

การประยุกต์การควบคุมคุณภาพกระบวนการเชิงสถิติในเทคนิคพิเศษทางรังสีรักษา

นายทวีป แสงแห่งธรรม

วิทยานิพนธ์นี้เป็นส่วนหนึ่งของการศึกษาตามหลักสูตรปริญญาวิทยาศาสตรดุษฎีบัณฑิต

สาขาวิชาวิศวกรรมนิวเคลียร์ ภาควิชาวิศวกรรมนิวเคลียร์

คณะวิศวกรรมศาสตร์ จุฬาลงกรณ์มหาวิทยาลัย

ปีการศึกษา 2555

ลิขสิทธิ์ของจุฬาลงกรณ์มหาวิทยาลัย

บทคัดย่อและแฟ้มข้อมูลฉบับเต็มของวิทยานิพนธ์ตั้งแต่ปีการศึกษา 2554 ที่ให้บริการในคลังปัญญาจุฬาฯ (CUIR)

เป็นแฟ้มข้อมูลของนิสิตเจ้าของวิทยานิพนธ์ที่ส่งผ่านทางบัณฑิตวิทยาลัย

The abstract and full text of theses from the academic year 2011 in Chulalongkorn University Intellectual Repository (CUIR)

are the thesis authors' files submitted through the Graduate School.

**APPLICATIONS OF STATISTICAL PROCESS CONTROL TO ADVANCED
RADIOTHERAPY TECHNIQUES**

Mr. Taweap Sanghangthum

**A Dissertation Submitted in Partial Fulfillment of the Requirements
for the Degree of Doctor of Engineering Program in Nuclear Engineering**

Department of Nuclear Engineering

Faculty of Engineering

Chulalongkorn University

Academic Year 2012

Copyright of Chulalongkorn University

Thesis Title	APPLICATIONS OF STATISTICAL PROCESS CONTROL TO ADVANCED RADIOTHERAPY TECHNIQUES
By	Mr. Taweap Sanghangthum
Field of Study	Nuclear Engineering
Thesis Advisor	Associate Professor Sivalee Suriyapee, M. Eng.
Thesis Co-advisor	Associate Professor Somyot Srisatit, M. Eng.
Thesis Co-advisor	Professor Todd Pawlicki, Ph.D.

Accepted by the Faculty of Engineering, Chulalongkorn University in Partial Fulfillment
of the Requirements for the Doctoral Degree

.....Dean of the Faculty of Engineering
(Associate Professor Boonsom Lerthirunwong, Ph.D.)

THESIS COMMITTEE

.....Chairman
(Associate Professor Supitcha Chanyotha, Ph.D.)

.....Thesis Advisor
(Associate Professor Sivalee Suriyapee, M.Eng.)

.....Thesis Co-advisor
(Associate Professor Somyot Srisatit, M.Eng.)

.....Thesis Co-advisor
(Professor Todd Pawlicki, Ph.D.)

.....Examiner
(Associate Professor Sunchai Nilswankosit, Ph.D.)

.....Examiner
(Assistant Professor Napassavong Rojanarowan, Ph.D.)

.....External Examiner
(Puangpen Tangboonduangjit, Ph.D.)

ทวีป แสงแห่งธรรม : การประยุกต์การควบคุมคุณภาพกระบวนการเชิงสถิติในเทคนิคพิเศษทางรังสีรักษา. (APPLICATIONS OF STATISTICAL PROCESS CONTROL TO ADVANCED RADIOTHERAPY TECHNIQUES) อ.ที่ปรึกษาวิทยานิพนธ์หลัก : รศ. ศิวลี สุริยาปี, อ.ที่ปรึกษาวิทยานิพนธ์ร่วม : รศ. สมยศ ศรีสถิตย์, Prof. Todd Pawlicki, Ph.D. 125 หน้า.

การควบคุมคุณภาพกระบวนการเชิงสถิติเป็นนวัตกรรมใหม่ในการประกันคุณภาพทางรังสีรักษา งานวิจัยนี้เป็นงานระยะแรกเริ่มที่นำกระบวนการเชิงสถิติมาประยุกต์ใช้เพื่อประเมินการตรวจสอบในเทคนิคพิเศษทางรังสีรักษา ทั้งนี้เพื่อเพิ่มความสามารถของกระบวนการประกันคุณภาพ ในงานส่วนแรกเป็นการใช้แผนภูมิควบคุมแบบ X สร้างขีดจำกัดควบคุมจาก 278 แผนการรักษาในเทคนิคปรับความเข้ม และ 159 แผนการรักษาในเทคนิคปรับความเข้มรอบตัวสำหรับมะเร็งหลังโพรงจมูก และใช้ดัชนีชี้วัดความสามารถของกระบวนการเพื่อวัดความสามารถของกระบวนการตรวจสอบแผนการรักษา ผลการศึกษาพบว่าแผนภูมิควบคุมสามารถแยกความผิดปกติออกจากความคลาดเคลื่อนแบบสุ่มได้ โดยมีขีดจำกัดควบคุมในเทคนิคปรับความเข้มอยู่ที่ 85% และปรับความเข้มรอบตัวอยู่ที่ 90% งานส่วนที่สองใช้แผนภูมิควบคุมแบบ X และแผนภูมิควบคุมแบบ $EWMA$ สำหรับการวัดความคงที่ของปริมาณรังสีประจำสัปดาห์จากเครื่องเร่งอนุภาคในช่วงเวลา 2 ปี โดยปรับเปลี่ยนจำนวนจุดที่ใช้คำนวณค่าขีดจำกัดควบคุม จาก 1 ถึง 5 เดือน จากการทดลองพบว่าควรใช้ข้อมูลประมาณ 2-3 เดือนในการคำนวณแผนภูมิควบคุมแบบ X แต่ใช้ข้อมูล 1 เดือนก็เพียงพอสำหรับแผนภูมิควบคุมแบบ $EWMA$ และควรใช้อย่างน้อย 20 ข้อมูลที่อยู่ในช่วงควบคุมอย่างต่อเนื่องในการคำนวณดัชนีชี้วัดความสามารถของกระบวนการ งานวิจัยสุดท้ายเป็นการหาขีดจำกัดการยอมรับในข้อมูลที่มีลักษณะการกระจายแบบต่างๆ พบว่าการตรวจสอบความถูกต้องของปริมาณรังสีแบบจุดใน 631 แผนการรักษา มะเร็งต่อมลูกหมากแบบปรับความเข้มซึ่งมีลักษณะการกระจายของข้อมูลเป็นแบบปกติ มีค่าขีดจำกัดการยอมรับอยู่ที่ 3.6% ในส่วนการผ่านของค่า γ ใน 157 แผนการรักษาสำหรับเทคนิคการรักษาแบบปรับความเข้มรอบตัวสำหรับมะเร็งบริเวณศีรษะและลำคอ ซึ่งมีการกระจายของข้อมูลแบบเบ้ไปทางซ้าย มีค่าขีดจำกัดการยอมรับด้านล่างที่ 88.22% และส่วนของความสม่ำเสมอของปริมาณรังสีในก้อนมะเร็งจาก 150 แผนการรักษาแบบปรับความเข้มรอบตัว ซึ่งมีการกระจายของข้อมูลแบบเบ้ไปทางขวา มีค่าขีดจำกัดการยอมรับด้านบนที่ 0.19 การควบคุมคุณภาพกระบวนการเชิงสถิตินำมาใช้ในรังสีรักษาได้เป็นอย่างดี

ภาควิชา..... วิศวกรรมนิวเคลียร์..... ลายมือชื่อนิสิต.....
 สาขาวิชา..... วิศวกรรมนิวเคลียร์..... ลายมือชื่อ อ.ที่ปรึกษาวิทยานิพนธ์หลัก.....
 ปีการศึกษา..... 2555..... ลายมือชื่อ อ.ที่ปรึกษาวิทยานิพนธ์ร่วม.....
 ลายมือชื่อ อ.ที่ปรึกษาวิทยานิพนธ์ร่วม.....

5071869121 : MAJOR NUCLEAR ENGINEERING

KEYWORDS : STATISTICAL PROCESS CONTROL/ CONTROL CHART/ PROCESS CAPABILITY INDEX/ PATIENT SPECIFIC QA/ TOLERANCE LIMITS

TAWEAP SANGHANGTHUM: APPLICATIONS OF STATISTICAL PROCESS CONTROL TO ADVANCED RADIOTHERAPY TECHNIQUES. ADVISOR: ASSOC. PROF. SIVALEE SURIYAPEE, M.Eng., CO-ADVISOR : ASSOC. PROF. SOMYOT SRISATIT, M.Eng., PROF. TODD PAWLICKI, Ph.D., 125 pp.

The statistical process control (SPC) is the new novel tool in radiotherapy QA process. This research is one of the first studies that applied SPC concept to advanced radiotherapy techniques. For the first research part, the \bar{X} control chart was performed to establish the reasonable control limits of % gamma pass of nasopharyngeal case in 278 IMRT QA plans and 159 VMAT QA plans, and to assess the efficiency of QA process by using process capability index. The result showed lower control limit of gamma pass of IMRT and VMAT QA of 85% and 90%, respectively. The VMAT QA process was more capable with higher capability index than IMRT. The second part employed the \bar{X} and $EWMA$ charts for 2 years of weekly output constancy check. The number of point used to calculate control limits was varied from 1 to 5 months of data for all energies, and the λ and L were two more parameters variation. It was found that 2-3 months of data should be employed to calculate control limit of \bar{X} chart, and 1 month of data should be used to calculate $EWMA$ control limit. At least 20 in-control data point should be achieved to find the process capability and process acceptability with 95% confidence interval. The last part of research work was the setup of local tolerance limits in different data distribution types. Our local tolerance limit for normal distribution data type of percent point dose difference between measurement and calculation of 631 prostate IMRT QA plans was 3.6%. The appropriate lower tolerance limit for left-skewed distribution data type of percent gamma pass of 157 head and neck VMAT QA plans was 88.22%, which was lower than universal action limit. The upper tolerance limit for right-skewed distribution data type of homogeneity index of 150 VMAT PTV plans for head and neck cases was 0.19. The SPC can assist in the QA work in radiotherapy with more efficient than using traditional QA concept.

Department : Nuclear Engineering Student's Signature

Field of Study : Nuclear Engineering Advisor's Signature

Academic Year : 2012 Co-advisor's Signature

Co-advisor's Signature

ACKNOWLEDGEMENTS

I would like to express my deepest gratitude to Asso. Prof. Sivalee Suriyapee, my local supervisor, for valuable advice, supervision, constructive comments, and English proof. I am equally grateful to Prof. Todd Pawlicki, my co-advisor, for excellence scientific guidance, advice, and never-ending source of ideas about the research. I am also deeply thankful to Asso. Prof. Somyot Srisatit, my co-advisor, for valuable advice and fruitful discussion to my research and my study throughout the study course.

I would also like to extend my appreciation to my thesis committee from Chulalongkorn and Mahidol university, Asso. Prof. Dr. Supitcha Chanyotha, Asso. Prof. Dr. Sunchai Nilsuwankosit, Assis. Prof. Dr. Napassavong Rojanarowan, and Dr. Puangpen Tangboonduangjit, for their kindness in examining the dissertation defense and providing the comments and suggestions for the improvement.

My sincere appreciation goes to all lecturers and staff at Nuclear Engineering Department, Chulalongkorn University for their kind support and supply the knowledge in Nuclear Engineering.

I would also like to express my sincere gratitude to Chulalongkorn hospital and the entire staff at Department of Therapeutic Radiology and Oncology, especially for Assis. Prof. Dr. Chonlakiet Khorprasert (head of my department) for all support.

Special thanks to my colleagues, Miss Chotika Jumpangern, Mr. Sornjarod Oonsiri, Mr. Isra Israngkul-Na-Ayuthaya, Mrs. Puntawa Oonsiri, Miss Sumana Somboon, and Mr. Tanawat Tawonwong, who excellent helps in the laboratory experiments and works during I have studied.

I am greatly appreciated for financial supporting by the 90th Anniversary of Chulalongkorn University Fund (Ratchadaphiseksomphot Endowment Fund) and the IAEA's Doctoral CRP on "QA of the Physical Aspects of Advanced Technology in RT".

Last but not the least, I am grateful to my family for their encouragement, entirely care and understanding during the entire course of study.

CONTENTS

	Page
ABSTRACT IN THAI.....	iv
ABSTRACT IN ENGLISH.....	v
ACKNOWLEDGEMENTS.....	vi
CONTENTS.....	vii
LIST OF TABLES.....	xii
LIST OF FIGURES.....	xiii
LIST OF ABBREVIATIONS.....	xvii
CHAPTER I INTRODUCTION.....	1
1.1 Background and rationale.....	1
CHAPTER II LITERATURE REVIEWS.....	4
2.1 Theories.....	4
2.1.1 Statistical process control.....	4
A. Control chart.....	4
B. Process capability and acceptability.....	11
2.1.2 Radiation treatment technique.....	15
2.1.3 Gamma evaluation.....	19
2.1.4 Radiation output.....	21
2.2 Review of related literatures.....	23

	Page
CHAPTER III RESEARCH OBJECTIVES	26
3.1 Research objectives.....	26
3.2 Scope of dissertation.....	27
3.3 Keywords.....	27
CHAPTER IV METHODOLOGY	28
4.1 Materials.....	28
4.1.1 Linear accelerator.....	28
4.1.2 MapCHECK 2D diode array.....	31
4.1.3 ArcCHECK 3D diode array.....	32
4.1.4 Treatment planning system.....	33
4.1.5 IMRT/VMAT QA software.....	34
4.1.6 Dose constancy check.....	35
4.1.7 Farmer type ionization chamber.....	36
4.1.8 Dosimeter or electrometer.....	37
4.1.9 Solid water phantom.....	38
4.2 Methods.....	39
4.2.1 SPC analysis for patient-specific IMRT and VMAT QA.....	39
A. IMRT planning and QA.....	39

	Page
B. VMAT planning and QA.....	40
C. Statistical process control analysis.....	43
C.1 X control chart analysis.....	43
C.2 Process capability analysis.....	43
4.2.2 Linear accelerator output constancy checks using process control techniques.....	44
A. Shewhart-type control chart.....	45
B. EWMA chart.....	47
C. Process capability and acceptability.....	47
4.2.3 On setting tolerance limits for process monitoring in radiotherapy.....	48
A. Process capability index.....	50
B. Clinical cases.....	52
B1. A process with normal distribution data.....	53
B2. A process with left-skewed distribution data.....	53
B3. A process with right-skewed distribution data.....	55
4.3 Anticipated outcomes.....	57

	Page
CHAPTER V RESULTS	58
5.1 SPC analysis for patient-specific IMRT and VMAT QA.....	58
5.2 Retrospective analysis of linear accelerator output constancy checks using process control techniques.....	63
A. Shewhart-type control chart.....	63
B. EWMA chart.....	67
C. Process capability and acceptability.....	69
5.3 On setting tolerance and action limits for process monitoring.....	72
A. A process with normal distribution data.....	72
B. A process with left-skewed distribution data.....	74
C. A process with right-skewed distribution data.....	74
CHAPTER VI DISCUSSION	76
6.1. SPC analysis for patient-specific IMRT and VMAT QA.....	77
6.2. Retrospective analysis of linear accelerator output constancy checks using process control techniques.....	80
6.3 On setting tolerance and action limits for process monitoring.....	84
CHAPTER VII CONCLUSIONS	76
7.2 Conclusions.....	89
7.3 Recommendation for future work.....	91

	Page
REFERENCES	94
APPENDIX	102
BIOGRAPHY	123

LIST OF TABLES

Table	Page
5.1 The control limits of X chart between using all first 50 plans and out-of-control points removed for nasopharyngeal carcinoma IMRT and VMAT plans.....	60
5.2 The number of first run points before out-of-control limits and number of longest run points on the X-charts for 6 and 10 MV photon beams, and 6, 9, 12, 16, and 20 MeV electron beams	66
5.3 The number of measurements before the first out-of-control point is observed on the EWMA charts for 6 and 10 MV photon beams, and 6, 12 and 20 MeV using 1 to 3 months (4-12 data points) calculate the control limits for different smoothing parameter (λ) and limit width (L).....	70
5.4 The mean, SD, target, and skewness of clinical application data of % point dose difference for prostate IMRT QA (normal distribution), % gamma pass of VMAT nasopharynx QA (left-skewed distribution), and homogeneity index of head and neck plan (right-skewed distribution).....	73
5.5 The tolerance and action limits for clinical application data of % point dose difference of IMRT QA (normal distribution), % gamma pass of VMAT QA (left-skewed distribution), and homogeneity index (right-skewed distribution).....	75
7.1 The summary of research works with selected SPC tools.....	88
7.2 The example of radiotherapy QA with appropriate control chart type.....	91

LIST OF FIGURES

Figure	Page
2.1 A typical control chart.....	5
2.2 The measurement data with (a) chance and (b) assignable causes of variation.....	6
2.3 A flowchart for the selection of the correct control chart for different data types.....	7
2.4 The steps of creating and using a control chart to monitor and improve a process.....	11
2.5 Distributions with different capability ratio (C_p) and acceptability ratio (C_{pk}) showing their relationship to the process target, upper action limit (UAL) and lower action limit (LAL).....	13
2.6 Distributions with different Taguchi's capability ratio (C_{pm}) relationship upper action limit (UAL) and lower action limit (LAL).....	15
2.7 The verification process of intensity map of IMRT process.....	17
2.8 The isodose distribution of nasopharyngeal carcinoma plan for IMRT and VMAT treatment techniques.....	19
2.9 Geometrical representation of calculation concept of gamma evaluation method.....	21
4.1 Linear accelerator machines (Varian Medical Systems, Inc., Palo Alto, CA, USA) (a) Clinac 21EX with EPID, and (b) Clinac iX with EPID and OBI (CBCT).....	30

Figure	Page
4.2 Multileaves collimator (Varian Medical Systems, Inc., Palo Alto, CA, USA).....	30
4.3 MapCHECK 2D diode array (Sun Nuclear Corp., Melbourne, FL, USA).....	31
4.4 ArcCHECK 3D diode array (Sun Nuclear Corp., Melbourne, FL, USA).....	32
4.5 Eclipse treatment planning software (Varian Medical Systems, Palo Alto, CA, USA).....	33
4.6 SNC Patient software (Sun Nuclear Corp., Melbourne, FL, USA).....	34
4.7 The RBA-3 dose constancy check (GAMMEX rmi, Middleton, WI, USA)..	35
4.8 The FC65-P cylindrical ionization chamber (Scanditronix-Wellholfer Dosimetrie, Schwarzenbruck, Germany).....	36
4.9 The Dose1 dosimeter (Scanditronix-Wellholfer Dosimetrie, Schwarzenbruck, Germany).....	37
4.10 Solid water phantom or Virtual Water® (CIVCO medical solution, IA, USA).....	38
4.11 The setting up of a) MapCHECK for patient-specific IMRT verification and b) ArcCHECK for patient-specific VMAT verification.....	42
4.12 The dose volume histogram of PTV with D_2 , D_{98} , and D_{median}	56
5.1 The IMRT QA plan comparison of nasopharyngeal carcinoma in SNC patient software measured by MapCHECK and calculated by Eclipse.....	58
5.2 The VMAT QA plan comparison of nasopharyngeal carcinoma in SNC patient software measured by ArcCHECK and calculated by Eclipse.....	59

Figure	Page
5.3 Individual (\bar{X}) control chart of % gamma pass of patient-specific (a) IMRT QA and (b) VMAT QA for nasopharyngeal carcinoma plans with center line (CL) and lower control limit (LCL).....	62
5.4 The \bar{X} -control chart for output constancy check for 6 MV (a, b) and 12 MeV (c, d). The output data in first month used to calculate the control limit are displayed in (a) and (c), while (b) and (d) used four months of data. The solid lines are the process behavior limits and the center line.....	65
5.5 Signal to noise ratio (\bar{x}/σ) normalized by the number of in-control data points for the data in (a) 2009 and (b) 2010 for the first run of the data in-control for all energies.....	67
5.6 The Exponentially Weighted Moving Average ($EWMA$) chart for output constancy check measured by central ionization chamber of RBA-3 device with first month calculated control limits for (a) 6 MV; $\hat{\lambda}=0.05, L=2.492$, (b) 6 MV; $\hat{\lambda}=0.20, L=2.860$, (c) 12 MeV; $\hat{\lambda}=0.05, L=2.492$, and (d) 12 MeV; $\hat{\lambda}=0.20, L=2.860$	68
5.7 The capability ratio (C_p) and acceptability ratio (C_{pk}) of first run and longest run for output constancy check measured by central ionization chamber of RBA-3 device with different time to calculate the control limits for (a) 6 MV photon beams and (b) 12 MeV electron beams.....	69
5.8 The capability ratio (C_p) and acceptability ratio (C_{pk}) with the 95% CI for the process of linac output verification per energy using the first in-control run	

Figure	Page
and 2 months of data to calculate the control limits. Values of C_p and C_{pk} above the dashed horizontal line are considered acceptable.....	71
5.9 Histogram of percent dose difference between measured and calculated of patient-specific prostate IMRT QA as normal distribution data	73
5.10 Histogram of percent gamma passing rate of patient-specific nasopharyngeal carcinoma VMAT QA as a left-skewed distribution data.....	74
5.11 Histogram of homogeneity index of VMAT plan of head and neck cancer as a right-skewed distribution.....	75
6.1 The flow chart for using tolerance limit from process capability index method.....	87

ABBREVIATION

Abbreviation	Terms
QC	Quality control
QA	Quality assurance
ICRU	International Commission on Radiation Units and Measurements
AAPM	American Association of Physicists in Medicine
CT	Computed Tomography
FTA	Fault Tree Analysis
FMEA	Failure Mode and Effect Analysis
SPC	Statistical Process Control
IMRT	Intensity Modulated Radiation Therapy
VMAT	Volumetric Modulated Arc Therapy
PTV	Planning Target Volume
PCI	Process Capability Index
HI	Homogeneity Index
CL	Center Line
UCL	Upper Control Limit
LCL	Lower Control Limit
X/MR chart	Individual/Moving Range Chart
\bar{X} /R chart	Average/Range Chart
\bar{X} /S chart	Average/Standard Deviation Chart

Abbreviation	Terms
p chart	The proportions chart for defective with variable sample size
np chart	The proportions chart for defective with constant sample size
c chart	The counts control chart for defect with constant sample size
u chart	The counts control chart for defect with variable sample size
d	Constant value that depends on subgroup size
n	Number of subgroup size
$\bar{\bar{X}}$	Grand average data of several subgroups
A	Constant Value that depends on subgroup size
EWMA	Exponentially Weighted Moving Average
λ	The smoothing parameter for EWMA chart
L	The control limit width for EWMA chart
C_p	The process capability
C_{pk}	The process acceptability
C_{pm}	The Taguchi's process capability index
UAL	Upper Action Limit
LAL	Lower Action Limit
USL	Upper Specification Limit
LSL	Lower Specification Limit
T	The process target
2D	Two dimensional radiotherapy
3D-CRT	Three dimensional conformal radiotherapy

Abbreviation	Terms
MLC	Multileaf collimator
MRI	Magnetic Resonance Imaging
F	Quadratic objective function (cost function)
r_o	The priority or penalty or weighting factor
D_C	Calculated dose
D_o	Prescribed dose
TPS	Treatment planning system
MOSFET	Metal–oxide–semiconductor field-effect transistor
EDR film	Extended dose range film
EPID	Electronic Portal Imaging Device
DTA	Distance-to-agreement
Γ, γ	Gamma index
MU	Monitor Unit
cGy	centigray
R&R	Reproducibility and Repeatability
$P_p, P_{pk},$ and P_{pm}	The long term process performance indices
CBCT	Cone beam computed tomography
ms	millisecond
SIB	Simultaneous integrated boost
RBA	Radiation Beam Analyser
FC65P	Plastic farmer chamber with sensitive volume of 0.65 cm^3
POM	PolyOxyMethylene

Abbreviation	Terms
ηC	nanocoulomb
V	Electrical potential difference in voltage
IEC	International Electrotechnical Commission
LR	Low risk
HR	High risk
CW	Clockwise
CCW	Counterclockwise
IGRT	Image Guided Radiation Therapy
MV	Megavoltage
IAEA	International Atomic Energy Agency
TRS	Technical Report Series
SSD	Source-to-surface distance
SSK	Strahlenschutzkommission (German Commission on Radiological Protection)
IPEM	Institute of Physics and Engineering in Medicine
RCR	The Royal College of Radiologists
ESTRO	European Society for Therapeutic Radiology and Oncology
S	Skewness index
μm	micrometer
D_2	The absolute dose at 2% of the target volume (maximum dose)

D_{98}	The absolute dose at 98% of the target volume (minimum dose)
D_{median}	The median dose of target volume
N	The number of data points in month used to calculate the limits
QUASIMODO	QUality ASsurance of Intensity MODulated radiation Oncology
PMMA	Polymethyl methacrylate

CHAPTER I

INTRODUCTION

1.1 Background and Rational

Radiotherapy, radiation therapy, or radiation oncology is a complex clinical process of using ionizing radiation to treat a variety of diseases but primarily to local malignant tumors. Radiotherapy is one of the three most common types of cancer treatment, while other two methods are surgery and chemotherapy. It may be delivered radiotherapy alone or combined with other methods together to improve the potential of cancer treatment. The goal of radiotherapy is to give a high, conform, homogeneous and accurate radiation dose to well-defined target volume, while can spare dose to surrounding normal tissues with the fewest complications. The accuracy in each step of radiotherapy process is possible affected to tumor control and normal tissue complications. Quality control (QC) and quality assurance (QA) are the systematic procedure of monitoring and controlling all of the process to ensure that the process of product or service can pass the standard criteria. Nowadays, the role of quality and safety are more and more important parts in radiotherapy community, especially when using the sophisticated modern equipment and treatment technique. Radiotherapy is one of the top in rank of health care program that performed the QA system. The International Commission on Radiation Units and Measurements (ICRU) has a recommendation of uncertainty in dose delivery to patient at no greater than 5% [1, 2]. A comprehensive QA program should be performed to all possible sources of variation

aspects in patient treatment process in an effort to maintain the overall uncertainty. Mijnheer [3] divided QA in radiotherapy into 3 parts; treatment machine and equipments, treatment planning, and imaging system. The professional organizations in radiation oncology, such as the American Association of Physicists in Medicine (*AAPM*), have been proposed the QA programs and their limitations covered these three parts [4-7]. However, the QA should not be considered only machine and equipment, but also would include all of the process of radiation treatment, including doctor delineations, data and image transfer, time between CT and treatment, accuracy of billing, etc.

In radiotherapy QA process, the limitations are normally used distance, angle, or percent difference or used standard deviation method that based on machine function or experience, however, these traditional tools may not be enough to evaluate the quality in radiotherapy, especially in this era of quality and safety. Several methods are described for new modern QA tools in radiotherapy, for example: fault tree analysis (FTA) [8], failure mode and effect analysis (FMEA) [9] or statistical process control (SPC) [10]. The SPC is the high level QA tool in industrial engineering field, which is the field of highest level of quality control. Therefore, the SPC is possible to use in radiotherapy quality control in order to improve the efficiency of radiotherapy process. This study applies SPC to patient-specific intensity modulated radiation therapy (IMRT)/ volumetric modulated arc therapy (VMAT) QA by separating the systematic error from random error, and applied to output constancy check by investigation the number of data point for setting the control limit. This study also

utilizes the SPC concept to setup the suitable tolerance limits of planning target volume (PTV) homogeneity index and patient-specific QA.

CHAPTER II

LITERATURE REVIEWS

2.1 Theories

2.1.1 Statistical Process Control (SPC)

A. Control charts

Statistical Process Control (SPC) is the use of statistically based methods to evaluate a process or its output to achieve a state of control. Control chart (process behavior chart or Shewhart chart) is one of the seven basic tools of quality control for SPC, which was pioneered in 1924 by Walter A. Shewhart when he worked in Bell Telephone Laboratories. Control chart is a time ordered statistical tool used to distinguish between process variation resulting from “common causes” and variation resulting from “special causes”. The former causes can be referred to “random errors”, while latter causes represent “systematic errors”. Control chart has been used commonly in industrial manufacturing and business process for long time. It consists of three basic components; 1) center line (*CL*) that represents the mean value of the process data, 2) two horizontal lines called upper control limit (*UCL*) and lower control limit (*LCL*) that defines the limit of common variation causes, and 3) measurement data that plotted over the time series or sample number as shown in **Figure 2.1**. The filled dot in **Figure 2.1** expresses the systematic error point.

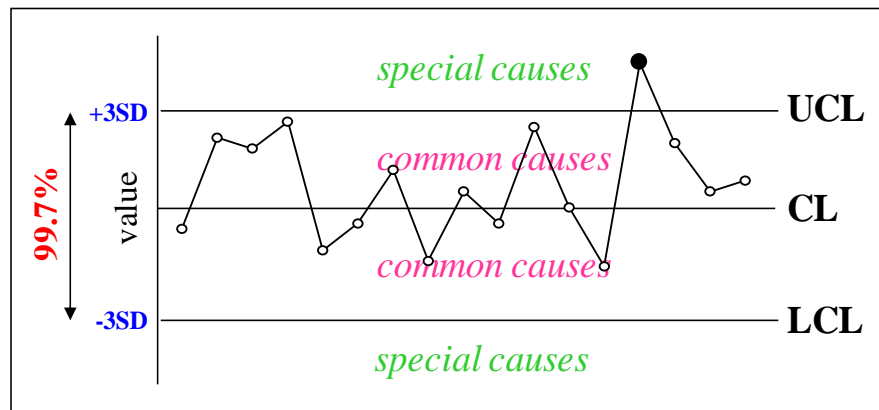


Figure 2.1. A typical control chart.

An important assumption when using control charts is that the measurement subgroups (or individual values) are independent. When the data fall within the *UCL* and *LCL*, then the process is said to be in control and only common (random) causes affect the process. However, if any data point is out of the control limits, then special (non-random) causes are affecting the process and the source(s) of the special cause need to be identified and removed from the process to bring the process back in-control. The causes of systematic variation can be shown in location, spread, and shape as illustrated in **Figure 2.2**. Conventionally, the *UCL* and *LCL* are set at ± 3 standard deviations from the center line [11]. This implies that 99.7% of the data points would fall within the control limits when the data is normally distributed. Then, when the process is in control, there is only a 0.3% chance that a point will be outside the control limits, i.e., a false positive.

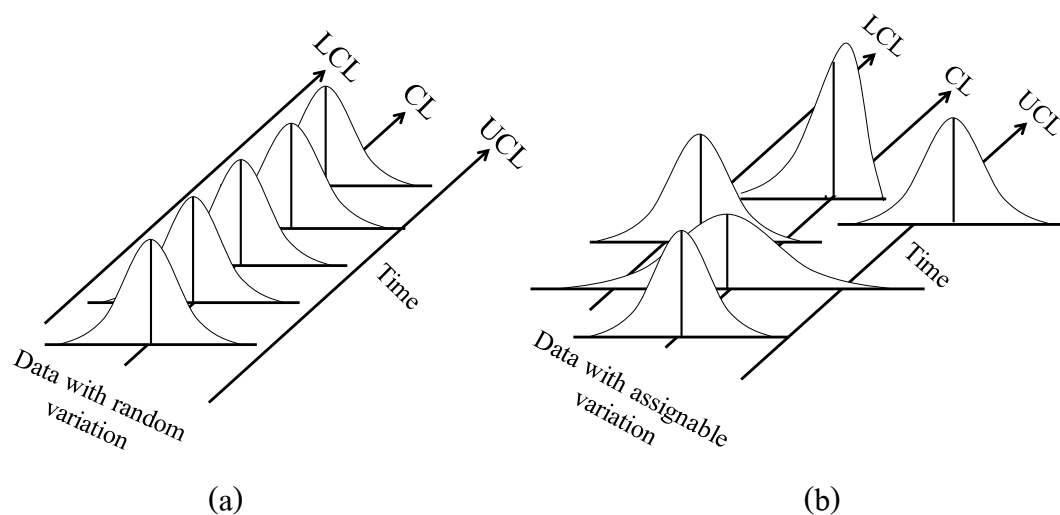


Figure 2.2. The measurement data with (a) chance and (b) assignable causes of variation.

There are two main types of control charts that depend on data type as shown in **Figure 2.3**; attribute control chart and variable control chart [12]. The former chart is suitable for discrete distribution data that expressed as yes/no, presence/absence, good/bad or function/non-function, while the latter chart is match for continuous data or measured on a numerical scale. The variable control chart is more suitable to radiotherapy QA. The two main categories of control chart are sub-divided into several other chart types. Each sub-category has a specific purpose. For the variable control chart, there are individual/moving range (X/MR), average/range (\bar{X}/R), and average/standard deviation (\bar{X}/S) charts that depend on subgroup size. If the number in each subgroup is one to nine, then the \bar{X}/R or \bar{X}/S charts should be used. If the subgroup size is ten or more, then the \bar{X}/S charts are recommended. One important assumption for variable control charts is that the measurement subgroups are independent of each other.

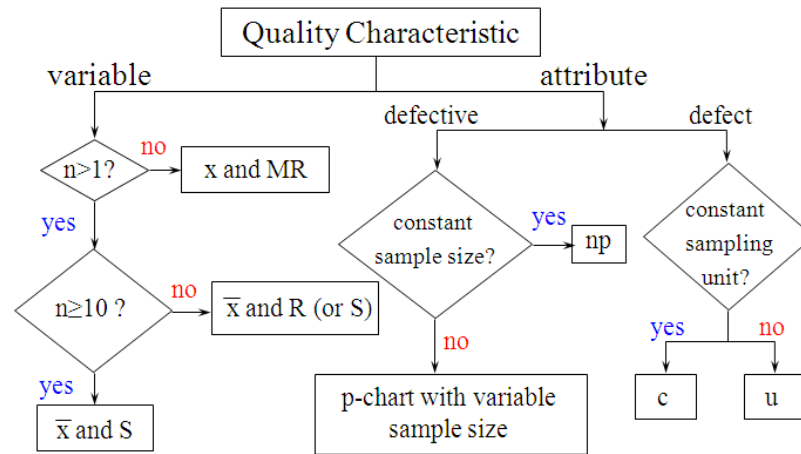


Figure 2.3. A flowchart for the selection of corrected control chart for different data types.

A.1 The individual and moving range (X/MR) charts

The X/MR charts are selected for individual value collected per time period. The examples of radiotherapy QA that can be applied this control chart type are daily output constancy check, daily water temperature of linear accelerator machine, point dose difference between measurement and calculation for IMRT QA, etc. The average and limits are calculated from Equation (2.1).

$$UCL_x = \bar{X} + 3 \frac{\overline{MR}}{d_2}, \quad CL_x = \bar{X}, \quad LCL_x = \bar{X} - 3 \frac{\overline{MR}}{d_2} \quad (2.1)$$

The moving range and their limits for output are calculated from Equation (2.2).

$$UCL_{MR} = \overline{MR} \left(1 + 3 \frac{d_3}{d_2}\right), \quad CL_{MR} = \overline{MR}, \quad LCL_{MR} = \overline{MR} \left(1 - 3 \frac{d_3}{d_2}\right) \quad (2.2)$$

The MR is the absolute value of the difference between two consecutive data points ($MR_i = |X_i - X_{i-1}|$). The \bar{X} and \overline{MR} are calculated as the average data and average

moving range over a specified number of data points. The constants d_2 and d_3 depend on n value, where n is the number of value in the subgroup. It is customary to use $n = 2$ for subgroup size 1 so d_2 is 1.128 and d_3 is 0.8525 [11].

A.2 The average and range (\bar{X}/R) charts

The \bar{X} and R charts are typically used for collected group of data in each time period. However, the number of data in each group should be constant and not larger than 10 data points. The examples of this control charts type in radiotherapy QA are dose from planar detector with specific point of measurement, output from five chamber detectors or subgroup method of individual data, or long term of reproducibility of detector that have measured several times in each measurement period. The mean and limits for average control chart are calculated from Equation (2.3).

$$UCL_{\bar{X}} = \bar{\bar{X}} + 3 \frac{\bar{R}}{d_2 \sqrt{n}}, \quad CL_{\bar{X}} = \bar{\bar{X}}, \quad LCL_{\bar{X}} = \bar{\bar{X}} - 3 \frac{\bar{R}}{d_2 \sqrt{n}} \quad (2.3)$$

where \bar{X} is the average data of each subgroup and $\bar{\bar{X}}$ is grand average data of several subgroups. The range and their limits can be calculated from Equation (2.1) but replaced \overline{MR} with \bar{R} , where R is the range of the value in each group ($R_i = X_{max} - X_{min}$). If the sample size in each subgroup is large, the accuracy of chart will reduce because range uses only two data in each group for calculation. The constants d_2 and d_3 depend on subgroup size n . If the calculated range is negative value, we use zero because range is not less than zero.

A.3 The average and standard deviation (\bar{X}/S) charts

The \bar{X} and S charts are also suitable for subgroup data the same as \bar{X}/R chart but \bar{X}/S is better in case of a large number of data in each subgroup. The sequence of charts setting up is the same with \bar{X}/R charts construction, however, the sample standard deviation is defined in Equation (2.4).

$$S = \sqrt{\frac{\sum_{i=1}^n (X_i - \bar{X})^2}{n-1}} \quad (2.4)$$

The average and control limits of \bar{X}/S chart are calculated from Equation (2.5).

$$UCL_{\bar{X}} = \bar{\bar{X}} + A_3\bar{S}, \quad CL_{\bar{X}} = \bar{\bar{X}}, \quad LCL_{\bar{X}} = \bar{\bar{X}} - A_3\bar{S} \quad (2.5)$$

The constant A_3 is tabulated for various subgroup size in text book [11].

A.4 Exponentially Weighted Moving Average (EWMA) chart

The EWMA chart is a special type of time order control chart used the history of output to calculate control limits. This chart is originally proposed by S W Roberts in 1959. Where the \bar{X}/mR charts are used to detect large changes in the process, the *EWMA* chart is suitable for detecting the gradual drifts in the process [12]. In the *EWMA* chart, the most recent data points are given a greater weight (λ). The degree of weight reduces with exponential function for prior data with $\lambda \cdot (1-\lambda), \lambda \cdot (1-\lambda)^2, \dots$, etc. The chart is match for subgroup size of 1. The *EWMA* equation is given by Equation (2.6).

$$EWMA_t = \lambda \cdot x_t + (1 - \lambda) \cdot EWMA_{t-1} \quad (2.6)$$

for $t = 1, 2, 3$, where x_t is the observation data at time t .

The average and limits for the *EWMA* chart are calculated from Equations (2.7).

$$UCL = \mu_0 + L \cdot \sigma \sqrt{\frac{\lambda}{2 - \lambda} [1 - (1 - \lambda)^{2t}]}, \quad CL = \mu_0, \quad LCL = \mu_0 - L \cdot \sigma \sqrt{\frac{\lambda}{2 - \lambda} [1 - (1 - \lambda)^{2t}]} \quad (2.7)$$

where μ_0 is the process average, t is the sample number, λ is the weighting factor (smoothing factor) with values $0 < \lambda \leq 1$, which makes the *EWMA* chart sensitive to small process drifts. A large λ value means a greater weight to recent data and less weight to old data. The parameter L is the width of the control limit. Difference than *X*-charts; the *UCL* and *LCL* are calculated with each new data point for *EWMA* charts. However, similar to *X*-charts, the *EWMA* chart also relies on the assumption that the samples (or individual values) are independent. The value of L and λ are chosen as a range of values that are a compromise between efficiency detection of process drifts and chart insensitivity to non-normal data [12]. When selecting the proper λ , the *EWMA* chart can be produced sensitive to a small or gradual drift in the process, whereas the Shewhart control procedure can only react in case of the last data point is outside a control limit.

The steps of control chart construction are shown as a flowchart in **Figure 2.4**. After the charts are selected by using the criteria from **Figure 2.3**, the data will be plotted on the charts. The control limits are calculated and the first lots of measurement data will be compared with control limits. If any data points are out-of control limits

and the sources of error can be found, those out-of-control points will be removed. The new control limits are recalculated for systematic error removed. Then, the next measurement data is plotted on the chart and compared with new control limits. If the data are outside control limit, the charts will immediately warn QA staff to get rid of the error.

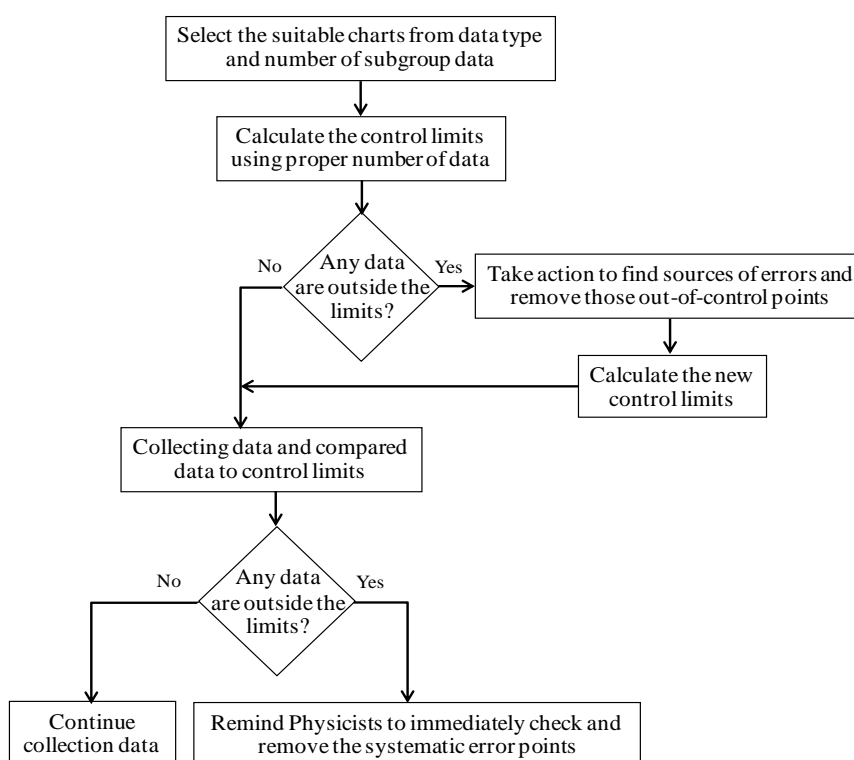


Figure 2.4. The steps of creating and using a control chart to monitor and improve a process.

B. Process capability and acceptability

The process capability indices are the measurement of process performance according to some requirements. In manufacturing, these requirements are usually called specifications. When a process or part is measured, it is compared to the

specification limits. In radiation oncology, the process or QC result is compared to the clinical or action limits. The process capability (C_p) and process acceptability (C_{pk}) are two commonly process capability indices (PCI) that have been used in industrial manufacturing for long time.

The process capability is used to compare the variation process of the data with respect to the upper and lower action limits to quantify action limit width relative to the dispersion of process data as shown in Equation (2.8),

$$C_p = \frac{UAL - LAL}{6 \cdot \sigma} \quad (2.8)$$

where UAL and LAL are the upper and lower action limits, respectively. The σ is the standard deviation of the data distribution. The greater the C_p value, the better of process is able to meet action limits as shown in **Figure 2.5**. A C_p value of 1.0 means that the data spread is equal to the action limit width. However in some process, a process can still be functioning poorly even with a high C_p value (see bottom image in **Figure 2.5**). So, the capability ratio alone is not enough to provide a full description of a process because C_p does not indicate the degree to which the process is centered on the target.

The process acceptability is another index that should be used to fully characterize a process. Acceptability describes how close the process center is to the nearest action limit. It is calculated from Equation (2.9).

$$C_{pk} = \min\left(\frac{UAL - \mu}{3 \cdot \sigma}, \frac{\mu - LAL}{3 \cdot \sigma}\right) \quad (2.9)$$

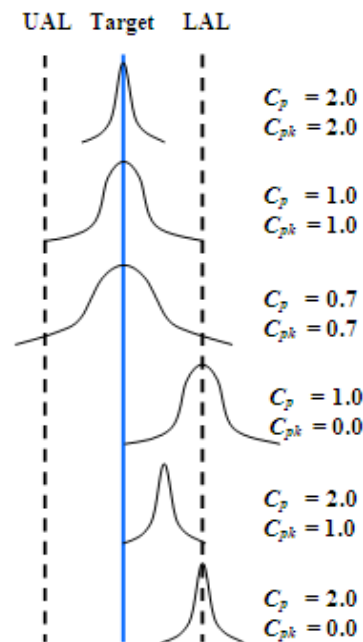


Figure 2.5. Distributions with different capability ratio (C_p) and acceptability ratio (C_{pk}) showing their relationship to the process target, upper action limit (UAL) and lower action limit (LAL).

If the process is on target, the value of capability ratio will equal to acceptability ratio. However, the capability ratio is higher than acceptability ratio in cases where a process is not on target as shown in **Figure 2.5**. When calculating C_p and C_{pk} ratios, it is important that the process is in-control, that is, no points outside the control limits on the \bar{X} -chart. This is because if the process is changing, then one cannot be confident that the process is subject to only random (or common) causes. Furthermore, the normal distribution upon which the capability and acceptability ratios depend is not assured. In this study, data normality was verified using the Anderson–Darling test statistic. For any non-normal distributions, the Johnson Transformation was used to normalize the data. The normalized data was then used to calculate C_p and

C_{pk} . The Anderson–Darling tests and Johnson Transformations were done in Minitab v16 software (Minitab Inc, State College, PA).

The C_p parameter explains how much the data dispersion but does not consider the process mean, while the C_{pk} index illustrates is another index that used to explain how close to the process center. The C_{pk} alone is inadequate to measure the process centering. The good process should have both C_p and C_{pk} as high as possible. However, these two indices just consider only the dispersion and closeness to the center of data. The center or average of data is correct value or not, it cannot explain from these two indexes. Chan et al. [13] originated the new process capability index, C_{pm} , based on Taguchi's loss function process that that use unary quadratic loss function replaced traditional step function. This index can explain the dispersion of process compared to specification limits and also take the process target into consideration in only one index. The standard two-side of C_{pm} can be calculated from Equation (2.10).

$$C_{pm} = \frac{UAL - LAL}{A\sqrt{\sigma^2 + (\bar{X} - T)^2}} \quad (2.10)$$

where UAL and LAL are the upper and lower action limits, respectively. A is a constant that depends on the quality you need, typically this constant is set to 6 for C_{pm} of 1.0 in case of perfect center at midpoint (guarantees that the total non-conformity yield is lesser than 0.27%) as shown in **Figure 2.6**.

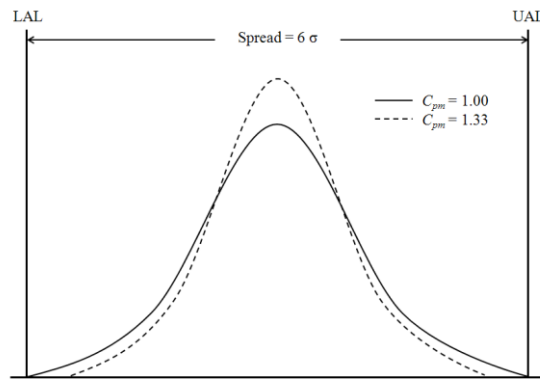


Figure 2.6. Distributions with different Taguchi's capability index (C_{pm}) relationship upper action limit (UAL) and lower action limit (LAL).

2.1.2 Radiation Treatment techniques

Radiotherapy is one of the main methods of cancer treatment. The radiation treatment technique has been developed from two dimensional radiotherapy (2D), three dimensional conformal radiotherapy (3D-CRT) to intensity modulated radiotherapy (IMRT), and volumetric modulated arc therapy (VMAT) [14]. The 2D treatment technique is the treatment technique used 2D image from conventional simulator for dose calculation. This technique is suitable for conventional treatment that typically uses single or two-parallel opposing fields. The 3D-CRT is based on CT image for dose calculation. The forward planning with suitable energy, number of beams, field weight, beam angle, multileaf collimator (MLC) shielding, compensators (wedge, bolus, or tissue compensator) are selected by planner to get the conform dose to target volume and less radiation dose to surrounding normal tissues.

The IMRT is the advanced treatment technique that radiation doses can be modulated by MLC movement or using compensator to perform the non-intensity pattern. The MLC-based is more commonly used to modulate the beam. This treatment

technique is planned on 3D image (CT or MRI) with computerized dose calculations to determine the suitable variation of intensity patterns in each treatment fields, however, the radiation dose will conform to the tumor shape and spare dose to normal tissues when combines all of fields together. Not only the prescribed dose need to be set, but the defined dose constraints for PTV and critical organs are also required for optimization. The inverse treatment planning with quadratic objective function (cost function) in Equation (2.11) is used to optimize based on properly dose constraints [15].

$$F = \frac{1}{N} \sum_n r_Q [D_c(n) - D_o(n)]^2 \quad (2.11)$$

where r_Q is the priority or penalty or weighting factor that weight the importance of structure Q . D_c and D_o are the prescribed and calculated dose, respectively. This formula relies on iteration method of least square type of estimation in statistical analysis. After finishing the optimization, the “*optimal fluence*” or desired intensity map of each planning fields are shown in **Figure 2.7**. The leaves motion of MLC will be calculated following the optimal fluence pattern. The leaves are speed-up in the light pixels and slow-down at dark pixels. There are two different approaches for MLC mode in IMRT technique; dynamic and segmented IMRT. The radiation can be exposed during MLC movement for the former IMRT mode, and vice versa for the latter IMRT mode. The dynamic MLC (DMLC) is more common to use for Varian linac. When finishing the leaves motion calculation, the radiation doses are calculated to get the “*actual fluence*” of each planning field. The actual fluence has some different from optimal fluence because the optimal fluence uses only mathematic

formula to optimize the fluence but the actual fluence is calculated with including the scatter, leaves leakage, and inhomogeneity corrections. These actual fluencies are imported to the treatment machine to perform the measurement and then the measured fluence is compared with calculated fluence (actual fluence). This step is for checking the accuracy of MLC movement and called patient-specific IMRT QA, which is necessary to do all cases before patient treatment. IMRT has become one of the catchwords of modern radiotherapy treatment and also becomes to the standard treatment technique for head and neck cancer treatment in many cancer centers [16] because of the clinical benefits of dose sparing to surrounding normal tissue, especially the salivary glands, and benefits of dose conformity to target volume compared to conventional radiotherapy [17, 18, 19].

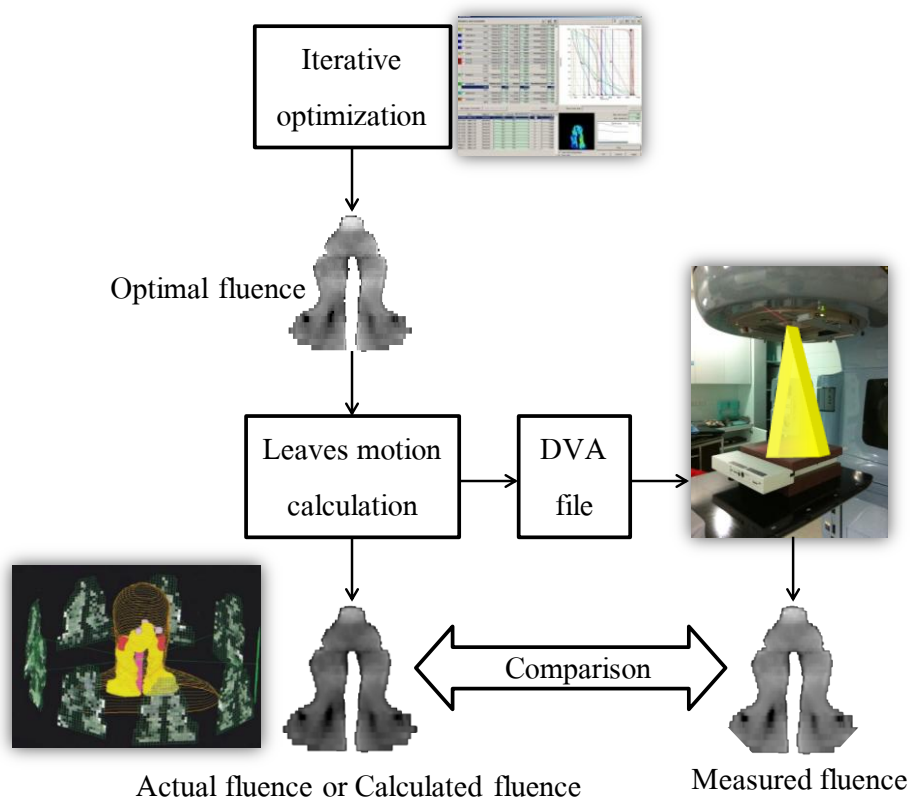


Figure 2.7 The verification process of intensity map of IMRT process.

The VMAT technique is the newest radiation treatment technique. It is a state-of-the-art radiotherapy treatment technique that combines the concept of two advanced techniques; dynamic arc and IMRT, together. The VMAT has more complicated than IMRT because VMAT is not only modulated the beam by two-ways MLC movement, but include the dose rate and gantry speed variation as well. During the radiation beam continuously delivery, the gantry rotates around patient with two-ways DMLC movement while the dose rate and gantry speed can be varied simultaneously. The VMAT plan has the potential to improve the dose conformity and coverage to target volume and normal tissue sparing compared to conventional technique [20]. However, the predominance of this technique than previous generation of modulated radiotherapy technique, IMRT, is the reduction of the number of monitor units (MUs) and also the delivery time [21]. The isodose distribution of IMRT and VMAT are quite equivalent but the latter technique has a smoother dose distribution as shown in **Figure 2.8**. Because both in IMRT and VMAT techniques, the radiation dose can be modulated by DMLC movement and VMAT technique has more variation factors that impact to radiation dose accuracy, the robust patient-specific quality assurance (QA) program of dose distribution of IMRT and VMAT technique was recommended to verify the correct treatment delivery before clinical treatment [22].

There are many dosimetric systems in market used to validate the IMRT or VMAT techniques by checking the accuracy of dose measurement or leaf sequences. In our view, it can be separated into 5 categories; *a) point dose* (e.g. ionization chamber, thermoluminescent dosimeter, MOSFET), *b) planar dose* (e.g. EDR film, EBT film, EPID, MapCHECK, MatriXX, seven29), *c) volume dose* (e.g. Delta4,

ArcCHECK, Compass, BankGel), *d) MLC verification* (e.g. David, DynalogFile), *e) MU verification* (e.g. RadCal, MU check). The planar QA tool is the most common used to verify the IMRT plans, while the volume dose QA tool is a popular one to validate the accuracy of VMAT plans. For traditionally medical physics aspect, percentage of dose difference, distance-to-agreement and gamma value are three commonly methods used to evaluate the result of plan verification.

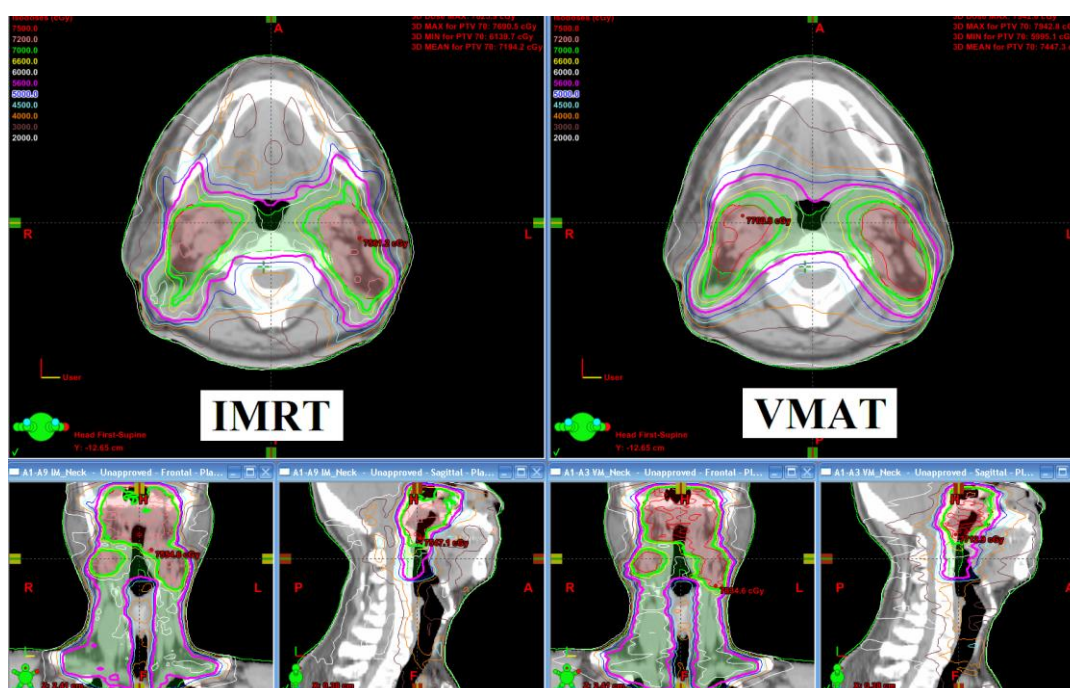


Figure 2.8. The isodose distribution of nasopharyngeal carcinoma plan for IMRT and VMAT treatment techniques.

2.1.3 Gamma Evaluation

The percent dose difference has been used to evaluate the dose difference between two set of data, for example the difference between calculation and measurement. However, this concept is difficult to evaluate in 2D planar or 3D volume

of dose difference. The simple qualitative evaluation of two set of dose distribution is the superimpose method. Van Dyk *et al.* [23] separate the region of dose into high and low dose gradient region. They recommended to use the percent different concept for low dose gradient region, and to employ the distance-to-agreement (*DTA*) tool for high dose gradient region. The *DTA* is the distance difference between a reference data point and the nearest data point with the same dose. Low *et al.* [24] proposed the concept of gamma evaluation for dose distribution comparison in quantitative method. The gamma index combines the concept of % dose difference and *DTA* criterion together by using the ellipse formula. The surface of ellipsoid represents the acceptance criterion, which is defined in Equation 2.12 and shown in **Figure 2.9**.

$$1 = \sqrt{\frac{\Delta r^2}{\Delta d_M^2} + \frac{\Delta D^2}{\Delta D_M^2}} \quad (2.12)$$

where Δr is the absolute distance difference between reference point [r_r] and compared point [r_c], while ΔD is the dose difference between dose at position r_c [$D_c(r_c)$] and reference dose at position r_r [$D_r(r_r)$]. If the dose difference at inquiry point is inside the ellipsoid, it will pass the criteria. Therefore, the gamma criteria can be defined in Equation (2.13).

$$\Gamma_r(r_c, D_c) \equiv \sqrt{\frac{\Delta r^2}{\Delta d_M^2} + \frac{\Delta D^2}{\Delta D_M^2}} \leq 1 \quad (2.13)$$

If the criteria of dose difference and *DTA* are the same value, such as 3% dose difference and 3mm distance-to-agreement, the ellipsoid becomes circle. The minimal value of $\Gamma_r(r_c, D_c)$ is defined as gamma quality index, $\gamma(r_r)$, of the reference point. The

point passing the specified criteria correspond with $\gamma(r_r) \leq 1$, while failed point that not passed the specified criteria represent with $\gamma(r_r) > 1$.

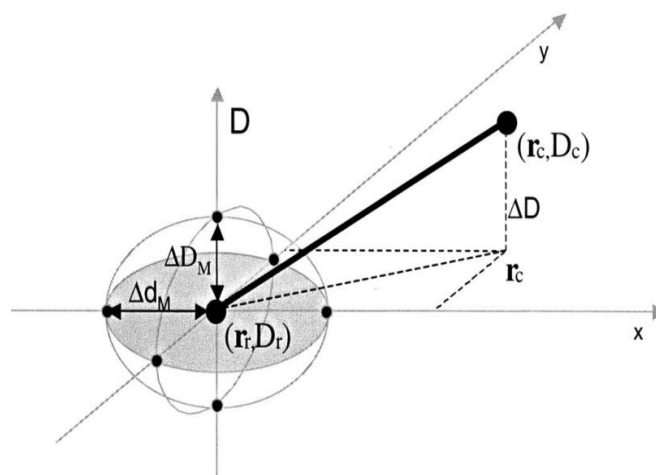


Figure 2.9. Geometrical representation of calculation concept of gamma evaluation method.

2.1.4 Radiation Output

The accuracy of absorbed dose in patient irradiated by X-rays or electron in radiotherapy depends on several factors. Linear accelerator (linac) output constancy is an important part of a regular QA program because the absolute dose delivered to the patient is a major factor in determining the outcome of treatment.

The monitor chamber is a device in linear accelerator treatment head used to count the radiation output. The gas filled ionization chambers (also called monitor chambers or simply ion chambers) are type of radiation detector using to measure the radiation dose output in term of monitor unit (MU) and monitor the beam position. The ion chamber system consists of two separate of parallel plate ionization chambers (four

quadrants), which are placed perpendicular to each other for radial and transverse directions to allow inplane and crossplane symmetry monitoring. These two ion chambers are also perpendicular to the radiation beam direction. The monitor chamber system has the feedback mechanism to disable the beam when reaching the MU setting or lack of beam symmetry. When the radiation passes gas in ion chamber, the gas molecules are ionized and then the positive ion and free electron are produced within the ion chamber. The created charge particles can be used to explain the basic electrical signal.

The output of our linear accelerator machine is calibrated in water phantom following the IAEA TRS-398 protocol as annual QA [25]. The each energy of output is adjusted to 1.00 cGy/MU at depth of maximum dose with 100 cm source to surface distance. The sensitivity of monitor ionization chamber of linear accelerator depends on several factors. Therefore, the output constancy check should be performed as a regular QA program. The 5 point monitor chambers device is typically used to roughly check the output of linac machine. The action limits are determined from the AAPM Task Group No.142 at $\pm 3.0\%$ of baseline for daily linear accelerator output checks [4]. In this work, we use this same criterion for weekly linear accelerator output checks.

2.2 Review of related literatures

Control charts have been commonly used in industrial manufacturing for many years and were used for healthcare monitoring and improvement more recently. However, control charts have just been applied in radiotherapy quality assurance as a modern QA tool in the few years.

Tennant R *et al* [26] monitored clinical variables for disease in individual patients using control chart. They searched data from MEDLINE, CINAHL, Embase and five other databases yielded 74 studies that include their criteria. They found that control chart is an effective tool in monitoring the clinical variables in individual patients of hypertension, asthma, renal function post-transplant and diabetes disease. The result showed the same or better performance of control chart compared to the sensitivity and specificity method that used as a standard.

Holli K *et al* [27] estimated the variation of field location in treatment planning for difference types of breast cancer by using reproducibility and repeatability (*R&R*) method with range control chart. The eleven experienced oncologists planned of treatment planning for 3 patients. From the range chart, they found that one of those physicians had large variation in treatment planning that means he needs more training.

Pawlicki T *et al* [10] were the first Physicist group who proposed SPC and control chart for radiotherapy QA. They explored average (*X-bar*) and range (*R*) charts as a modern QA tools in radiotherapy and they compared the benefit to traditional QA approach that used only acceptance criteria. In their work, control charts were applied to daily QA of output and flatness/symmetry as a pilot project. The *X-bar* and *R* charts were used to analyze daily linac output for a 10MV photon beam over 52 days.

Control chart limits were compared to standard deviation limits. They found that control charts were able to separate the systematic errors from random errors, while the general standard deviation cannot identify the same systematic changes in the process.

Breen SL *et al* [28] evaluated intensity modulated radiotherapy (IMRT) dosimetric verification using the concept of SPC. They verified the planning target volume (PTV) and spinal cord doses using ionization chamber on cylindrical phantom. The percentage of dose differences between measurement and 2 versions of PINNACLE treatment planning were plotted on control charts. They found that the upper and lower limits of version 6.2 were larger than the version 7.6 because of the limitations of multileaf collimator (MLC) in old version.

Pawlicki T *et al* [29] investigated the IMRT QA using SPC. They compared 7 institutes IMRT QA doses between measurement and calculation using the average chart to compare the treatment planning dose, measured dose, and the dose calculated from secondary independent software for head and neck and prostate. They found that IMRT QA results varied between the measurement and the independent computer calculations. There were only 11 of 24 processes pass the control criteria. The process ability and process target of prostate cases were better than head and neck cases.

Gerard K *et al* [30] used \bar{X}/MR and EWMA charts to evaluate patient specific IMRT QA for head & neck and prostate plans that were planned in CADPLAN and ECLIPSE treatment planning system. Moreover, they compared the results to clinical specifications using the short term process capability index (C_{pk}) and long term process performance indices (P_p , P_{pk} , and P_{pm}). The results showed that IMRT QA was in control for both head & neck and prostate plans. For three performance indices, it

showed smaller than 1.00 in head & neck and close to 1.00 in prostate. This implies that they need to improve the process centering and process dispersion.

Able CM *et al* [31] used control chart to monitor the reproducibility of steering coil currents by looking the change in beam flatness and symmetry. The \bar{X}/R control chart can be efficiency detected high-alarm with downward trend in transverse angle and low-alarm in transverse position and radial angle before a beam steering failure.

Nordstrom F *et al* [32] applied SPC to investigate the monitor unit verification from multicenter. The result also showed that different centers have different limits with different site of treatment. The process capability index is almost 1.00 in all institutes.

CHAPTER III

Research Objectives

The SPC concept is a new novel tool in radiotherapy QA process. This study extends the research work of Pawlicki [10, 29] to control the output variation in both photon and electron beams by using Shewhart control chart, EWMA chart and PCI. Until now, there are only few publications used control chart in IMRT QA process but there is no one used SPC in VMAT technique. This is the first study that applied SPC method to radiotherapy QA in VMAT and compared with IMRT treatment technique. The PCI concept to set the tolerance limits in radiotherapy field in different types of data distribution is also pioneer investigation in this research.

3.1 Research objectives

1. To set the lower control limit of percent gamma pass in head and neck VMAT QA cases using the X/MR control charts, and to evaluate the performance of VMAT QA from process capability index
2. To determine optimal control charts for linac output constancy monitoring by using X/MR and EWMA control chart, and to assess the efficiency of QA process by capability ratio and acceptability ratio.
3. To set the local tolerance limits via the process capability index method of point dose difference in prostate IMRT QA in case of normal distribution data type, percentage of gamma pass in nasopharyngeal VMAT QA that represents the data

in a left-skewed distribution type, and the homogeneity index of head and neck VMAT plan as a right-skewed distribution data type.

3.2 Scope of dissertation

The SPC, especially control charts and process capability indices, is applied to patient specific IMRT and VMAT QA for head and neck region, and applied to weekly linac output constancy check.

3.3 Keywords

- Statistical process control
- Control chart
- Process capability index
- Output
- Patient-specific IMRT/VMAT QA

CHAPTER IV

RESEARCH METHODOLOGY

4.1 Materials

4.1.1 Linear accelerator

The linear accelerator (linac) is the machine that uses high-frequency electromagnetic waves to accelerate electron in linear accelerator tube to high energies. The photon beams are produced when high energy electrons hit the target. However, the target is moved-out when electron mode is selected. The linacs used in the experiments are Clinac 21EX (**Figure 4.1(a)**), Clinac 23EX, and Clinac iX (**Figure 4.1(b)**). All machines belong to Varian Company (Varian Medical Systems, Inc., Palo Alto, CA, USA).

The Clinac 21EX provides dual photon beam energies of 6 and 10 MV, and 5 electron energies of 6, 9, 12, 16, and 20 MeV electron beams. This machine is equipped with 80 multileaf collimators (MLC), which the width of each collimator is 1 cm at isocenter. This machine can be operated with 3D-CRT and IMRT treatment techniques.

The Clinac 23EX is capable to deliver 6 and 15 MV photon beams, and 4, 6, 9, 12, 16, and 20 MeV electron beams. This machine is equipped with 120 multileaf collimators (MLC), which the width of leaves is 5 mm at the central 20 cm and 1 cm at the 10 cm outer of each side for the maximum field size of 40x40 cm². This machine

can be operated with 3D-CRT, IMRT, and VMAT treatment techniques. The Clinac 23EX machine has a kV x-ray source using for setup field verification.

The Clinac iX or RapidArc machine supplies the dual photon beams of 6 and 10 MV and 6 electron energies the same as Clinac 23EX. The MLC of this machine are also the same type with Clinac 23EX. This machine also has another kV x-ray source and capable to treat the patient in 3D-CRT, IMRT, and VMAT treatment techniques.

The distance from x-ray target to isocenter of all machines is 100 cm. The Varian MLC shown in **Figure 4.2** consists of two banks of tungsten leaves which individually move under computer control. The MLC set is mounted below the conventional collimator in the same direction of X-jaws. The MLC can move in both step-and-shoot and dynamic, but only dynamic movement is used in this study.

The stationary therapy dose rate varied from 100 MU/min to 600 MU/min is available in six-fixed step for 2D, 3D-CRT, Dynamic Arc, and IMRT treatment techniques. The fixed at 400 MU/min dose rate were used in these treatment techniques in our department. For the VMAT technique, the dose rate is varied during beam-on to modulate the beam, which 600 MU/min is the maximum dose rate setting.



(a)

(b)

Figure 4.1. Linear accelerator machines (Varian Medical Systems, Inc., Palo Alto, CA, USA) (a) Clinac 21EX with EPID, and (b) Clinac iX with EPID and OBI (CBCT).



Figure 4.2. Multileaves collimator (Varian Medical Systems, Inc., Palo Alto, CA, USA).

4.1.2 MapCHECK 2D diode array

The MapCHECK, model 1175, (Sun Nuclear Corp., Melbourne, FL, USA) is a 2-dimensional diode array [33]. This device composes of 445 n-type solid state detectors for the area of $22 \times 22 \text{ cm}^2$ as shown in **Figure 4.3**. The inner 221 detectors cover the central part for area of $10 \times 10 \text{ cm}^2$ with 0.707 cm diagonal spacing, while outer 224 detectors have 1.414 cm spacing in diagonal. The active area of each detector is $0.8 \times 0.8 \text{ mm}^2$ and the active detector volume of each detector is 0.000019 cm^3 . The MapCHECK has linear depth of detector junction from top of overlay of 1.35 cm inherent buildup that equivalent to 2.00 g/cm^2 water. The dose limit of MapCHECK is 330 cGy . This device was employed to verify the patient-specific IMRT QA with 0° gantry angle for this study.

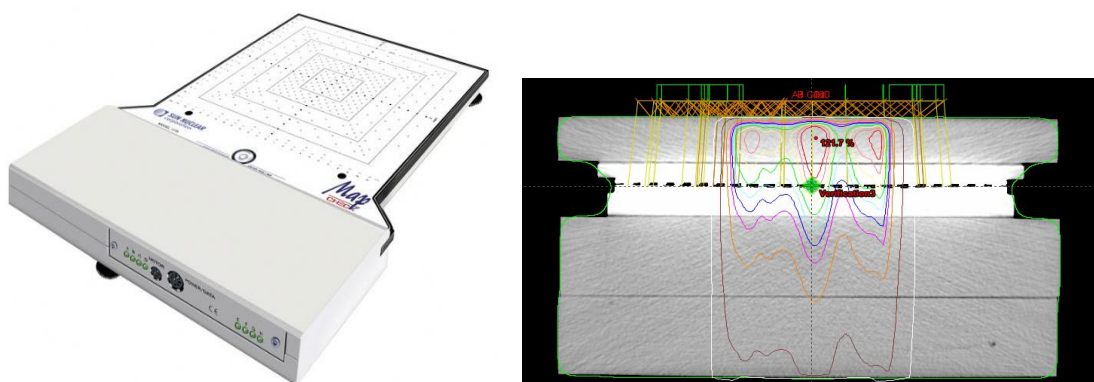


Figure 4.3. MapCHECK 2D diode array (Sun Nuclear Corp., Melbourne, FL, USA).

4.1.3 ArcCHECK 2D diode array

Figure 4.4 shows the ArcCHECK, model 1220, (Sun Nuclear Corp., Melbourne, FL, USA) cylindrical diode array as a 3-dimensional beam dosimetry QA system [34]. This device composes of 1386 n-type solid state detectors with active size of $0.8 \times 0.8 \text{ mm}^2$ and active volume of 0.000019 cm^3 in each detector. The detectors are arranged in helical array (HeliGrid) with 1 cm spacing along cylindrical and 1 cm along circumference for 21.0 cm in detector array length (spiral height). The detectors are embedded in a 2.85 cm linear depth of acrylic buildup that equivalent to 3.28 g/cm^3 density depth. All detectors are perpendicular to the beam for all gantry angles. The ArcCHECK is divided into two sections, which the inner section is 15 cm in diameter of acrylic insertion capable to insert a thimble ionization chamber for central axis dose measurement. If the inner section is removed, the accuracy of inhomogeneity correction of treatment planning can be checked. This device has no limited dose of measurement because each detector sensors are updated the measurement dose in every 50 ms. The ArcCHECK was designed specifically for rotational dosimetry. This device was used to verify the patient-specific VMAT QA with real gantry angle.

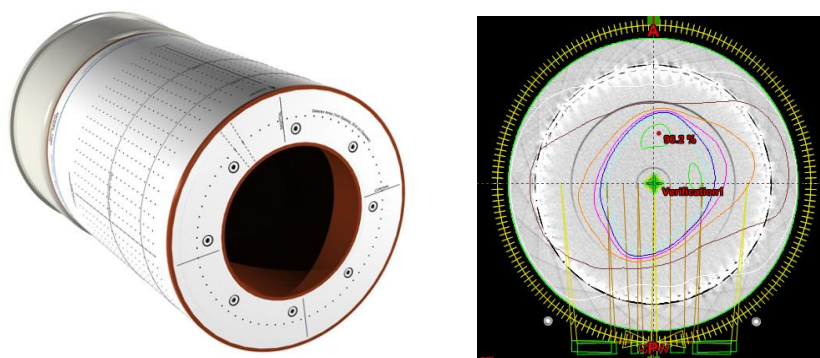


Figure 4.4. ArcCHECK 3D diode array (Sun Nuclear Corp., Melbourne, FL, USA).

4.1.4 Treatment planning system

The treatment planning system in **Figure 4.5** is used in the experiment is Eclipse software version of 7.3.10 and then upgrade to 8.9.17 manufactured by Varian Associates Palo Alto, CA. The former planning versions can plan the photon for 2D, 3D conformal, Dynamic Arc, and IMRT treatment techniques, while the latter version is possible to perform more in VMAT technique. These planning systems are also utilized for electron beam planning and supported for brachytherapy and proton beam therapy planning. The example plan in **Figure 4.5** is IMRT of nasopharyngeal carcinoma with SIB treatment technique.

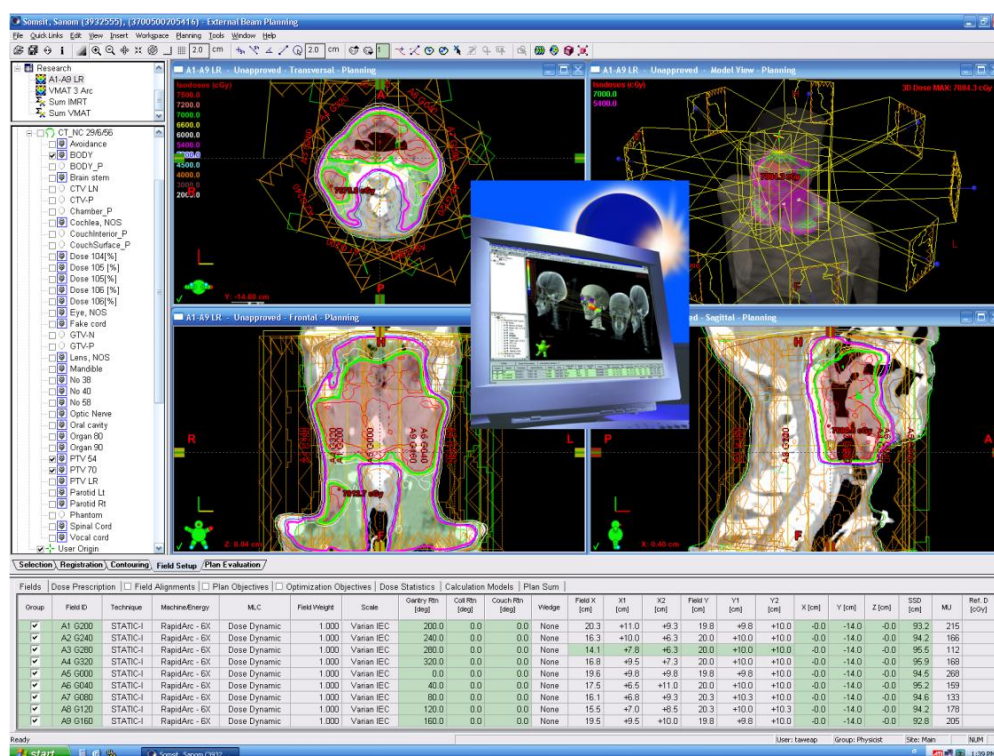


Figure 4.5. Eclipse treatment planning software (Varian Medical Systems, Palo Alto, CA, USA).

4.1.5 IMRT/VMAT QA software

The SNC Patient software (Sun Nuclear Corp., Melbourne, FL, USA) version 6.1 is software for IMRT/VMAT QA evaluation. The IMRT QA verification software is shown in **Figure 4.6**. This software is used to compare two data sets of dose distribution (normally between planning calculation and MapCHECK/ArcCHECK measurement). It can be evaluated the plan in absolute or relative, and gamma or only DTA analysis. It can display in profile comparison across a selected axis. This software has a function of Calc Shift that can determine the misalignment between the planned and measured dose map and automatically corrects for the misalignment.

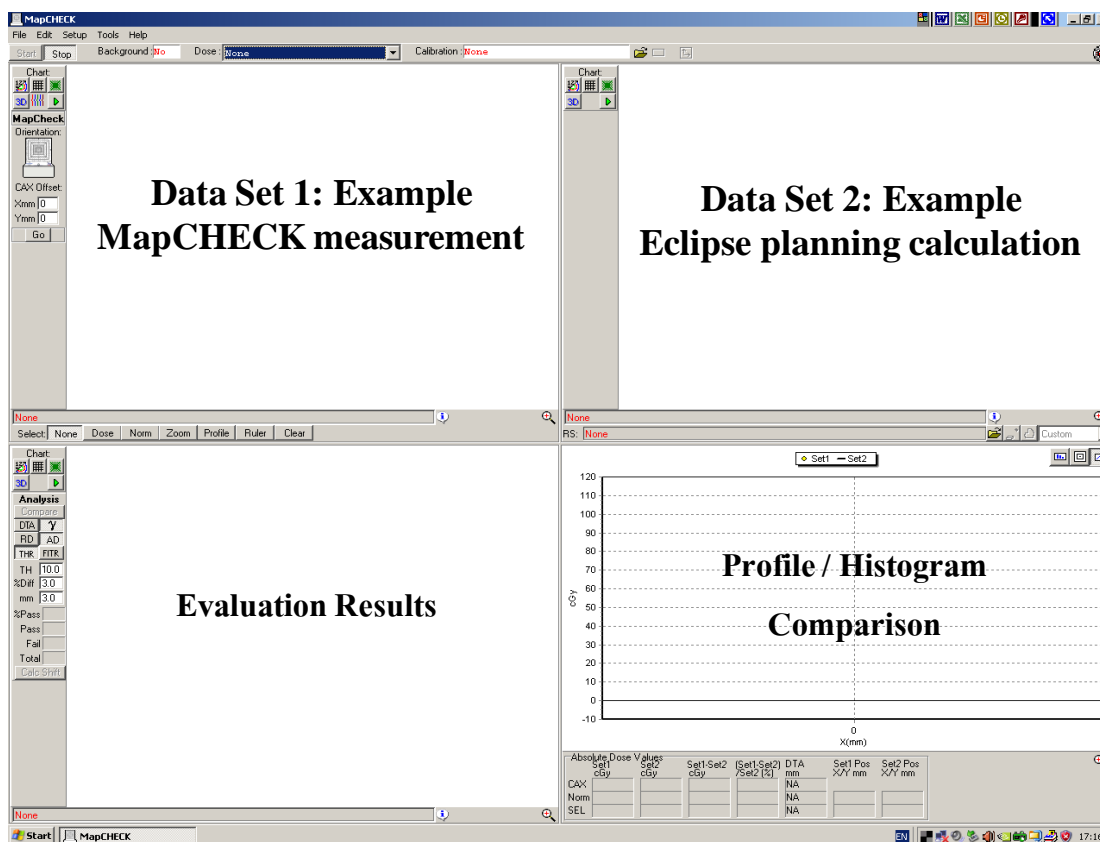


Figure 4.6. SNC Patient software (Sun Nuclear Corp., Melbourne, FL, USA).

4.1.6 Dose constancy check

The Protea System Corporation Radiation Beam Analyser (RBA-3) dose constancy check (GAMMEX rmi, Middleton, WI, USA) is exhibited in **Figure 4.7**. The RBA-3 consists of five parallel plate chambers of 0.2 cm^3 volume, one is placed centrally and four other chambers are located on the radial and lateral planes at 8 cm displaced from center [35]. The chambers are covered with the 14 mm lateral Perspex surrounding the chamber, and are placed below a 4 mm thick Perspex sheet. The central ionization chamber reading was used to represent linac output, while the other four act for flatness/symmetry. The RBA-3 has a thermometer and barometer inside that can correct the chamber signal automatically for temperature and pressure effect.

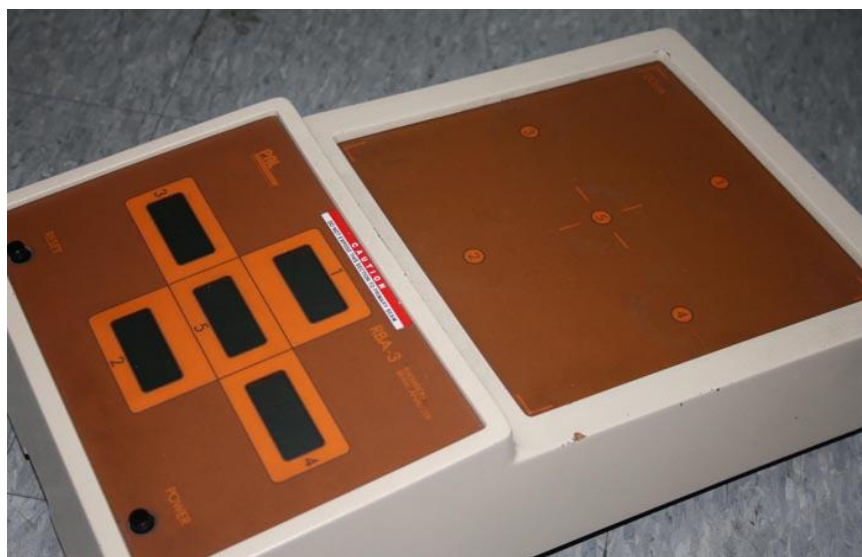


Figure 4.7. The RBA-3 dose constancy check (GAMMEX rmi, Middleton, WI, USA).

4.1.7 Farmer type ionization chamber

The ionization chamber used to verify the prostate IMRT QA plan as a point dose verification is shown in **Figure 4.8**. This waterproof chamber is FC65P farmer type chamber (Scanditronix-Wellhofer Dosimetrie, Schwarzenbruck, Germany) [36]. The chamber consists of POM (PolyOxyMethylene, CH_2O plus additives) for outer electrode with a density of 1.4 g/cm^3 and aluminum for inner electrode with a density of 2.7 g/cm^3 . The nominal active volume of the chamber is 0.65 cm^3 . This chamber has leakage current lesser than $\pm 5 \times 10^{-15} \text{ A}$, and sensitivity of 21 nC/Gy . The reference polarizing voltage is $+300 \text{ V}$. The chamber was calibrated by secondary standard dosimetry laboratory in every 2 years.



Figure 4.8. The FC65-P cylindrical ionization chamber (Scanditronix-Wellhofer Dosimetrie, Schwarzenbruck, Germany).

4.1.8 Dosimeter or Electrometer

The Dose1 dosimeter (Scanditronix-Wellhofer Dosimetrie, Schwarzenbruck, Germany) is a charge measuring device that used couple with ion chamber. The Dose1 shown in **Figure 4.9** is a reference class dosimeter according to IEC 60731 for dosimetry. This device is not only support with ionization chamber, but it is possible to connect with semiconductors and diamond detector as well.



Figure 4.9. The Dose1 dosimeter (Scanditronix-Wellhofer Dosimetrie, Schwarzenbruck, Germany).

4.1.9 Solid water phantom

The solid water phantom or Virtual Water[®] (CIVCO medical solution, IA, USA) selected in our studies is shown in **Figure 4.10**. This phantom is water-equivalent phantom that made from epoxy resin based mixture used to perform routine in radiotherapy QA. The physical properties of this phantom are 1.03 g/cm³ of mass density (water equivalent), and 3.34×10^{23} electron/g of electron density. The size of Virtual Water is 30x30 cm² with various thicknesses ranging from 0.2 to 5.0 cm. The phantoms are designed for detector insertion for 2.0 cm slab. This type of phantom dose not exhibits the charge storage effects.



Figure 4.10. Solid water phantom or Virtual Water[®] (CIVCO medical solution, IA, USA).

4.2 Methods

The experiment is divided into three parts.

4.2.1 SPC analysis for patient-specific IMRT and VMAT QA

In this part, the possible systematic errors and the appropriate control limits of percent gamma pass of patient-specific IMRT and VMAT QA were investigated using \bar{X} control chart because each QA plan has one data of gamma pass. The nasopharyngeal carcinoma plan was selected in this study due to the large number of cases. We used the MapCHECK as a two-dimensional (2D) diode arrays to verify the patient-specific IMRT QA and chose the ArcCHECK for 3D diode arrays to verify the patient-specific VMAT QA. Moreover, the process capability index was used to evaluate the QA performance process.

A. IMRT planning and QA

The relatively large scale of patient-specific IMRT QA of 278 nasopharyngeal carcinoma plans for about two years during year 2007 to 2009 has been considered using a MapCHECK 2D diode array. Almost all of the nasopharyngeal carcinoma IMRT plans performed with 9 equi-angular beam arrangements of coplanar technique with dynamic MLC-based generated by the Eclipse treatment planning system (version 7.3.10) for 6 MV on a Varian Clinac 21EX or 23EX linear accelerator. Most of the plans are sequential techniques of 200 cGy in 25 fractions for PTV-LR and 200 cGy in 10 fractions more for PTV-HR, while some plans are simultaneous integrated boost technique in 33 fractions of 169.7 cGy/fraction for PTV-LR and 212.1 cGy/fraction for PTV-HR. After patient plan was approved by radiation oncologist, physicists created

the pretreatment verification plan on MapCHECK detector based on the composite plan at 0° degree gantry angle. The MapCHECK was employed to verify the IMRT QA. The SSD on MapCHECK surface was set at 98.65 cm and then it was covered by 3 cm of solid water phantom as shown in **Figure 4.11 (a)**. Therefore, the water equivalent depth of total buildup was 5 cm at the source to axis distance of 100 cm. However, before the IMRT plans were verified, the absolute dose of 200 cGy was calibrated at every date of QA session to reduce the effect of output variation. The SNC software was chosen to evaluate the plan comparison between measurement and calculation. The comparison was evaluated in absolute dose with gamma index. The gamma criteria of 3% dose difference between measurement and calculation and 3 mm distance-to-agreement ($\gamma_{3\%/3\text{mm}}$) with 10% threshold was selected to evaluate the plan verification [37]. The threshold dose means the minimum isodose in percentage compared to maximum dose, which above dose level used to analyze. The gamma index was applied from ellipses formula by using the dose and distance difference between measurement and calculation. The point that had gamma value higher than 1.00 was not passed the criteria. The percentage of evaluated measurement points passing the criteria can be called % pass or percent gamma pass or gamma passing rate.

B. VMAT planning and QA

The RapidArc machine has been installed in Thailand at our institute in 2010. The 159 VMAT plans of nasopharyngeal carcinoma during year 2010-2011 were optimized and calculated by Eclipse treatment planning system version of 8.9.17. The

plans were performed with 6 MV photon energy by using 2 full arcs (185° to 175° CW and CCW rotation) and 1 partial arc (185° to 0° CW). In our experience, the 2.5 arc was an optimal number of arc for treating head and neck region. It was not only to improve the dose conformity, the homogeneity to PTV and the dose sparing to normal tissue, but also to stop the gantry angle to be ready for next patient setup. The maximum repetition rate was set to 600 MU/min and the medium thickness of Exact IGRT couch top structure was inserted in the planning to improve the accuracy of dose calculation. The collimator rotation was set at 340° for CW arc and 20° for CCW arc to reduce tongue-and-groove effect. The field size was manual set by the planner before optimization, and the maximum field in X-axis was be limited at 16 cm as the recommended from Varian's specialist to get the best optimization. The VMAT plan was different from IMRT plan that most of the VMAT plans were simultaneous integrated boost (SIB) technique in 33 fractions and some plans are sequential techniques in 25 fractions for PTV-LR and 10 fractions more for PTV-HR. The physicist planned in both IMRT and VMAT techniques as shown in **Figure 2.8**, which the IMRT was planned first and then the dose constraints from IMRT were guided to optimize the VMAT plan. The oncologist would select the VMAT or IMRT plan to treat the patient by considering from DVH and isodose evaluation. If the VMAT plan was selected, the ArcCHECK cylindrical diode array was employed for patient-specific QA. The ArcCHECK and the MapCHECK were from the same company, which both of these devices used the same detector material. After VMAT plan was approved by radiation oncologist, the VMAT plan was recalculated in ArcCHECK phantom based on composite plan for the same patient plan of monitor unit to get the

same MLC movement, same dose rate variation, and same gantry speed modulation. The isocenter was set at the center of ArcCHECK by using laser and cross-hair, the SSD of 86.60 cm would read on ArcCHECK surface as shown in **Figure 4.11 (b)**. All detectors of ArcCHECK were perpendicular to the beam for all angles. This device was also calibrated in absolute dose of 200 cGy at $10 \times 10 \text{ cm}^2$ field size for every QA session date. After dose calibration, the VMAT QA plan could be measured in composite plan with real gantry angle. The measured doses from ArcCHECK were compared to calculated doses from planning in the SNC patient software. The $\gamma_{3\%/3\text{mm}}$ and 10% dose threshold [37] was also used to analyze the VMAT QA results the same as IMRT QA criteria.

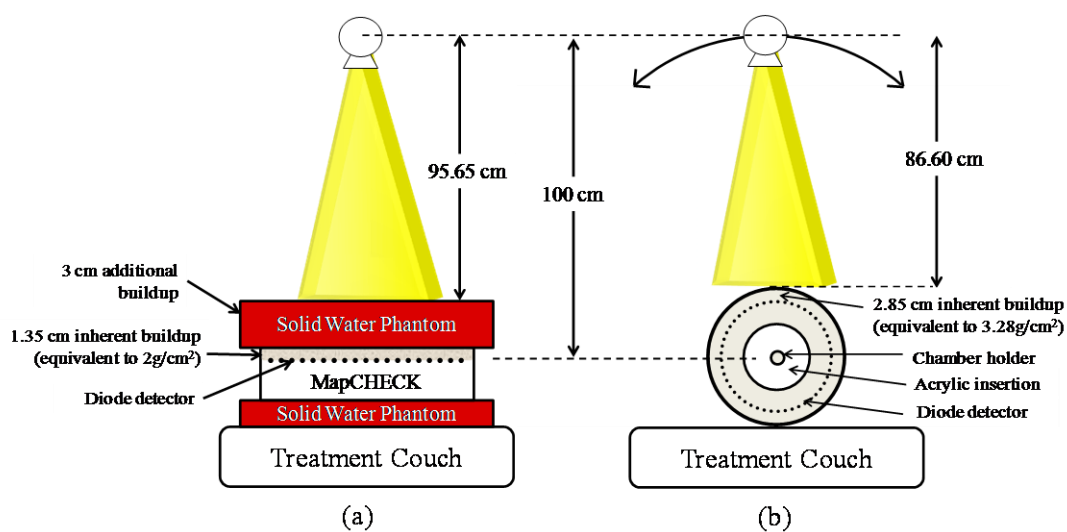


Figure 4.11. The setting up of a) MapCHECK for patient-specific IMRT verification and b) ArcCHECK for patient-specific VMAT verification.

C. Statistical process control analysis

C.1 X control chart analysis

The individual (\bar{X}) control chart was used to monitor and control the variation of process QA. The percentages of gamma pass of IMRT and VMAT QA plans between difference of MapCHECK/ArcCHECK measurement and Eclipse calculation are plotted on \bar{X} control chart with plan number. The first fifty data points were used to calculate the control limits according to Montgomery [12] who recommended that at least 20 data points should be used to calculate control limit. However, if there were any out-of-control data points and we could find the sources of error, those out-of-control points will be removed. Then the CL and control limits were recalculated to get the corrected control limits from random error only.

C.2 Process capability analysis

The process capability indices are the measure of process performance according to the specification or action limits. The C_p and C_{pk} are two commonly process capability indices that have been used in industrial engineering for long time. The C_p parameter explains how much the data dispersion but does not consider the process mean, while the C_{pk} index illustrates how close the process center but does not take the dispersion into account. The new index, C_{pm} , combines those two indices together to adequately describe process performance in one index. The C_{pm} can be calculated from Equation (2.10).

\bar{x} is an average of % gamma pass, while σ is the standard deviation of % gamma pass. USL and LSL are the upper and lower specification limits, respectively. If there are no standard criteria for specification limit, we can replace LSL with LCL . T is the process target value that can be assumed to the average of gamma pass value in condition of no target value. In case of the patient-specific IMRT and VMAT QA, however, one-sided lower specification should be set. It should not have the upper specification limit because the higher passing rate, the better result. The C_{pm} from Equation (2.10) can be modified to C_{pml} as shown in the Equation (4.1).

$$C_{pml} = \frac{\bar{X} - LSL}{1.46\sqrt{\sigma^2 + (\bar{X} - T)^2}} \quad (4.1)$$

The constant 1.46 is recommended by Pillet [38] in case of one-side specification limit case. The higher C_{pml} value you calculated, the more efficiency result you get. In industrial engineering, the process capability index value was accepted at 1.00 for the high quality of QA process.

4.2.2 Linear accelerator output constancy checks using process control techniques

Linear accelerator (linac) output constancy has always been an important part of a regular QA program because the absolute dose delivered to the patient is a major factor in determining the outcome of treatment. In this study, we applied Shewhart-type control charts, *EWMA* charts, and capability indices for 2 years linac constancy QA during 2009 to 2010. These methods give more information than the traditional QA approach which defines the action limit at only value of $\pm 3.0\%$ from based line

[4]. The SPC concept can explain the trend of data that we can monitor and expect the out-of-control limits before the serious problem has occurred. The goal of this experiment part is to determine an optimal implementation of these process control tools as part of a comprehensive QA strategy for linac output constancy verification and monitoring.

The output of a Varian Clinac 21EX linear accelerator machine (Varian Medical Systems, Palo Alto, CA) for 6 and 10 MV photon beams, and 6, 9, 12, 16, and 20 MeV electron beams was calibrated following the IAEA TRS-398 protocol [25]. The routine output verification of all energies was undertaken with a Protea System Corporation Radiation Beam Analyser (RBA-3) dose constancy check (GAMMEX rmi, Middleton, WI) [35]. The data were collected by a physicist or physicist student once per week from January 2009 to August 2010. Fifty monitor units were delivered per reading with a $20 \times 20 \text{ cm}^2$ field size/cone size at 100 cm source-to-surface distance (SSD) with 1.8 cm additional buildup of Perspex for 10 MV photon beams and with 0.8 cm additional buildup for 6 MV photon beams and all electron energy. The RBA-3 was setup using the optical distance indicator and positioning lasers. The action limits for all energies was $\pm 3\%$ of baseline.

Following our institutional protocol, at the end of each year a full calibration of output in solid water phantom was done. If the output for any energy was determined to be outside $\pm 1.0\%$ of 1.0 cGy/MU, then the output for that energy was adjusted until the output equaled 1.0 cGy/MU and new baseline values for the RBA-3 were acquired.

A. Shewhart-type control chart

The UCL and LCL are calculated using the linac output data stream and are different for each energy. When the data fall within the UCL and LCL , then the process is said to be in-control and only common (random) causes affect the process. However, if any data point is out of the control limits, then special (non-random) causes are affecting the process and the source(s) of the special cause need to be identified and removed from the process to bring the process back in-control.

Since each output constancy check can be considered for a subgroup of size one, individual (\bar{X}) charts were used. The average and limits are calculated from Equation (2.1).

R is the range of a subgroup and d_2 is a bias correction constant that depends on the subgroup size n . It is customary to use the constant value $d_2 = 1.128$ for subgroup size $n = 1$. In the case of $n = 1$, the range is taken as the moving range, MR , which is the absolute value of the difference between two consecutive data points ($MR_i = |X_i - X_{i-1}|$). The \bar{X} is calculated as the average over a specified number of data points or subgroups and the average moving range, \overline{MR} , is calculated over the same data points.

We investigated control chart limits as a function of the number of data points to calculate the limits ($n = 1$). The data of first 4, 8, 12, 16, and 20 points, representing to 1, 2, 3, 4, and 5 months, were varied to calculate the control limits in each year for each beam energy. However, if there were any points in the calculation limit that were out-of-control and the source of the error was known, then those out-of-control points were removed and the control limits were recalculated [12]. The effect that the number of data used to calculate the control limits has on the detection of out-of-control

process behavior is investigated by comparing the signal to noise ratio (\bar{x}/σ) over the data used.

B. Exponentially Weighted Moving Average (EWMA) chart

Where the X -chart is used to detect large changes in the process, the *EWMA* chart is used to detect gradual drifts in the process. From the previous data, the output is normally gradual shift. So, the EWMA chart might be more suitable in this case. The *EWMA* equation is given by Equation (2.6). The λ is the weighting or smoothing factor with values $0 < \lambda \leq 1$, which makes the *EWMA* chart sensitive to small process drifts. A large λ value means a greater weight to recent data. The parameter L is the width of the control limit. Difference than X -charts; the *UCL* and *LCL* are calculated with each new data point for *EWMA* charts. However, similar to X -charts, the *EWMA* charts also rely on the assumption that the samples (or individual values) are independent.

We varied the parameters λ and L such that $\lambda = 0.05, L = 2.492$; $\lambda = 0.10, L = 2.703$; and $\lambda = 0.20, L = 2.860$ and the number of points used to estimate μ_0 and σ were varied from 1 to 5 months. Note, μ_0 is the same as the \bar{X} the X -charts. The values of λ and L were chosen as a range of values that are the compromise between efficient detection of process drifts and chart insensitivity to non-normal data.

C. Process capability and acceptability

For routine linear accelerator output checks, the action limits are determined from the AAPM Task Group No.142 at $\pm 3.0\%$ of baseline for daily linear accelerator

output checks [4]. In this work, we use this same criterion for weekly linear accelerator output checks. The process capability indices, C_p and C_{pk} , were chosen for this work because they are industry standards.

To investigate the impact of run length on the interpretation of capability and acceptability, we have used the first run and longest run of in-control points in each year to calculate the C_p and C_{pk} for each energy as well as the number of data points used to calculate the X -chart limits upon which the C_p and C_{pk} are determined. The first run is the number of data points until reaching the first out-of-control point, while the longest run is the number of longest consecutive data points within the control limits.

It is important to note that C_p and C_{pk} in Equations (2.8) and (2.9) are usually point estimates approximated by using the sample standard deviation (or \overline{MR}/d_2) to estimate σ and the sample average to estimate μ . Therefore, C_p and C_{pk} are subject to statistical fluctuations and confidence intervals should be reported. We used the sample standard deviation and average to determine C_p and C_{pk} and results are reported at the 95% confidence interval.

4.2.3 On setting tolerance limits for process monitoring in radiotherapy

This part proposed a systematic approach and set the local tolerance limits based on the process capability index method. This study also explained how to apply process capability index to find the tolerance limits with different types of data distribution in real clinical situations in radiotherapy QA. The three clinical QA conditions depended on distribution type of data are the % point dose difference of 631 prostate IMRT QA plans for normal distribution data type, the % gamma pass of 157

nasopharynx VMAT QA plans for left-skewed data distribution type, and the PTV homogeneity index of 150 head and neck VMAT plans for right-skewed data distribution type.

Quality assurance is a systematic procedure of monitoring and controlling all of the process to ensure that the process of product or service can pass criteria. The criterion is typically referred to tolerance limit or action limit. However, there is no universal definition to define these two limits. Even in radiology field, it has some confusion between these two terms. The SSK [39] has a publication paper on “Quality Control of Nuclear Medicine Equipment” that defined tighter in action limit compared with tolerance limit. The example from this publication is (reference value + 5%) for action level and (reference value + 10%) for tolerance level of sensitivity of planer gamma cameras. However, the radiotherapy field defined totally converse way from above definition. ESTRO group shows the definition of tolerance and action levels in “guidelines for the verification of IMRT” [40], and the college of radiographer, IPEM, and RCR has definition of the tolerance and action limits in “On target: ensuring geometric accuracy in radiotherapy” [41]. They said the action limit is normally set at twice of tolerance limit. The example of radiotherapy limit in tolerance and action limits is $\pm 3\%$ dose difference for tolerance limit and $\pm 5\%$ dose difference for action limit for IMRT point dose verification [40] or Palta [41] defined action limit of gantry, MLC, and table isocenter at 1.0 mm radius and tolerance limit at 0.75 mm radius. In this study, we follow the definition from radiotherapy field. Our opinion is that the action limit should be set by expert for standard criteria, while the appropriated tolerance limit should be set for each institute because of different environment,

different machine, and also different QA device. If the QA result exceeds action limit, it should be no longer performed the equipment or treat patient and physicist should take an action as soon as possible. If the QA result falls between tolerance limit and action limit, the physicist should be investigated until suitable moment. If the QA difference between measured and ideal value is lower than tolerance limit, no need to take any action.

PCI is one of the common tools of SPC used to evaluate the ability of process compared with specification limits and process centering. There was few medical physicist groups applied process capability family to radiotherapy QA [30, 32]. The limitation from PCI should be better than traditional limitation setting because PCI takes the process target into the consideration.

After QA measurement, the physicist needs to evaluate the QA results that pass or not pass. AAPM and ESTRO are symbolized of medical physicist groups of USA and Europe who try to set the criteria for accepted QA measurement result. The different QA measurements or different data types have different methods to design the passing criteria. Most of the QA data types in radiotherapy physics are defined in percentage, distance, or angle different from the ideal value. However, the methods to define these limitations are different. Some of them relied on the machine function or experience of user, while some limitations used the statistical method to set the limitation, for example standard deviation or percentile. This study shows some example and explains how to use the PCI to define the tolerance limits in all three types of data distribution.

A. Taguchi's Process capability index

The new process capability index (C_{pm}), based on Taguchi's loss function replaced with the traditional step function, shown in Equation (2.10) was used in this study. The constant A depends on the quality you need, typically this constant is set to 6 for C_{pm} of 1.0 in case of perfect center at midpoint. However, every case in this study set the C_{pm} at 1.33 for an optimal operating process as shown in **Figure 2.6**. Although the constant A is normally used at 6 for 6 standard deviation units in industrial manufacturing, however, it is quite large value for radiotherapy QA aspect. When we use the Minitab to random normal distribution data with perfect centering for 1000 data, we found that the constant A of 3 is the best fit with using 95th percentile and mean+1.96 SD methods (the standard methods used in some guidelines of ESTRO and AAPM, respectively). Therefore, we select 3 for constant A of normal distribution data. The σ is the process standard deviation, \bar{X} is the process mean and T refers the process target value that is normally the midpoint between UTL and LTL .

The tolerance range, different between UTL and LTL , is calculated from Equation (4.2).

$$Tolerance_Range = [C_{pm} \times A \sqrt{\sigma^2 + (\bar{X} - T)^2}] \quad (4.2)$$

The tolerance limit is tolerance range divide by 2. So, it can be calculated from Equation (4.3).

$$\pm Tolerance = [C_{pm} \times A \sqrt{\sigma^2 + (\bar{X} - T)^2}] / 2 \quad (4.3)$$

The C_{pm} in Equation (2.10) is changed to C_{pml} and C_{pmu} for finding only lower tolerance and upper tolerance limits, respectively. The C_{pml} can be defined by Equation (4.4).

$$C_{pml} = \frac{\bar{X} - LTL}{A\sqrt{\sigma^2 + (\bar{X} - T)^2}} \quad (4.4)$$

From Equation (3.4), the LTL can be found from Equation (4.5).

$$LTL = \bar{X} - [C_{pml} \times A\sqrt{\sigma^2 + (\bar{X} - T)^2}] \quad (4.5)$$

In the same way, the UTL is calculated from Equation (4.6).

$$UTL = \bar{X} + [C_{pmu} \times A\sqrt{\sigma^2 + (\bar{X} - T)^2}] \quad (4.6)$$

For the one-side tolerance limit, the Taguchi's loss function, KX^2 , was used in the calculation. The constant A of one-side tolerance limit is different from two-side tolerance limits. The selection of A depends on desired quality. Based on Pillet [38] solving, constant A was selected at 1.46.

B. Clinical cases

The QA in clinical cases also divided into 3 data distribution types. The type of distribution data was differentiated by skewness value. The skewness is a measure of the asymmetry of the probability distribution that will close to 0, negative, and positive in case of normal, left-skewed, and right-skewed distribution data, respectively. The skewness formula is shown in Equation (4.7).

$$S = \frac{n}{(n-1)(n-2)} \sum_{i=1}^n \left(\frac{X_i - \bar{X}}{SD} \right)^3 \quad (4.7)$$

We show the investigation of point dose differences in prostate IMRT QA as a normal distribution data, percentage of gamma pass in nasopharyngeal VMAT QA as a left-skewed distribution data, and homogeneity index of head and neck of VMAT plan as a right-skewed distribution data.

B1. A process with normal distribution data

The normal distribution (Gaussian distribution) is the most common types of distribution in natural processes. The shape of this distribution resembles a bell. The characteristic of this distribution is the highest frequency group at mean value and symmetrical reduces of frequency as tails to right and left from the mean value. If the data are normal, the mean, mode, and median are the same value. The kurtosis of normal distribution depends on the SD value. The example of normal distribution data is the score of examination. Many students get score around the mean value, while only some students get high or low score. The examples in radiotherapy QA are patient setup errors (target at 0.0 cm), output constancy check (target at 1.0 cGy/MU), or point dose difference between measurement and calculation. The last example is shown in this study.

The cylindrical ionization chamber of 0.6 cm³ volume was used to verify the point dose measurement. The ion chamber was set at 10.0 cm depth in solid water phantom with SAD treatment technique. This pretreatment verification plan was based on composited plan at 0° degree gantry angle. The 631 prostate IMRT plans were used to investigate in this study. The measured doses from ion chamber were compared with

calculated dose from treatment planning by using percentage of dose different to evaluate the QA plan.

B2. A process with left-skewed distribution data

This skewed distribution is not symmetry data on the right and left from the mode of data because it has a natural prevents outcomes on one side. The left or right-skewed distributions are according to the tail direction. The negative or left-skewed distribution shows the long tail on the left side with few low values, the mass of distribution data is concentrated on the right side. The tolerance limit of left-skewed distribution is normally focused to only the *LTL*. The calculated skewness is negative value. The example of left-skewed distribution data is the score of easy examination. Many students get the high score (but not more than full score; target), while only some students get low score. The case of the patient-specific QA that used gamma index evaluation is good clinical example for a process with left-skewed distribution. This distribution needs only one-sided lower tolerance limit. It should not have the upper tolerance limit because the higher passing rate, the better result you will get. The maximum of percent gamma pass is fixed at 100% and this is the target value. This study used the percent gamma pass of VMAT QA for nasopharyngeal cancer plans for the example of this clinical case. At our institution, the ArcCHECK 3D diode array (Sun Nuclear Corporation, Melbourne, FL) was employed as a standard QA device for patient-specific VMAT QA.

The ArcCHECK was set on treatment couch by using laser and cross-hair at 86.60 cm SSD on ArcCHECK surface. After using control chart to separate systematic error from random error, two of systematic error plans were removed from this study.

One error is from very small field that is not good enough to analyze by low resolution detector of ArcCHECK, while another error is due to human error. The remainder 157 VMAT plans of nasopharyngeal carcinoma from one year data were used to evaluate in this example. The measured doses from ArcCHECK were compared to calculated doses from Eclipse planning in ArcCHECK software. The gamma index with the criteria of 3% dose differences and 3 mm distance-to-agreement ($\gamma_{3\%/3\text{mm}}$) with 10% dose threshold on 3D mode analysis was used to analyze the QA results [24].

For the gamma evaluation, AAPM Task Group number 119 [5] defines the action limit of gamma evaluation from IMRT QA by using 1.96σ , while QUASIMODO project [42] from ESTRO group used 95th percentile to specify the limitation of percent gamma evaluation. We applied these calculation methods to define the lower limit of VMAT QA. The percentile can be calculated from Equation (4.8).

$$P = \frac{[cf + (f/2)] \times 100}{N} \quad (4.8)$$

where cf represents cumulative frequency and f is frequency. N is the total number of data.

B3. A process with right-skewed distribution data

In contrast with left-skewed distribution, the positive or right-skew distribution has long tail on the right side with few high values. The large frequency of data is lie on the left side. The specification limit of this distribution is generally concentrated to the *UTL*. The skewness value is more than zero for right-skewed distribution. The

example of right-skewed distribution data is the score of difficult examination. Many students get the low score, while only some students get quite high score. However, this example will get low capability because the target is full score but most of the students get low score. Another example is the gold plate making. The target thickness of gold plate is as thin as possible. In practice, most of the gold plate can make very thin thickness (but thicker than 0 μm thickness), while some of them has large thickness. This case will get high capability with a *USL*. The clinical example of this distribution data is homogeneity index (*HI*) of PTV. There are several formulas for HI. Our institute selects the formula from Gutierrez [43] that can be defined by Equation (4.9).

$$HI = \frac{D_2 - D_{98}}{D_{median}} \quad (4.9)$$

where D_2 and D_{98} considered to be the maximum and minimum doses those represents the PTV doses at 2% and 98% of the target volume, respectively. The D_{median} is median dose of the PTV as shown in **Figure 4.12**. The lesser value of *HI* corresponds to a more homogeneous dose of PTV. The ideal value of *HI* is zero that means very sharp dose-volume histogram of PTV. The *HI* of example case in **Figure 4.12** is 0.10.

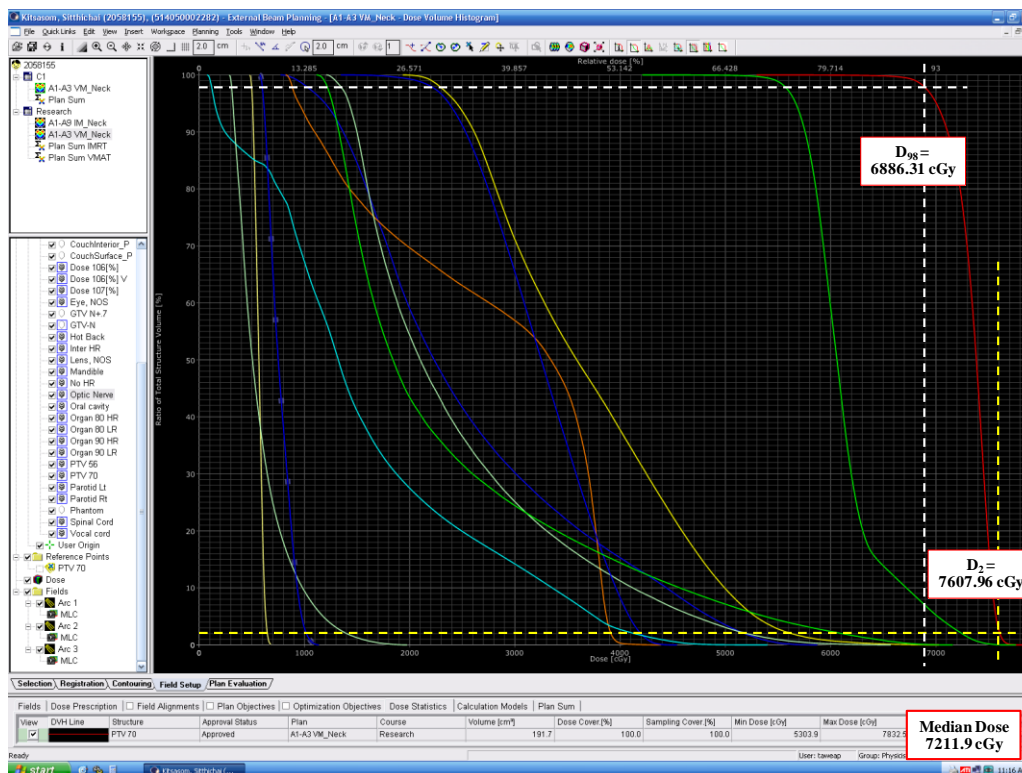


Figure 4.12. The dose volume histogram of PTV with D_2 , D_{98} , and D_{median} .

The right-skew distribution example was evaluated from 150 VMAT plans for head and neck cancer. The Eclipse planning version of 8.9.17 was used in this study. All of our plans were based on 6 MV photon beams with 2 full rotational arcs and 1 half rotational arc. The plans were optimized and calculated by random experienced physicists and were approved by radiation oncology before doing the plan evaluation.

4.3 Anticipated outcomes

1. Demonstrate the use and benefit of control charts to existing quality control procedures in radiotherapy of patient-specific IMRT and VMAT QA, linac output constancy monitoring, and PTV homogeneity index.
2. Determine the optimal control charts for linac output constancy monitoring.
3. Provide the suitable tolerance limits that define high quality for QA process.

CHAPTER V

RESULTS

5.1 SPC analysis for patient-specific IMRT and VMAT QA

The nasopharyngeal IMRT and VMAT QA plans were compared between the MapCHECK/ArcCHECK measurement and Eclipse treatment planning using SNC patient software. The % gamma passes were plotted on X control chart to estimate the suitable tolerance control limits.

Figure 5.1 shows IMRT QA plan comparison in SNC patient software consists of 4 panel screens, which are the dose map of data set 1 (MapCHECK measured), dose map data set 2 (Eclipse calculated), profile across a selected axis comparison panel, and plan evaluation panel with fail points shown, following the clockwise direction starting from right upper panel screen. The evaluation panel shows the out-of-criterion points that red point represents the higher measured dose than calculated dose and vice versa for the blue dot.

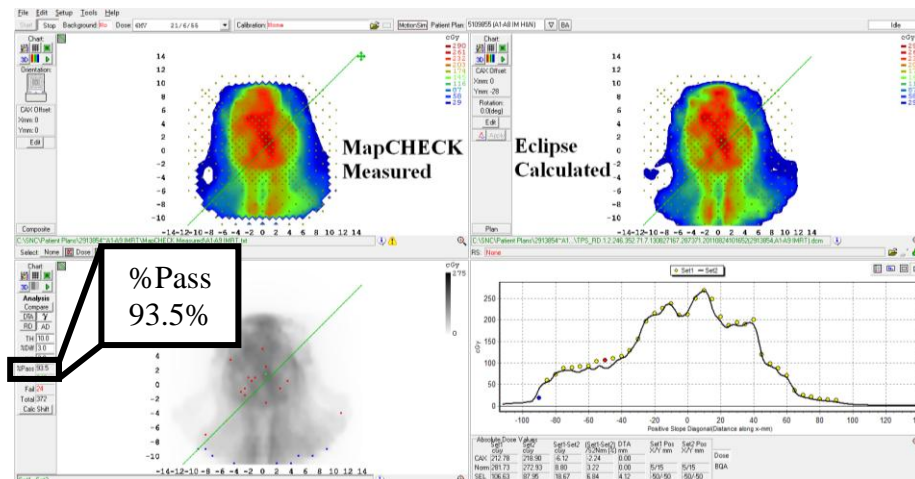


Figure 5.1. The IMRT QA plan comparison of nasopharyngeal carcinoma in SNC patient software measured by MapCHECK and calculated by Eclipse. The dots in left lower panel represent out-of gamma criterion points. The red dot implies the dose from MapCHECK measurement is higher than Eclipse calculation, while the blue dot represents the dose from MapCHECK measurement is lower than Eclipse calculation.

Figure 5.2 presents VMAT QA plan comparison in SNC patient software consists of 4 panel screens, which are the dose map of data set 1 (ArcCHECK measured) in left upper window, dose map data set 2 (Eclipse calculated) in right upper window, plan evaluation panel with fail points shown in central panel, and profile comparison in lower panel.

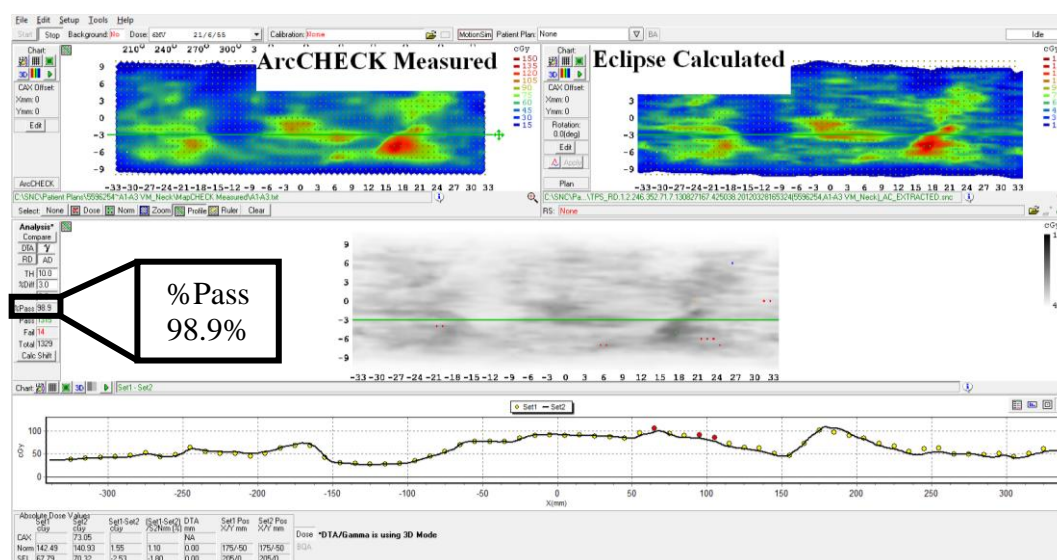


Figure 5.2. The VMAT QA plan comparison of nasopharyngeal carcinoma in SNC patient software measured by ArcCHECK and calculated by Eclipse.

The raw data of % gamma pass in IMRT and VMAT QA for nasopharyngeal carcinoma are shown in appendix I and II, respectively. When using first 50 points of gamma pass value calculated the CL , UCL , and LCL of IMRT plans, a systematic error was identified for point numbers 26, 32, 33 and 34 (from **Figure 5.3 (a)**). Therefore, these four points were removed and then new limitations were recalculated. For the VMAT QA, the data point number 26 was lower than LCL when using first 50 points calculated limits. This data point was not actual systematic error because this case used very small field size with complicated plan and also the ArcCHECK detectors were low resolution. We decided to remove this data point from the control limit calculation.

Table 5.1. The control limits of X chart between using all first 50 plans and out-of-control points removed for nasopharyngeal carcinoma IMRT and VMAT plans.

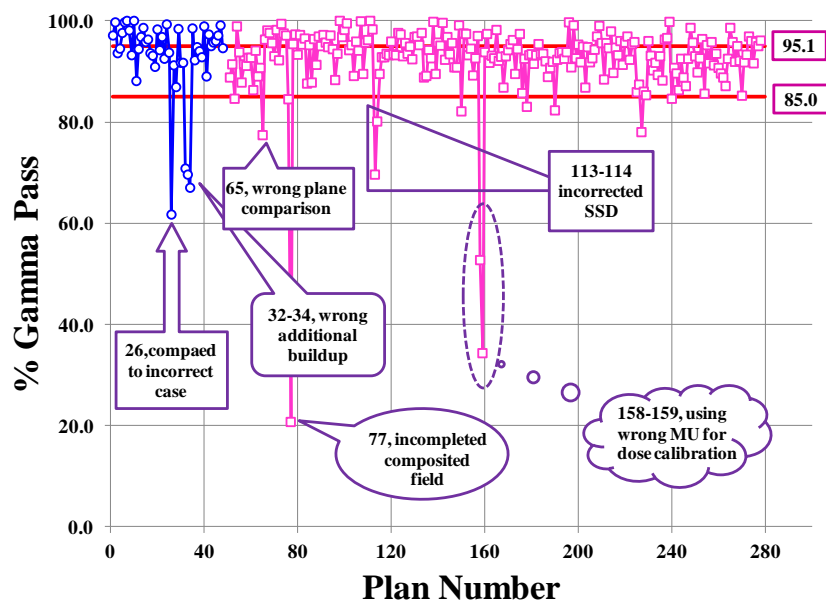
Techniques	control limits calculated from first fifty plans			control limits calculated from first fifty plans with systematic errors removed		
	UCL	CL	LCL	UCL	CL	LCL
IMRT	107.9	92.9	77.8	105.1	95.1	85.0
VMAT	103.5	96.5	89.5	103.1	96.7	90.3

The comparison of limitation results between first fifty point calculation and systematic error removed in X charts of IMRT and VMAT QA is displayed in **Table 5.1**. When those systematic errors were removed, the calculation limits in both IMRT and VMAT QA were narrower. The UCL , CL , and LCL of IMRT QA after systematic

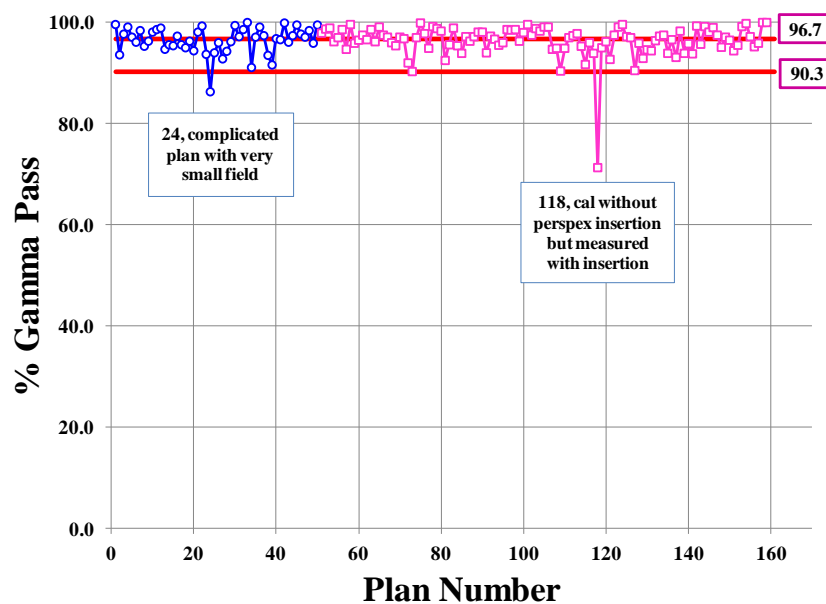
error removed were 105.1%, 95.1%, and 85.0%, respectively. The *UCL*, *CL*, and *LCL* of VMAT QA when systematic error removed were 103.1%, 96.7%, and 90.3%, respectively. Because the maximum value of gamma evaluation was 100%, the *UCL* should not be considered. The *LCL* was only one parameter to define the passing criteria of percent gamma pass.

After the control limits set, the continuing QA data were plotted on the chart. When the QA data point shows out-of-control limits, the chart is react the Physicist to immediately check the errors. **Figure 5.3 (a)** is the *X* control chart of IMRT QA results. The control limits from first 50 points was used to calculate for systematic error removed. It showed less than 3.6% of the points were (10 from 278 points) outside the control limit due to systematic error, however, there were some out-of-control points (6 from 278 points) that close to *LCL* but it was not demonstrated the systematic error. Most of these points were due to complicated plans with large area of high doses and high dose gradients. The remainder 262 plans from 278 plans (>94%) were within the control limit that implied random error of QA process. Almost all of the systematic error points were due to the human error, so the source of errors should be found and removed.

Figure 5.3 (b) is the *X* control chart of VMAT QA results. The control limits was calculated from first 50 points. We found one out-of-control points from complicated plan with small field size. Therefore, we removed that out-of-control point and used only 49 points to calculate the control limit. The chart detected two systematic error and three near-mis error points.



(a)



(b)

Figure 5.3. Individual (\bar{X}) control chart of % gamma pass of patient-specific (a) IMRT QA and (b) VMAT QA for nasopharyngeal carcinoma plans with center line (CL) and lower control limit (LCL). The open circle sign represents the calculated points of the control limits (without systematic error points), while the open square points are the data points of remainder IMRT QA results.

If the IMRT and VMAT QA result were compared, it was significantly higher *CL* and *LCL* of VMAT than IMRT. When we evaluated the plan by using the average and SD of all IMRT and VMAT plan with systematic error removed, it showed the average of % gamma pass at $93.7\% \pm 3.7\%$ for IMRT QA and $96.6\% \pm 2.2\%$ for VMAT QA. This implied that the VMAT technique had more efficiency to treat because the measured dose distribution of VMAT case from diode array was closer to the predicted dose from Eclipse treatment planning than IMRT study. The result was confirmed by process capability index C_{pml} values of 1.60 and 1.99 for IMRT and VMAT, respectively. This C_{pml} values were based on systematic error removed.

5.2 Linear accelerator output constancy checks using process control techniques

The linac output was analyzed for all energies (6 and 10 MV photon beams, and 6, 9, 12, 16, and 20 MeV electron beams) by varying the number of control limits calculation points from 1, 2, 3, 4, and 5 month of data in both \bar{X} and *EWMA* charts to find the appropriate data for calculating the control limit.

A. Shewhart-type control chart

The example of \bar{X} -control charts for output consistency are shown for one photon (6 MV) and one electron (12 MeV) energy in **Figure 5.4**. The first 44 data points belong to year 2009, and the remainders are the output values for year 2010. The raw data appear in appendix III. The two figures on the left use first month of data to calculate control limits, while right two figures use first four months for calculating limits.

In 2009, point number 15 was a systematic error owing to setup error where a junior physicist set a 100 cm SSD on surface of RBA-3 instead of a 100 cm SSD on Perspex phantom. For all charts where point 15 was out-of-control over the time used to calculate the limits, it was removed and new control limits were calculated. This resulted in only an average of 0.1% change in the control chart limit width for all energies. The average output in year 2009 was lower than 1.0 cGy/MU while, most of the output data in year 2010 were higher than 1.0 cGy/MU. Point number 31 also had an error in RBA-3 setup. The outputs were checked the day after (point 32). When using 1 month of data to calculate the limits, point number 43 was out-of-control for almost all energies (but not for 12 MeV as shown in **Figure 5.4**). The measurements were repeated two days later (point 44) and the result still showed out-of-control process behavior (e.g., **Figure 5.4 (a)**). Therefore, it was decided to do the full calibration in water phantom, which confirmed deviations of more than 1.0 cGy/MU for all energies. The outputs were then calibrated to 1.0 cGy/MU starting at point 45 (**Figure 5.4 a-d**). After point 74 in 2010, the process showed consistent the out-of-control behavior. A full calibration was done about one month before the scheduled time (i.e., at point 84).

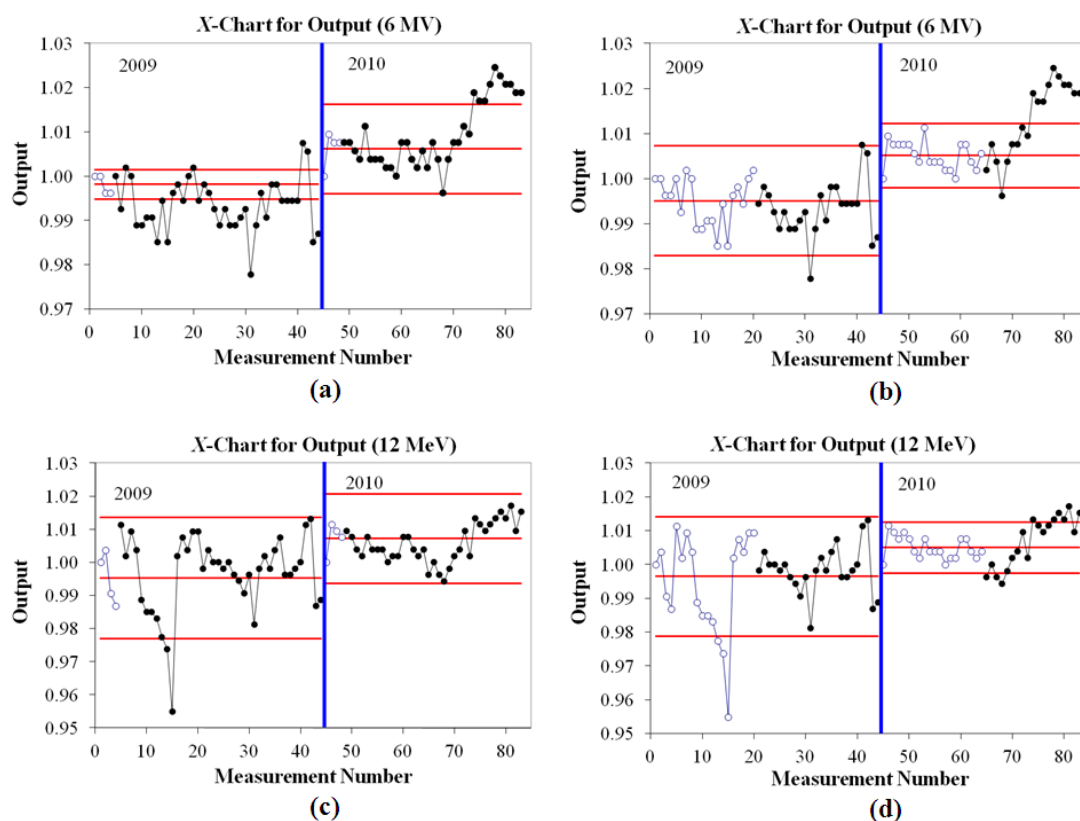


Figure 5.4. The X -control chart for output constancy check for 6 MV (a, b) and 12 MeV (c, d). The output data in first month used to calculate the control limit are displayed in (a) and (c), while (b) and (d) used four months of data. The solid lines are the process behavior limits and the center line. The open circles are the data points used to calculate the control limits.

The number of consecutive in-control data points on X -charts is important because in-control process behavior is the basis for the correct interpretation of process capability and acceptability. **Table 5.2** displays the number of first run points and number of longest run points before an out-of-control point is detected from the X -chart for 6 and 10 MV photon beams, and 6, 9, 12, 16, and 20 MeV electron beams with different number of data points used to calculate the limits.

Table 5.2. The number of first run points before out-of-control limits and number of longest run points on the X -charts for 6 and 10 MV photon beams, and 6, 9, 12, 16, and 20 MeV electron beams. Each month is equal to 4 data points. N is the number of data points in month used to calculate the limits.

N (month)	6X '09		10X '09		6E '09		9E '09		12E '09		16E '09		20E '09	
	1 st	Long	1 st	Long	1 st	Long	1 st	Long	1 st	Long	1 st	Long	1 st	Long
1	5	5	5	7	5	5	8	11	13	29	6	12	5	11
2	12	15	12	15	14	15	14	15	13	29	14	15	14	15
3	12	15	14	15	14	15	14	15	13	29	14	15	14	15
4	30	30	30	30	30	30	14	15	13	29	14	15	14	29
5	30	30	30	30	14	15	12	15	12	29	14	15	14	15

Figure 5.5 shows signal to noise ratio for each energy in 2009 and 2010. The 4 data points used to calculate control limit has large variation in each energy, so the first month of data show large signal to noise ratio variation in each energy. There is a clear trend that by month 2 or 3 (8 to 12 data points), the limits are stable. The process is more stable in 2010 (see **Figure 5.5 (b)**), which shows that the overall value of normalized signal to noise is improved.

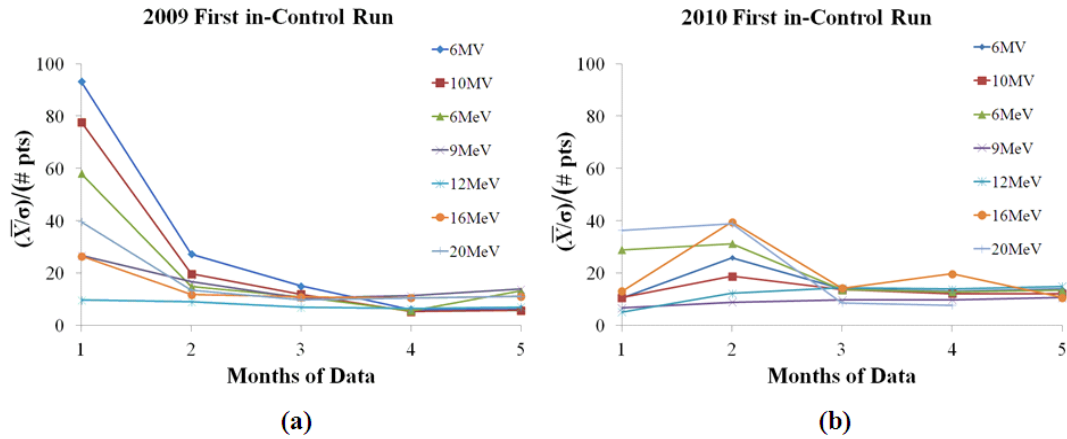


Figure 5.5. Signal to noise ratio (\bar{x}/σ) normalized by the number of in-control data points for the data in (a) 2009 and (b) 2010 for the first run of the data in-control for all energies.

B. Exponentially Weighted Moving Average (*EWMA*) Chart

EWMA charts are useful to detect slow drifts of a process. This chart type was not only varied the number of calculated point from 1 to 5 months for all photon and electron energies, but also varied the 3 set of parameters $\hat{\lambda}$ and L . The *EWMA* chart in **Figure 4.6** displays an example of the output measurements for 6 MV photon beam and 12 MeV electron beam with $\hat{\lambda} = 0.05$, $L = 2.492$, and $\hat{\lambda} = 0.20$, $L = 2.860$ and using 1 month (4 points) in the calculation to estimate μ_0 and σ from the raw data in appendix IV. The greater $\hat{\lambda}$ and L are selected, the larger limit width becomes as shown in **Figure 5.6**. The processes for all energies exhibit out-of-control behavior. For 12 MeV in 2009 and different $\hat{\lambda}$ and L , the *EWMA* charts detect out-of-control process behavior at points 14 or 15. Similar results are found for 6 MV in 2009 at point 9 or 10. For 6 MV in 2009 ($\hat{\lambda}=0.2$), the process wanders in- and out-of-control starting at point 10 and similar behavior is seen for the 12 MeV process.

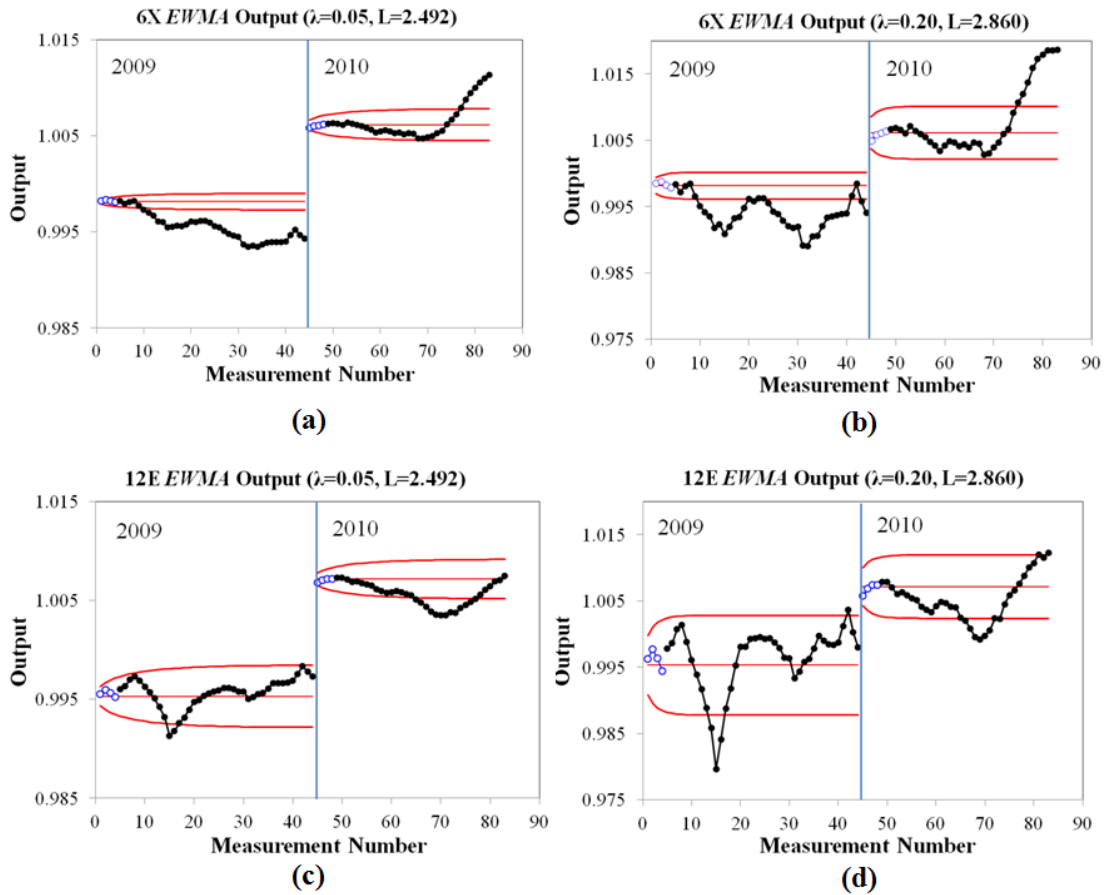


Figure 5.6. The Exponentially Weighted Moving Average (*EWMA*) chart for output constancy check measured by central ionization chamber of RBA-3 device with first month calculated control limits for (a) 6 MV; $\lambda=0.05$, $L=2.492$, (b) 6 MV; $\lambda=0.20$, $L=2.860$, (c) 12 MeV; $\lambda=0.05$, $L=2.492$, and (d) 12 MeV; $\lambda=0.20$, $L=2.860$. The open circles are the points used to calculate control limit and the filled dots are collecting output data. The solid red line represents control limits.

Table 5.3 shows number of first in-control run points from *EWMA* chart of photon beams and some energy of electron beams for 1 to 3 months (4-12 points) in example used to calculate the control limits at different λ and L parameters. For a given number of points used to estimate μ_0 and σ , there was not a significantly

different of number of first run point's in-control for different λ and L parameters (Table 5.3). The processes are stable over a longer period of time in 2010 compared to 2009 before eventually going and remaining out-of-control.

C. Process capability and acceptability

Process capability ratio and process acceptability ratio, C_p and C_{pk} , were used to characterize the process performance of radiation routine output the linac. The data for the year 12 MeV in 2009 and 6 MV, 9 MeV, and 20 MeV in 2010 were non-normal and consequently transformed to normal prior to calculating the process capability and acceptability. Figure 5.7 displays the C_p and C_{pk} values with different time to calculate the control limit for 6 MV (a) and 12 MeV (b) in both first run and longest run for 2009 and 2010.

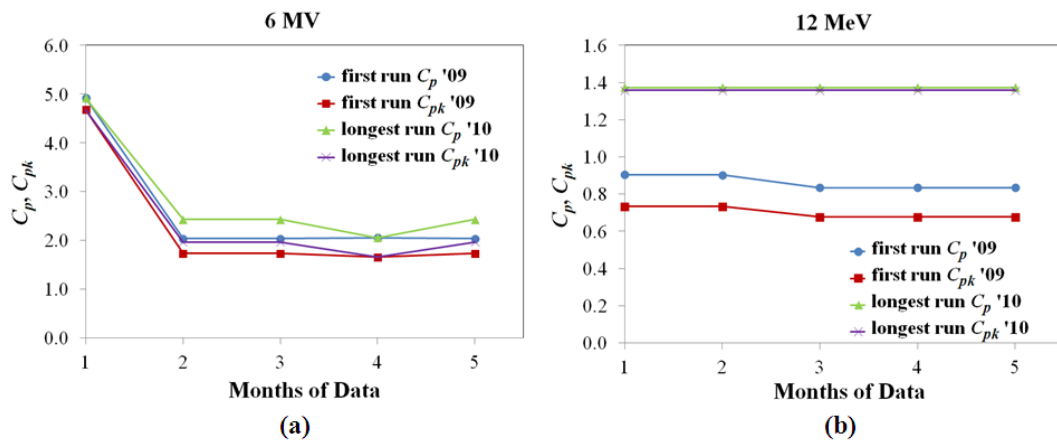


Figure 5.7. The capability ratio (C_p) and acceptability ratio (C_{pk}) of first run and longest run for output constancy check measured by central ionization chamber of RBA-3 device with different time to calculate the control limits for (a) 6 MV photon beams and (b) 12 MeV electron beams.

Table 5.3. The number of measurements before the first out-of-control point is observed on the *EWMA* charts for 6 and 10 MV photon beams, and 6, 12 and 20 MeV electron beams using 1 to 3 months (4-12 data points) to calculate the control limits for different smoothing parameter (λ) and limit width (L). N is the number of data points in month used to calculate the limits.

N (month)	Parameters	6X		10 X		6E		12E		20E	
		'09	'10	'09	'10	'09	'10	'09	'10	'09	'10
1	$\lambda=0.05, L=2.492$	9	33	8	24	9	13	15	21	13	13
	$\lambda=0.10, L=2.703$	10	32	9	24	9	13	15	21	12	12
	$\lambda=0.20, L=2.860$	10	31	9	24	9	13	14	21	12	11
2	$\lambda=0.05, L=2.492$	11	24	12	23	12	13	13	21	12	11
	$\lambda=0.10, L=2.703$	11	24	11	23	12	13	12	21	12	11
	$\lambda=0.20, L=2.860$	10	24	11	24	10	12	12	21	12	11
3	$\lambda=0.05, L=2.492$	31	24	29	24	29	21	15	22	0	17
	$\lambda=0.10, L=2.703$	31	24	16	24	29	21	15	21	15	16
	$\lambda=0.20, L=2.860$	15	24	15	24	15	21	14	21	15	15

Figure 5.8 shows a comparison of calculated C_p and C_{pk} with 95% confidence interval calculated using the first in-control run of data for all photon and electron energies in the years 2009 and 2010. The result showed C_{pk} values were lower than C_p values for all energies, which implied the process has some shift from the target values and is also evident on the \bar{X} -charts. However, both C_p and C_{pk} were higher than 1.0 for most energies except 12 MeV in year 2009 and 20 MeV in 2010.

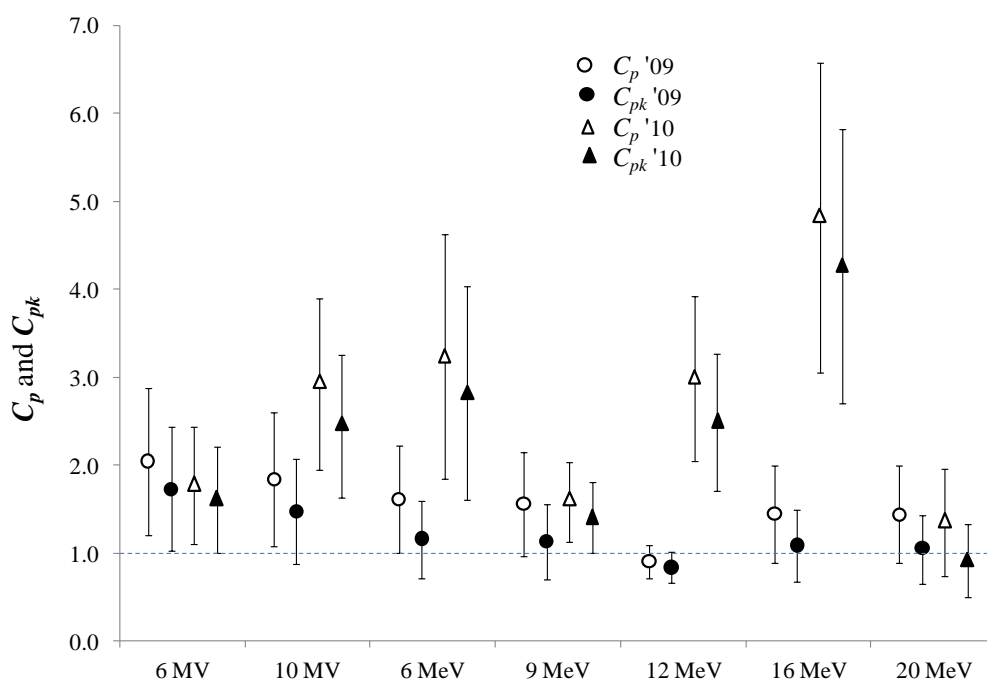


Figure 5.8. The capability ratio (C_p) and acceptability ratio (C_{pk}) with the 95% confidence interval for the process of linac output verification per energy using the first in-control run and 2 months of data to calculate the control limits. Values of C_p and C_{pk} above the dashed horizontal line are considered acceptable (also see

Figure 2.5).

5.3 On setting tolerance limits for process monitoring in radiotherapy

The tolerance limits using process capability index concept are set for 3 types of data distribution. The point dose differences in prostate IMRT QA is a normal distribution data, the percentage of gamma pass in nasopharyngeal VMAT QA is a left-skewed distribution data, and the PTV homogeneity index of head and neck of VMAT plan is a right-skewed distribution data.

A. A process with normal distribution data

The skewness of point dose difference of IMRT QA result is -0.09, which is shown in Table I, while the normal distribution fit of this %error scenario is shown in **Figure 5.9**. The % point dose difference of all data is displayed in appendix V. The **Table 5.4** also shows average and standard deviation of percent point dose different of 0.18% and 1.79%, respectively. Our local calculated tolerance limit of point dose difference for IMRT QA plan from C_{pm} method is $\pm 3.60\%$, while the ESTRO group has been defined the action limits at $\pm 5\%$.

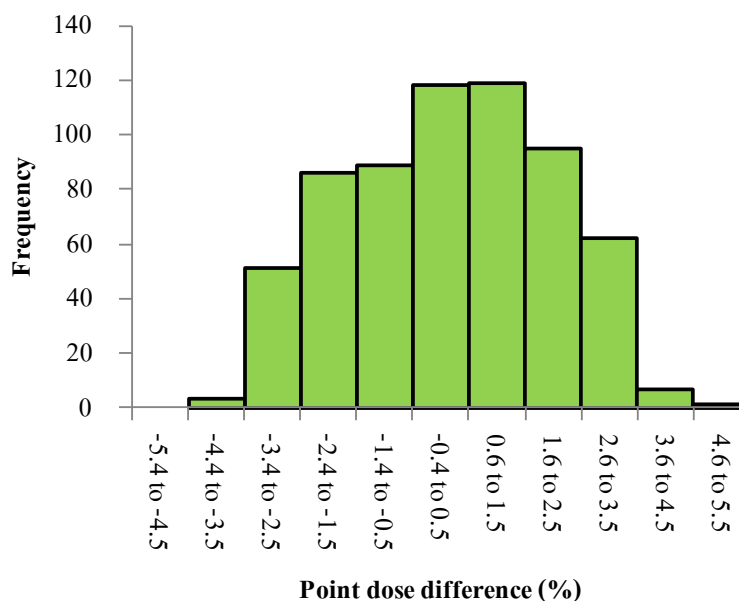


Figure 5.9. Histogram of percent dose difference between measured and calculated of patient-specific prostate IMRT QA as normal distribution data.

Table 5.4. The mean, SD, target, and skewness of clinical application data of % point dose difference for prostate IMRT QA (normal distribution), % gamma pass of VMAT nasopharynx QA (left-skewed distribution), and homogeneity index of head and neck plan (right-skewed distribution).

Parameters	% point dose diff (normal dist.)	% gamma pass (Lt.-skewed dist.)	HI (Rt.-skewed dist.)
Mean	0.18	96.63	0.10
SD	1.79	2.19	0.40
Target	0.00	100.00	0.0
Skewness	-0.09	-0.70	1.39

B. A process with left-skewed distribution data

The skeweness of percent gamma pass of nasopharyngeal carcinoma VMAT QA is -0.70. The raw data are presented in appendix VI. The average of this data is $96.63 \pm 2.19\%$ that is shown in **Table 5.3**. The distribution of percent gamma pass was plotted and shows in **Figure 5.10**.

The results from Table II shows our lower tolerance limit (*LTL*) of percent gamma pass from C_{pm} method at 88.82%, while calculated action limit from AAPM Task Group No. 119 and QUASIMODO project methods shows lower action limit (*LAL*) of 92.33% and 92.66%, respectively.

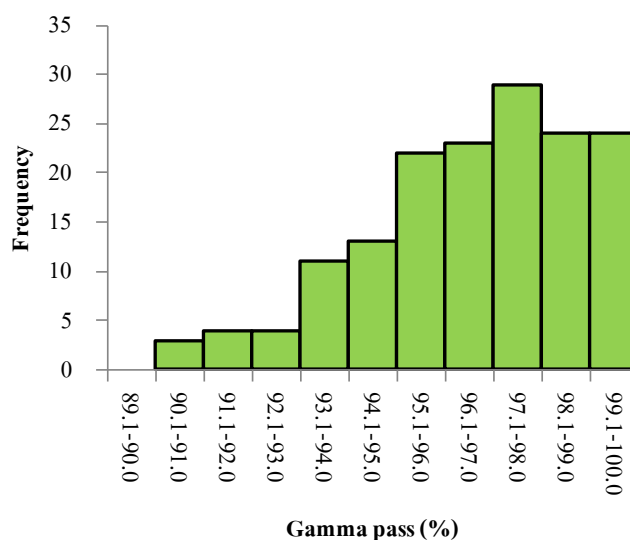


Figure 5.10. Histogram of percent gamma passing rate of patient-specific nasopharyngeal carcinoma VMAT QA as a left-skewed distribution data.

C. A process with right-skewed distribution data

Our average *HI* result of VMAT QA of head and neck cases is 0.1 ± 0.4 as shown in **Table 5.5** and the histogram result is shown in **Figure 5.11**. The data of this

research part is shown in appendix VI. The table also shows the skewness value of 1.39 that confirmed the right-skewed. The upper tolerance limit (*UTL*) of our *HI* is 0.19. There are no standard criteria from expert field from this *HI* formula.

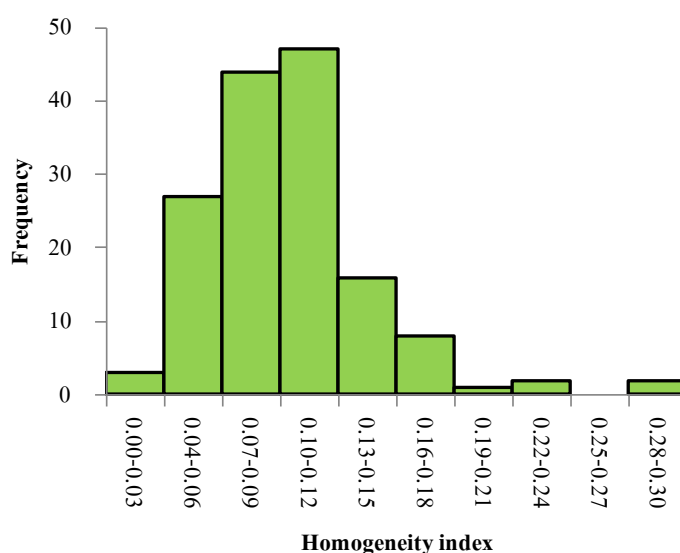


Figure 5.11. Histogram of homogeneity index of VMAT plan of head and neck cancer as a right-skewed distribution.

Table 5.5. The tolerance and action limits for clinical application data of % point dose difference of IMRT QA (normal distribution), % gamma pass of VMAT QA (left-skewed distribution), and homogeneity index (right-skewed distribution).

QA methods	Tolerance	Action
% point dose difference	± 3.60	$\pm 5\%$ (ESTRO)
% gamma pass	88.82%	92.33% (AAPM TG 119)
		92.66% (QUASIMODO)
Homogeneity index	0.19	-

CHAPTER VI

DISCUSSION

The statistical process control has been used in many fields such as industrial, business, and healthcare. The concept of SPC has also been applied to radiotherapy QA for few years to increase the efficiency of QA process, especially in advanced treatment techniques. Control chart is an effective tool to detect the uncontrolled variations by separating that variation from random variation. If the chart indicates that the process is under control then it can be used with confidence for random error data. However, if the chart indicates the out-of-control process, it will assist the QA staff to determine the source of variation. Then, eliminated outside limits point and bring result back into control simultaneously. It is not only the out-of-control points implied the systematic error, but the data pattern from the chart can explain possible systematic error as well. For example, if the data jump or suddenly move, it would be come from human or machine error. If the data are still within control limit but data are significantly separated into two groups. We should look back to the procedure that data were collected from two QA personnel or collected in two separate times like in the morning and evening. In case of the chart shows the trend upward or downward pattern, it might be due to the degrading in sensitivity of machine or detector itself. If the chart displays the cycle pattern, it normally responses to the cycle time of measurement.

There are many types of control chart, which the users need to understand the selection of suitable chart. For the Shewhart control chart, it depends on the data type

and number of subgroups as shown in **Figure 2.3**. There is another special chart, EWMA chart, which is more sensitive to detect the small shift in the process. The Shewhart chart would be used to detect the variation process larger than $\pm 1.5\sigma$, while the EWMA is more sensitive to find out the variation process smaller than $\pm 1.5\sigma$.

The discussion part is separated to 3 parts following the methodology and results parts.

6.1. SPC analysis for patient-specific IMRT and VMAT QA

The IMRT or VMAT techniques are the standard treatment technique in head and neck region at our center. There were some publications compared the clinical evaluation between IMRT and VMAT treatment techniques [20-21]. The VMAT had smoother dose distribution as demonstrated in **Figure 2.7**, and the treatment time was reduced. The dose conformity to PTV and dose to normal tissues for two techniques were comparable. However, there were only few dosimetric studies compared the QA results between IMRT and VMAT. We know that these two treatment techniques are quite complicated plans in head and neck region. The QA results are important and would be one of the indicators to select the technique.

The MapCHECK 2D diode array is a device to verify the patient-specific IMRT QA in our routine, while the ArcCHECK 3D diode array is selected for the VMAT technique. Although gamma evaluation is a standard tool for 2D to 3D planar dose QA, in this work, the control chart and process capability index are the optional tool applied to analyze IMRT and VMAT QA results in the other fashion to assist the decision of the best treatment technique.

From **Figure 5.1 (a)**, the systematic errors presented in the charts are due to;

wrong case comparison (point 26) of same patient first name but different surname, incorrect depth of additional buildup (points 32, 33, 34) from 3 cm to 4 cm, export the wrong slice plane from planning for dose comparison (point 65), incomplete composite field (point 77) using 7 fields combination instead of 9 fields, SSD setup error (point 113-114) from confusing student setup of 2.0 cm depth instead of 1.35 cm PMMA inherent buildup, and incorrect calibration dose (points 158-159) by using the monitor unit of 10 MV to calibrate 6 MV energy. The remainder out-of-control points are due to complicated plans itself. Although the VMAT planning employed more beam parameters to modulate the radiation dose than IMRT technique, the VMAT QA results are surprisingly better than IMRT QA. This is because the VMAT uses more of an aperture optimization that results in a more homogeneous dose distribution, lesser complexity of plan, and lesser high dose gradient with lesser MUs. The consequence is better match of VMAT dose distribution between measurement and planning than IMRT. Therefore, the VMAT *LCL* is higher than IMRT *LCL*. The process capability index, C_{pml} , value of VMAT plan is also higher than IMRT QA. It means that the passing rate of VMAT QA is closer to 100% and lesser variation of result than IMRT QA. Because the C_{pml} is 1.60 for IMRT QA and 1.99 for VMAT QA, this implies the processes of both IMRT and VMAT QA are quite satisfied.

The average of % gamma pass of IMRT QA is significantly lower than VMAT QA ($93.7\% \pm 3.7\%$ for IMRT excluding systematic error result and $96.6\% \pm 2.2\%$ for VMAT). Our gamma passing of IMRT QA from MapCHECK is not too difference with Lucas's study [44] who showed the passing rate of $92.7\% \pm 4.7\%$ for head and neck QA plan. Also, our VMAT QA result is comparable with Scorsetti's [45] who

presented the average gamma agreement index of head and neck VMAT QA of 96.7% \pm 2.1%. One more reason that the passing rate of VMAT QA is higher than IMRT QA in our result is our VMAT plans were calculated in newer version of more accuracy in dose calculation. We find many systematic errors from IMRT QA because of human error but there is a few systematic errors occurred in VMAT nasopharyngeal carcinoma plan. This is due to the ease of using the ArcCHECK, no need of additional buildup, simple setting up, and no plane selection in planning, the chance of systematic error is reduced. We find one systematic error in VMAT QA (point number 118), which is cause by the calculation without acrylic insertion but measuring with insertion. Another one is not actual systematic error (point 24) but it is the effect of low resolution of detector of ArcCHECK. This plan is the boost to only gross tumor, so the field size is very small. The areas that not pass the gamma criteria are only at the edge of field.

The tolerance level of the patient-specific QA for the acceptance process was proposed by many groups, such as Venselaar *et al.*[46], Palta *et al.*[40], Stock *et al.*[47], De Martin *et al.*[48], Basran and Woo [49], Both *et al.*[50], etc, however, those limits are mainly focused to only IMRT QA. For example, Basran & Woo [49], and Both *et al.*[50] recommended the local control limits for IMRT head and neck cases using MapCHECK are 88% and 90% gamma pass, respectively. There are no standard criteria to set the threshold limit of VMAT treatment technique. In this work, the calculated limit can be set at 85.0% gamma passing for nasopharyngeal carcinoma IMRT QA and about 90.0% for VMAT QA when the \bar{X} control chart is used. These *LCLs* are the cut-off limit for separating the systematic error from random variation of

our institute.

6.2. Linear accelerator output constancy checks using process control techniques

The output data should be compared to clinically appropriate action limits to decide whether a specific data point is acceptable for clinical use at that instant time [4]. For process monitoring and improvement, the output data need to be compared to the control limits. Our data indicates that the control limits are typically smaller than the action limits for routine output verification. The goal, then, is to calculate the control limits as soon as reliable limits are achievable. The results in **Figure 5.3** and **Table 5.2** demonstrate that using only four points (1 month) to calculate the control limits results in variable limits are not enough. When the number of data points to calculate the limits is increased, the results become more consistent. This is demonstrated in the normalized signal to noise ratio of **Figure 5.5**. This figure also shows that a more stable process (e.g., data of 2010) leads to better normalized signal to noise ratio (lower values in 2010 compared to 2009). Based on these results, we recommend that between 2-3 months of data (8-12 data points) should be used to calculate the control limits. This is also consistent with the findings of Pawlicki *et al.* for data from IMRT QA point dose measurements compared to planning systems or independent computer verifications [30]. It should be reiterated that each data point is also compared to the clinical action limits for acceptability. There is no risk to the patient in using 1 month (4 data points), for example, to calculate the control limits. However, unstable control limits means that one may miss some process changes if the limits are too wide or experience some false positives if the limits are too narrow. One

can mitigate anomalous interpretation of process behavior by calculating the control limits after 8-12 data points have been acquired.

If out-of-control points occurs over the time used to calculate the control limits and the reason for those out-of-control points is known (and can be addressed), then those out-of-control points can be removed from the control limit calculations. However, based on our results, changing in the control chart limit width is small when removing these points. Therefore, one can omit this procedure when calculating control limits without affecting the usefulness of the charts. It is not necessary to be overly concerned with being overly precise in determination of the control limits. It is more important to use the correct procedure to calculate the limits and that control limits should be calculated for each energy and each machine. Analysis of output constancy using this approach will tell more about the process than using a one-size-fits-all action limit approach to output constancy verification.

Control limits are point binomial estimates and there is an uncertainty associated with the calculation (similar to the process capability and acceptability indices). Determining confidence limits on each control limit is again overly complicating the procedure and will likely make interpretation of the results more complicated. For process capability and acceptability, it makes sense to calculate confidence limits because those ratios are used to make a definitive statement of process performance at a specific instance in time.

Gerard *et al.* presented the use of *EWMA* charts for IMRT QA [31]. It was concluded that *EWMA* charts were an efficient tool to detect the small and slow drifts occurred from MLC error in their IMRT dose delivery process. However, effects of the

smoothing parameter (λ) and the control limit width (L) were not presented. Our investigation of different values of λ and L indicate that when the parameters of λ and L increase, the limit width is also larger. **Figure 5.6** and **Table 5.3** demonstrate that using 4 data points (1 month) results in initial parameters μ_0 , σ , and control limits efficiently detected the slow process changes. We surmise that the slow process change is due to linac output drifts of the linac monitor ion chamber as described by Grattan and Hounsell [51]. As to the choice of λ and L , we recommend that $\lambda = 0.1$ and $L = 2.703$ be used. This choice is based on the fact that the *EWMA* control limits are narrower than the $\pm 3.0\%$ action limits. If the data has a very large drift variability with *EWMA* control limits greater than $\pm 3.0\%$, it might be advisable to use $\lambda = 0.05$ and $L = 2.492$ to quickly identify and correct the reason for the drifting process. Almost all of the out-of-control points on the *X*-chart are due to RBA-3 setup errors from junior physicist or physics student. This indicates that efforts toward more training and/or standardization are warranted. The slow linac drift errors are detected on the *EWMA* charts and eventually on the *X*-chart as well.

Although the process for all energies gradually change after point 74, the process is still within the clinical action limits. Because the *EWMA* chart is not as effective in detecting sudden large shifts in the process and the *X*-chart is relatively slow in responding to gradual shift process shifts, using these two charts together might be the best approach for on-line process monitoring as indicated by Woodall and Mahmoud [52]. However, there is some indication that *EWMA* charts can be used without *X*-charts to detect both large process changes and slow drifts so long as the

EWMA charts are based on the squared deviations from the target [53]. This could be a direction for future investigations.

Gerard *et al.*[31] simultaneously evaluated long-term capability indices (P_p , P_{pk} , and P_{pm}) to the process of IMRT QA. Long-term means these indices are applied over long runs of a process when a process may or may not be in-control so one needs to be careful when interpreting long-term capability indices. Breen *et al.* [29] and Nordström *et al.* [33] applied C_p and C_{pk} to the processes of IMRT QA and independent computer calculation checks, respectively. Both authors make a distinction when calculating C_{pk} for non-normal data by using the non-parametric form of those equations. In this work, we use the parametric versions of the indices but transformed the non-normal distributions. The previous works did not report confidence intervals, which we feel the important to understand the reliability of the process ability and capability. If we consider the 95% confidence interval, then only the 6 MV process is both capable and acceptable in 2009 whereas only the 20 MeV process is neither capable or acceptable in 2010. When using only a few data points (e.g., ≤ 25), the point estimates C_p and C_{pk} are associated with a large variability (**Figure 5.7** and **Table 5.2**). Given these issues, we recommend for waiting to calculate the C_p and C_{pk} until there are at least 25 or more in-control data points. Even though we use the simple standard deviation to calculate C_p and C_{pk} , the data are in-control and normal, the same results are obtained when the estimate \overline{MR}/d_2 is used to calculate C_p and C_{pk} . Ultimately, other process indices such as C_{pc} [54] or C_{pm} [13] that are insensitive to the form of the distribution and simultaneously evaluate the process variability and centering may be better. In any case, process indices should be used for high-level communication or documentation

about process performance, for example, to department administrators, accreditation bodies, or inter-institutional process comparisons.

In this work, linac output constancy is verified on a weekly basis. The frequency of any QA activity depends on factors such as; magnitude of error that could result without checking, time and cost of the QA procedures, and the opportunity costs of not being able to do other work. Due to the possible errors of the linac output deviates significantly from the baseline, output verification should be performed daily. The results of this work are also applicable to daily output checks. In the case of daily output checks, one can use the first 2-3 weeks of data to construct the \bar{X} -chart and the first week of data to build the *EWMA* chart.

Lastly, one should take care not to adjust the process within the noise of the system. If the control charts still show constant output within the control limits (and within clinical action limits), then the full calibration in water phantom would still be performed but output adjustment might not be necessary. Optimal strategies for process adjustments should be considered but this is out of the scope of this work and should be an area for future research.

6.3. On setting tolerance limits for process monitoring in radiotherapy

Every process has variation. One variation can be accepted as a random error, while another variation is systematic error that has significant deviation data from real value. The variation in the process need to control within the limitation, while systematic deviation that out-of limitation should be removed. The limitation aspects can be typically separated into tolerance limits and action limits. However, there is no universal definition of either tolerance or action limits. The appropriate setting of these

limits depends on local environment including the equipment used in QA or type of cases treated. Therefore, QA staff in each institute should set for their own limitation. In this study, the tolerance limits are defined as the minimum and/or maximum appropriate values of a QA data. If they are exceeded these tolerance limits, we should keep an eye on the QA process for potential problems and correct it in suitable time. The action limits are more restrict than tolerance limits. It can be said that the action limits are the cut-off or acceptable criteria. If the QA data are exceeded action limits, physicist mandatory to take action as soon as possible to find the cause of error and get rid of those error value and then bring the process back into random variation. Therefore, each institute should define their own tolerance limit, while the expert group should define international action limit.

PCIs are typically used to calculate the ability of QA process but this study look back. We define the Taguchi's PCI (C_{pm}) value at 1.33 for the good quality first, and then calculate the limits that can get the good process quality. The limitation from C_{pm} method is better tool than traditional method because the C_{pm} method takes the process target into consideration. If the average result of process has shifted from real target value, the calculated tolerance limit is possible to lower than action limit as shown in our clinical case of gamma evaluation of VMAT QA. This is because action limit from traditional method does not consider the target value.

A. In clinical cases, we calculate tolerance limits for the process of patient-specific ion chamber prostate IMRT QA for a normal distribution. This example process gives very good results because the average data of percent point dose difference is 0.18 that close to target value of zero and the standard deviation is not too

high. The calculated tolerance limit from C_{pm} method is lower than action limit from ESTRO definition. Therefore, if the QA result is between $\pm 3.61\%$ to $\pm 5.0\%$, we should beware to the QA process but if the QA result gives more than $\pm 5.0\%$, that plan should not be used to real clinical treatment.

B. The second clinical case that we give an example is calculation of *LTL* for the process of patient-specific nasopharyngeal VMAT QA using ArcCHECK for a left-skewed distribution. The result shows average gamma passing rate and SD of 96.6% and 2.2%, respectively. Our study is comparable with the result of Scorsetti *et al.* [45] that presented the average gamma agreement index of head and neck VMAT QA of $96.7\% \pm 2.1\%$. When we apply the gamma evaluation of IMRT to VMAT QA by using AAPM TG 119 and QUASIMODO protocol, we find that our *LTL* is lower than those *LAT*. This is implied that we need the improvement of the process to shift the process mean closer to target by using flow chart of **Figure 6.1**.

C. The last clinical example for right-skewed distribution is homogeneity index of PTV. Until now, there are no exact limitation criteria of *HI* from this formula. It just says that the smaller value corresponded to more homogeneous irradiation of the target volume. We find only the *HI* limitation of stereotactic that cannot apply to our case. When we follow the method from flow chart of **Figure 6.1**, we can set our local *HI* at 0.19 for head and neck VMAT plan.

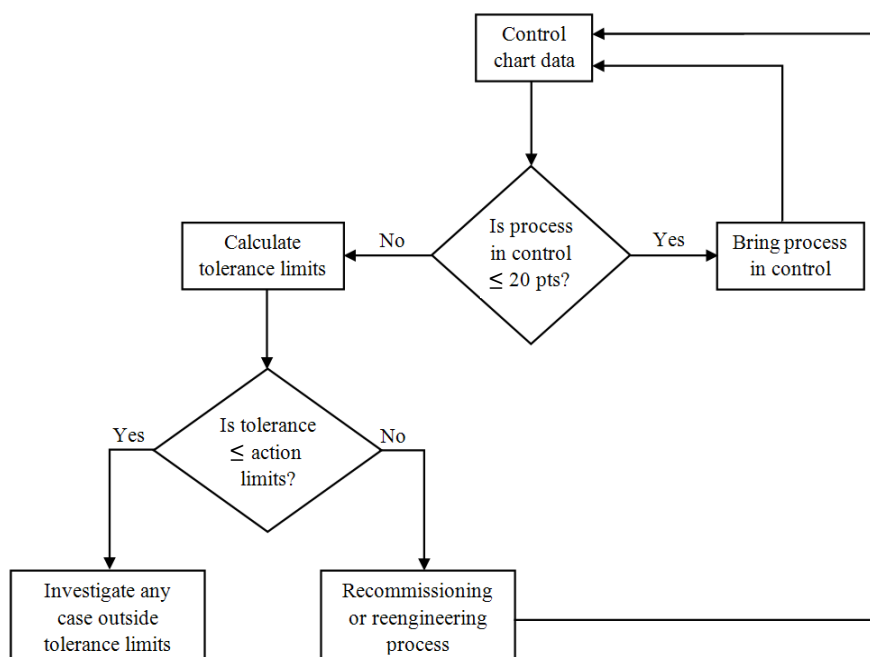


Figure 6.1. The flow chart for using tolerance limit from process capability index method.

One more thing should be take care that is the good process capability should be relied on the random data only. The user should use control chart to monitor and control the variation of the QA process and get-rid-of the out-of-control points due to systematic error before calculate the process capability or find the limitation of QA process. Moreover, the C_{pm} should be calculated for at least 20 in-control data points as shown in **Figure 6.1**.

The control chart can be applied to almost all cases in radiotherapy QA, however, it might not be suitable for the annually QA due to the limited of data number. The process capability index is another SPC tool used to evaluate the efficiency of the whole QA process, which is possible to apply for all process in radiotherapy QA. After we get the data and select the suitable control chart, we should

calculate the control limits with proper number. The question is how many data point represents the proper number. The text book [11] recommends using 20-25 data points to calculate control limits. In my opinion, it should depend on the frequency of data collection and the variation of data. For example, we cannot wait for 20-25 data points (about 2 years) for monthly QA without any control limits. We should trade-off between accuracy and time without control limit. The signal to noise (as in **Figure 5.5**) ought to apply to find the appropriate number of data point for calculating the control limits. If the continuing data fall within control limits for quite stable variation, the lesser frequent of data collection is recommended. The next question is when we should recalculate the control limits. We should recalculate the control limits when we have any changes in the QA process, such as device, method, or even version. Moreover, we could calculate the new control limit in case we need to improve the QA process.

CHAPTER VII

CONCLUSIONS

7.1 Conclusions

The concept of industrial engineering QA using statistical process control; SPC (control chart, *EWMA* charts, and process capability indices) provide a new perspective view on the process of radiotherapy QA as a modern QA tool. The research is one of the first groups who applied SPC method to radiotherapy QA, especially for the advanced radiotherapy techniques in order to minimize error and maximize quality in radiotherapy QA process for patient safety. The SPC tools are utilized in order to evaluate the output constancy check, PTV homogeneity index and patient-specific IMRT/VMAT QA. The concluded of the research works with different SPC tools in each experiment is shown in **Table 7.1**.

Table 7.1 The summary of this research works with selected SPC tools.

SPC analysis for patient-specific IMRT and VMAT QA	Linear accelerator output constancy checks using process control techniques	On setting tolerance limits for process monitoring		
		Normal Distribution	Left-Skewed Distribution	Right-Skewed Distribution
- 278 Naso. IMRT QA - 159 Naso. VMAT QA	2 years output constancy check	% point dose diff of 631 prostate IMRT QA plans	% gamma pass of 157 Naso. VMAT QA plans	PTV HI of 150 H&N VMAT plans
X-chart and C_{pml}	X-chart, EWMA chart, and C_p, C_{pk}	C_{pm}	C_{pml}	C_{pmu}
Aim: LCL	Aim: LCL, UCL and number to cal. limits	Aim: $\pm TL$	Aim: LTL	Aim: UTL

The first research is “SPC analysis for patient-specific IMRT and VMAT QA”

This research establish the appropriate X lower control limit of percent gamma pass from patient-specific IMRT QA verify with MapCHECK 2D arrays and patient-specific VMAT QA verify with ArcCHECK 3D diode arrays for nasopharyngeal carcinoma plan. Moreover, this research also evaluated the process of IMRT and VMAT QA performance using process capability index.

The second part is “Linear accelerator output constancy checks using process control techniques”. This part applied Shewhart-type control charts, *EWMA* charts, and capability indices for linac constancy check for both photon and electron energies. This study also determined an optimal implementation of the process control tools as part of a comprehensive QA strategy for linac output constancy verification and monitoring.

The last one is “On setting tolerance limits for process monitoring in radiotherapy”. This research part proposed a systematic approach to set the local tolerance limits based on the process capability index method in different data types relied on clinical situation in radiotherapy QA. It composed of the point dose difference in prostate IMRT QA as normal distribution data type, gamma pass of nasopharynx VMAT QA as a left-skewed distribution data, and PTV homogeneity index of head and neck VMAT plans as a right-skewed distribution data.

The results from our experiments can be concluded that:

- 1) The lower control limits of percent gamma pass of nasopharyngeal carcinoma plan for IMRT and VMAT in our institute are 85% and 90%, respectively,

2) Both IMRT and VMAT QA process are capable, which is better in VMAT QA (process capability of 1.99) than in IMRT QA (process capability of 1.66). Most of the out-of-limit points from IMRT QA are due to human error, this indicates the efforts toward more training of person and standardization of the techniques,

3) The first 8-12 data points (2-3 months for weekly output constancy check and 2-3 weeks for daily verifications) should be employed to calculate \bar{X} -chart control limits, the first 4-6 data points (1 month for weekly verifications and 1 week for daily verifications) should be used to calculate $EWMA$ control limits using $\lambda = 0.1$ and $L = 2.703$,

4) The tolerance limit, process capability (C_p) and process acceptability (C_{pk}) should be carefully calculated using at 95% confidence interval with the noise data only with at least 20 in-control data points and then monitor the processes against the tolerance and action limits and carefully interrogate any case that is outside the tolerance and action limits prior to treatment, otherwise a “not able to be reported” should be documented,

5) The setting up of our local tolerance limits of percent point dose difference of prostate IMRT QA is $\pm 3.6\%$,

6) The appropriated lower tolerance limits of percent gamma pass of head and neck VMAT QA is 88.82%, however, this process should be improved to get higher value than universal action limit,

7) The upper tolerance limit of HI of VMAT PTV for head and neck cases is 0.19.

This study opens the new perspective about the better QA concept by using the highest level QA tools to other institutions. The results are healthcare benefit to the patients in other cancer centers. These results are just the guideline; they should calculate by themselves because the differences in machine, immobilization, software version, environment, etc have different limits.

7.2 Recommendation for future work

The SPC concept can be used to improve the QA process in many fields. In radiotherapy QA, the SPC is possible to apply in various types of QA method. The **Table 7.2** shows some examples in radiotherapy QA with suitable chart type selection.

Table 7.2 The example of radiotherapy QA with appropriate control chart type.

QA type	Control chart	Condition
ODI reading	X/MR	daily QA
Linac water temperature	X/MR	morning check
Output constancy	X/MR	measured with central detector
Output constancy	\bar{X}/R or \bar{X}/S	measured several times with IC
Flatness/Symmetry	\bar{X}/R	average for 4 points from daily QA
Steering coil current	X/MR	
% Point dose difference	X/MR	
Gamma evaluation for IMRT/VMAT QA	X/MR	
Patient setup error (with mask)	$EWMA$	deviation $< 1.5\sigma$
Short term repeatability measurement	$EWMA$	deviation $< 1.5\sigma$
Conformation number for planning	X/MR	
Source position check in brachytherapy	X/MR	
Time between simulation-to-treatment	X/MR	

For the next step of SPC concept, when the systematic errors are separated from random errors using control charts and process capability index, all of the possible errors will be mapped to cause-and-effect diagram by using 4M+1E concept (Man, Machine, Material, Method, and Environment). Finally, brainstorming the physicist group is necessary to assign the severity, frequency of occurrence, capability of detection of the failure mode and then calculate the RPN. Lastly, the whole process by responsibility of medical physicist with combination of highly quality QA tools in this concept will reduce the possible risk of error and increase the capability of patient safety in radiotherapy QA.

REFERENCES

- [1] International Commission on Radiation Units and Measurements. Determination of absorbed dose in a patient irradiated by beams of x or gamma rays in radiotherapy procedures. ICRU Report No. 24, Washington DC, 1976.
- [2] International Commission on Radiation Units and Measurements. Use of computer in external beam radiotherapy procedure with high energy photons and electrons. ICRU Report No. 42, Washington DC, 1988.
- [3] Mijnheer, B.J. QA in radiotherapy: Physical and technical aspect. Qual Assur Health Care 4 (March 1992): 9-18.
- [4] Klien, E.E., et al. Task Group 142 report: Quality assurance of medical accelerators. Med Phys 36 (September 2009): 4197–4212.
- [5] Ezzell, G.A., et al. IMRT commissioning: Multiple institution planning and dosimetry comparisons, a report from AAPM Task Group 119. Med Phys 36 (November 2009): 5359–5373.
- [6] Fraass, B., et al. American Association of Physicists in Medicine Radiation Therapy Committee Task Group 53: Quality assurance for clinical radiotherapy treatment planning. Med Phys 25 (October 1998): 1773–1829.
- [7] Bissonnette, J.B., et al. Quality assurance for image-guided radiation therapy utilizing CT-based technologies: A report of the AAPM TG-179. Med Phys 39 (April 2012): 1946–1963.

- [8] Ekaette, E, Lee, R.C., Cooke, D.L., Iftody, S., and Craighead, P. Probabilistic fault tree analysis of a radiation treatment system. Risk Analysis 27 (December 2007): 1395-1410.
- [9] Huq, M.S., et al. A method for evaluating quality assurance needs in radiation therapy. Int J Radiat Oncol Biol Phys. 71 (May 2008): S170-S173.
- [10] Pawlicki, T., Whitaker, M., and Boyer, A.L. Statistical process control for radiotherapy quality assurance. Med Phys 32 (September 2005): 2777-2786.
- [11] Wheeler, D.J., and Chambers, D.S. Understanding statistical process control. 2nd ed, Knoxville: SPC Press, 1992.
- [12] Montgomery, D.C. Introduction to statistical quality control. 3rd ed, New York: Wiley, 1996.
- [13] Chan, L.K., Cheng, S.W., and Spiring, F.A. A new measure of process capability: C_{pm} . Journal of Quality Technology 2 (July 1988): 162-175.
- [14] Bucci, M.K., Bevan, A., and Roach, M. Advances in Radiation Therapy: Conventional to 3D, to IMRT, to 4D, and Beyond. CA Cancer J Clin 55 (March 2005): 117–134.
- [15] Mundt, A.J., and Roeske, J.C. Intensity modulated radiation therapy: a clinical perspective. Ontario: BC Decker, 2005.
- [16] Alvarez-Moret, J., Pohl, F., Koelbl, O., and Dobler, B. Evaluation of volumetric modulated are therapy (VMAT) with Oncentra MasterPlan® for the treatment of head and neck cancer. Radiat Oncol 5 (November 2010): 110.
- [17] Chao, K.S., et al. Intensity-modulated radiation therapy reduces late salivary toxicity without compro-mising tumor control in patients with oropharyngeal

- carcinoma: a comparison with conventional techniques. Radiother Oncol. 61 (December 2001): 275-280.
- [18] Dirix, P., Nuyts, S., and Van den Bogaert, W. Radiation-induced xerostomia in patients with head and neck cancer: a literature review. Cancer 107 (December 2006): 2525-2534.
- [19] Fang, F.M., et al. Intensity-modulated or conformal radiotherapy improves the quality of life of patients with nasopharyngeal carcinoma: comparison of four radiotherapy techniques. Cancer 109 (January 2007): 313-321.
- [20] Vanetti, E., et al. Volumetric modulated arc radiotherapy for carcinomas of the oro-pharynx, hypo-pharynx and larynx: a treatment planning comparison with fixed field IMRT. Radiother Oncol 92 (January 2009): 111-117.
- [21] Oliver, M., Ansbacher, W., and Beckham, W.A. Comparing planning time, delivery time and plan quality for IMRT, RapidArc and Tomotherapy. J Appl Clin Med Phys 10 (October 2009): 117-131.
- [22] Ezzel, G.A., et al. Guidance document on delivery, treatment planning, and clinical implementation of IMRT: report of the IMRT Subcommittee of the AAPM Radiation Therapy Committee. Med Phys 30 (August 2003): 2089-2115.
- [23] Van Dyk, J., Barnett, R.B., Cygler, J.E., and Shragge, P.C. Commissioning and quality assurance of treatment planning computers. Int J Radiat Oncol Biol Phys 26 (May 1993): 261-273.
- [24] Low, D.A., Harms, W.B., Mutic, S., and Purdy, J.A. A technique for the quantitative evaluation of dose distributions. Med Phys 25 (May 1998): 656-

661.

- [25] Andreo, P., et al. Absorbed dose determination in external beam radiotherapy: An International Code of Practice for Dosimetry Based on Standards of Absorbed Dose to Water, IAEA Technical Report Series No. 398, Vienna: IAEA. 2000.
- [26] Tennant, R., Mohammed, M.A., Coleman, J.J., and Martin, U. Monitoring patients using control charts: a systematic review. International Journal for Quality in Health Care 19 (November 2007): 187–194.
- [27] Holli, K., Laippala, P., Ojala, A., and Pitkanen, M. Quality control in health care: an experiment in radiotherapy planning for breast cancer patients after mastectomy. Int J Radiat Oncol Biol Phys 44 (July 1999): 827-833.
- [28] Breen, S.L., Moseley, D.J., Zhang, B., and Sharpe, M.B. Statistical process control for IMRT dosimetric verification. Med Phys 35 (October 2008): 4417-4425.
- [29] Pawlicki, T., et al. Moving from IMRT QA measurements toward independent computer calculations using control charts. Radiother Oncol 89 (December 2009): 330-337.
- [30] Gerard, K., Grandhay, J.P., Marchesi, V., Kafrouni, H., Husson, F., and Aletti, P. A comprehensive analysis of the IMRT dose delivery process using statistical process control (SPC). Med Phys 36 (April 2009): 1275-1285.
- [31] Able, C.M., Hampton, C.J., Baydush, A.H., and Munley, M.T. Initial investigation using statistical process control for quality control of accelerator beam steering. Radiat Oncol. 6 (December 2011): 180-188.

- [32] Nordström, F., Wetterstedt, S., Johnsson, S., Ceberg, C., and Back, S.A.J. Control chart analysis of data from a multicenter monitor unit verification study. Radiother Oncol 102 (January 2012): 364-370.
- [33] MapCHECKTM user's guide, Model 1175. 2-dimensional array for quality assurance testing of IMRT and compensator fields. Sun Nuclear Corporation.
- [34] ArcCHECKTM user's guide. The ultimate 4D QA solution. Sun Nuclear Corporation.
- [35] Mill, J.A., and Smith, J.M. Technical note: Assessment of a radiotherapy beam analyzer. The British Journal of Radiology 64 (June 1991): 547-548.
- [36] FC65P ionization chamber user's guide. Scanditronix Wellhofer, 2001.
- [37] Nelms, B.E., and Simon, J.A. A survey on planar IMRT QA analysis. J Appl Clin Med Phys 8 (March 2007): 1-15.
- [38] Pillet, M., Rochon, S., and Duclos, E. SPC-Generalization of capability index C_{pm} : case of unilateral tolerances. Quality Engineering 10 (September 1997): 171-176.
- [39] Quality Control of Nuclear Medicine Equipment – Definition of Action Levels and Tolerance Limits. Recommendation of the Commission on Radiological Protection. (2010): 1-11.
- [40] Alber, M., et al. ESTRO booklet no.9; Guidelines for the verification of IMRT. ESTRO (2008).
- [41] Palta, J.R., Kim, S., Li, J.G., and Liu, C. Tolerance limits and action levels for planning and delivery of IMRT. In: Intensity-Modulated Radiation Therapy:

- The State Of The Art. American Association of Physicists in Medicine Medical Physics. Monograph No. 29, (2003): 593–612.
- [42] Gillis, S., Wagter, C.D., Bohsung, J., Perrin, B., Williams, P., and Mijnheer, B.J. An inter-centre quality assurance network for IMRT verification: Results of the ESTRO QUASIMODO project. Radiother Oncol 76 (September 2005): 340-353.
- [43] Gutierrez, A.N., et al. Whole brain radiotherapy with hippocampal avoidance and simultaneously integrated brain metastases boost: a planning study. Int J Radiat Oncol Biol Phys 69 (October 2007): 589-597.
- [44] Lucas, E., Fan, J., and Franklin, R. IMRT QA comparison using MapCheck and portal dosimetry. AAPM Midwest chapter spring meeting. April 19, 2008.
- [45] Scorsetti, M., et al. Early clinical experience with volumetric modulated arc therapy in head and neck cancer patients. Radia Oncol 5 (October 2010): 93-103.
- [46] Venselaar, J., Welleweerd, H., and Mijnheer, B. Tolerances for the accuracy of photon beam dose calculations of treatment planning systems. Radiother Oncol 60 (April 2001): 191-201.
- [47] Stock, M., Kroupa, B., and Georg, D. Interpretation and evaluation of the gamma index and the gamma index angle for the verification of IMRT hybrid plans. Phys Med Biol 50 (February 2005): 399-411.
- [48] De Martin, E., et al. Agreement criteria between expected and measured field fluences in IMRT of head and neck cancer: the importance and use of the γ histograms statistical analysis. Radiother Oncol 85 (November 2007): 399-406.

- [49] Basron, P.S., and Woo, M.K. An analysis of tolerance levels in IMRT quality assurance procedures. Med Phys 35 (June 2008): 2300-2307.
- [50] Both, S., et al. A study to establish reasonable action limits for patient-specific quality assurance in intensity-modulated radiation therapy. J Appl Clin Med Phys 8 (February 2007): 1-8.
- [51] Grattan, M.W.D., and Hounsell, A.R. Analysis of output trends from Varian 2100C/D and 600C/D accelerators. Phys Med Biol 56 (November 2010): N11–N19.
- [52] Woodall, W.H., and Mahmoud, A.M. The inertial properties of quality control charts. Technometrics 47 (November 2005): 425-436.
- [53] Reynolds, M.R., and Stoumbos, Z.G. Should exponentially weighted moving average and cumulative sum charts be used with Shewhart limits? Technometrics 47 (November 2005): 409-424.
- [54] Luceño, A. A process capability ratio with reliable confidence intervals. Commun. Statis. – Simula 25 (January 1996): 235-246.

APPENDIX I

The data of % gamma pass in IMRT QA for nasopharyngeal carcinoma.

No	Gamma (3%, 3mm)	No	Gamma (3%, 3mm)	No	Gamma (3%, 3mm)	No	Gamma (3%, 3mm)
1	97.1	26	61.7	51	88.8	76	84.5
2	99.7	27	91.2	52	91.4	77	20.7
3	93.6	28	86.9	53	84.6	78	95.4
4	94.5	29	98.4	54	98.9	79	97.3
5	97.6	30	91.7	55	93.8	80	93.3
6	99.7	31	91.7	56	87.8	81	97.2
7	100	32	70.8	57	91.4	82	95.3
8	98.1	33	69.6	58	91.1	83	96.5
9	93.2	34	67	59	92.7	84	87.6
10	100	35	98.5	60	92.7	85	95.2
11	88.1	36	92.2	61	86.3	86	87.8
12	94.4	37	94.8	62	94.1	87	96.4
13	96.8	38	94	63	89	88	91.3
14	98.6	39	92.8	64	90.7	89	96.9
15	95.8	40	98.9	65	77.4	90	95
16	96.3	41	89	66	96.3	91	97.2
17	93.6	42	97.3	67	98.1	92	95.7
18	93.1	43	95	68	97.6	93	94.8
19	90.9	44	95.7	69	95.6	94	97.1
20	98.3	45	96	70	93	95	94.4
21	94.2	46	97.1	71	98.2	96	88.3
22	96.8	47	99.1	72	92.2	97	93.5
23	92.5	48	94.6	73	99.4	98	100
24	99.3	49	91.8	74	97.5	99	96.8
25	93.7	50	91	75	97.1	100	98.2

The data of % gamma pass in IMRT QA for nasopharyngeal carcinoma (Cont.).

No	Gamma (3%, 3mm)	No	Gamma (3%, 3mm)	No	Gamma (3%, 3mm)	No	Gamma (3%, 3mm)
101	99.5	126	95.6	151	97.5	176	85.7
102	94.2	127	93.5	152	97.4	177	92.5
103	95.2	128	94.9	153	93.2	178	83
104	89.1	129	92.4	154	94.5	179	93.2
105	95.9	130	96.8	155	89.2	180	93.4
106	94.1	131	96.9	156	92.6	181	91.5
107	99.9	132	95.2	157	97	182	93.2
108	89.5	133	97.6	158	52.7	183	95.4
109	95.7	134	88.8	159	34.3	184	93.4
110	96.2	135	89.1	160	93.8	185	93.5
111	100	136	94.2	161	97.4	186	92
112	98.3	137	92.6	162	91.7	187	88.9
113	69.6	138	99.8	163	93.1	188	90.7
114	80.1	139	89.5	164	92.6	189	91.9
115	89.5	140	95.7	165	98.2	190	82.3
116	92.8	141	95.1	166	92.1	191	92.3
117	92.8	142	99.6	167	92.9	192	93.6
118	93.5	143	92.3	168	86.8	193	93.8
119	93.2	144	96.8	169	93	194	92.5
120	95.9	145	93.4	170	94.2	195	93.8
121	93.4	146	95.6	171	95.4	196	99.7
122	93.2	147	90.8	172	96.2	197	90.8
123	97.6	148	90.8	173	89.5	198	99.1
124	97.3	149	99.1	174	94.4	199	92.6
125	93	150	82.1	175	97.4	200	95.3

The data of % gamma pass in IMRT QA for nasopharyngeal carcinoma (Cont.).

No	Gamma (3%, 3mm)	No	Gamma (3%, 3mm)	No	Gamma (3%, 3mm)	No	Gamma (3%, 3mm)
201	91.8	226	87.4	251	89.8	276	95.8
202	94.9	227	78	252	92.6	277	95
203	86.8	228	86	253	96.4	278	96.1
204	94.8	229	85.3	254	85.6		
205	91.8	230	96	255	95.2		
206	92.6	231	93.1	256	91.6		
207	94.3	232	90.2	257	95.8		
208	96.9	233	91.7	258	91.2		
209	99	234	89.3	259	93.5		
210	95.6	235	93	260	90.7		
211	88.4	236	88.2	261	89.6		
212	95.6	237	96.3	262	88.8		
213	94.6	238	96.6	263	87.1		
214	97.9	239	99.8	264	92.5		
215	89.7	240	84.6	265	98.6		
216	94.7	241	90.7	266	95.8		
217	93.2	242	89.6	267	91.9		
218	96	243	86.3	268	95		
219	91.3	244	92.5	269	92.1		
220	95.7	245	88.8	270	85.2		
221	96.9	246	87.1	271	91.8		
222	92.3	247	92.5	272	93.3		
223	95.4	248	98.6	273	96.9		
224	95.8	249	95.7	274	96		
225	85.9	250	93	275	91.6		

APPENDIX II

The data of % gamma pass in VMAT QA for nasopharyngeal carcinoma.

No	Gamma (3%, 3mm)	No	Gamma (3%, 3mm)	No	Gamma (3%, 3mm)	No	Gamma (3%, 3mm)
1	99.6	26	96.0	51	97.9	76	97.8
2	93.6	27	92.8	52	98.7	77	94.9
3	97.7	28	94.3	53	98.9	78	99.2
4	99.1	29	96.2	54	96.2	79	98.8
5	97.1	30	99.4	55	97.0	80	98.3
6	96.1	31	97.2	56	98.6	81	92.5
7	98.4	32	98.6	57	94.7	82	95.6
8	95.3	33	100.0	58	99.6	83	98.9
9	96.3	34	91.1	59	95.9	84	95.4
10	98.1	35	97.1	60	96.5	85	93.9
11	98.6	36	99.1	61	97.5	86	97.2
12	98.9	37	97.4	62	96.6	87	96.3
13	94.7	38	93.5	63	98.6	88	97.2
14	95.6	39	91.6	64	96.2	89	98.1
15	95.4	40	96.8	65	99.1	90	98.1
16	97.3	41	96.6	66	97.5	91	94.0
17	95.6	42	99.9	67	97.1	92	97.3
18	95.0	43	96.1	68	96.0	93	96.7
19	96.3	44	97.4	69	95.4	94	95.5
20	94.4	45	99.5	70	97.1	95	96.0
21	98.1	46	97.7	71	96.8	96	98.6
22	99.3	47	97.1	72	92.0	97	98.5
23	93.7	48	98.4	73	90.3	98	98.6
24	86.3	49	95.9	74	97.0	99	96.3
25	94.0	50	99.5	75	99.9	100	98.0

The data of % gamma pass in VMAT QA for nasopharyngeal carcinoma (Cont.).

No	Gamma (3%, 3mm)	No	Gamma (3%, 3mm)	No	Gamma (3%, 3mm)
101	99.6	126	97.0	151	94.4
102	97.5	127	90.5	152	95.5
103	98.8	128	95.9	153	99.2
104	98.3	129	92.9	154	99.8
105	99.1	130	94.6	155	97.2
106	99.1	131	94.4	156	95.2
107	94.7	132	96.4	157	95.9
108	94.9	133	97.3	158	100
109	90.4	134	97.5	159	100
110	94.9	135	93.9		
111	97.0	136	96.6		
112	97.4	137	93.1		
113	97.8	138	98.3		
114	95.3	139	93.9		
115	91.7	140	95.8		
116	96.0	141	93.8		
117	93.9	142	99.3		
118	71.3	143	95.7		
119	95.0	144	99.2		
120	96.2	145	98.1		
121	92.7	146	99.0		
122	97.5	147	97.5		
123	99.1	148	95.1		
124	99.6	149	97.1		
125	97.2	150	96.5		

APPENDIX III

The output constancy data measured by central detector from RBA-3.

	Date	6MV	10MV	6MeV	9MeV	12MeV	16MeV	20MeV
1	10/12/2008	1.000	1.000	1.000	1.000	1.000	1.000	1.000
2	17/12/2008	1.000	1.000	1.000	1.000	1.004	0.998	1.000
3	24/12/2008	0.996	0.995	0.996	0.994	0.991	0.989	0.991
4	6/1/2009	0.996	0.998	0.993	0.990	0.987	0.988	0.991
5	21/1/2009	1.000	0.998	0.996	1.000	1.011	0.998	1.002
6	27/1/2009	0.993	0.987	0.986	0.990	1.002	0.993	0.988
7	6/2/2009	1.002	0.998	0.998	1.000	1.009	1.005	0.998
8	17/2/2009	1.000	0.998	0.993	0.996	1.004	1.000	1.000
9	27/2/2009	0.989	0.987	0.984	0.987	0.989	0.991	0.986
10	4/3/2009	0.989	0.987	0.984	0.987	0.985	0.991	0.984
11	12/3/2009	0.991	0.989	0.991	0.987	0.985	0.989	0.990
12	18/3/2009	0.991	0.989	0.987	0.985	0.983	0.988	0.984
13	25/3/2009	0.985	0.984	0.982	0.981	0.977	0.982	0.981
14	1/4/2009	0.994	0.991	0.989	0.990	0.974	0.982	0.990
15	17/4/2009	0.985	0.980	0.978	0.977	0.955	0.979	0.972
16	22/4/2009	0.996	0.989	0.991	0.992	1.002	0.993	0.997
17	29/4/2009	0.998	0.996	0.993	0.998	1.008	1.000	0.997
18	6/5/2009	0.994	0.991	0.989	0.996	1.004	0.996	0.998
19	15/5/2009	1.000	0.996	0.993	0.996	1.009	0.998	0.997
20	20/5/2009	1.002	0.998	0.996	1.000	1.009	1.002	1.000
21	27/5/2009	0.994	0.993	0.989	0.989	0.998	0.995	0.991
22	2/6/2009	0.998	0.993	0.991	0.992	1.004	0.995	0.997
23	11/6/2009	0.996	0.993	0.991	0.992	1.000	0.996	1.000
24	18/6/2009	0.993	0.987	0.989	0.990	1.000	0.991	0.990
25	23/6/2009	0.989	0.987	0.987	0.989	0.998	0.991	0.990
26	2/7/2009	0.993	0.991	0.989	0.990	1.000	0.993	0.993
27	9/7/2009	0.989	0.987	0.984	0.987	0.996	0.988	0.988
28	15/7/2009	0.989	0.991	0.986	0.987	0.994	1.005	0.991

The output constancy data measured by central detector from RBA-3. (cont.).

	Date	6MV	10MV	6MeV	9MeV	12MeV	16MeV	20MeV
29	22/7/2009	0.991	0.987	0.982	0.987	0.991	0.989	0.991
30	30/7/2009	0.993	0.989	0.986	0.989	0.996	0.995	0.993
31	6/8/2009	0.978	0.978	0.968	0.971	0.981	0.973	0.976
32	10/8/2009	0.989	0.989	0.984	0.985	0.998	0.995	0.991
33	12/8/2009	0.996	0.993	0.987	0.990	1.002	0.995	0.993
34	19/8/2009	0.991	0.987	0.984	0.989	0.998	0.991	0.990
35	25/8/2009	0.998	0.996	0.991	0.994	1.004	0.993	0.993
36	8/9/2009	0.998	0.998	0.995	0.998	1.008	1.002	1.002
37	22/9/2009	0.994	0.995	0.986	0.989	0.996	0.991	0.993
38	30/9/2009	0.994	0.989	0.987	0.987	0.996	0.988	0.988
39	9/10/2009	0.994	0.993	0.989	0.989	0.998	0.988	0.990
40	16/10/2009	0.994	0.996	0.987	0.989	1.000	0.996	0.997
41	29/10/2009	1.007	1.007	0.996	1.002	1.011	1.011	1.009
42	3/11/2009	1.006	1.005	1.000	1.002	1.013	1.007	1.009
43	11/11/2009	0.985	0.985	0.975	0.977	0.987	0.984	0.984
44	13/11/2009	0.987	0.985	0.977	0.979	0.989	0.982	0.984
45	15/11/2009	1.000	1.000	1.000	1.000	1.000	1.000	1.000
46	20/11/2009	1.009	1.009	1.007	1.012	1.011	1.006	1.007
47	24/11/2009	1.008	1.007	1.005	1.010	1.010	1.004	1.005
48	30/11/2009	1.008	1.007	1.005	1.010	1.008	1.002	1.004
49	12/12/2009	1.008	1.006	1.007	1.012	1.010	1.004	1.009
50	15/12/2009	1.008	1.007	1.005	1.010	1.008	1.004	1.007
51	25/12/2009	1.006	1.004	1.005	1.006	1.004	1.004	1.007
52	6/1/2010	1.004	1.004	1.000	1.006	1.002	1.002	1.004
53	14/1/2010	1.011	1.011	1.005	1.013	1.008	1.007	1.009
54	21/1/2010	1.004	1.004	1.000	1.008	1.004	1.004	0.993
55	1/2/2010	1.004	1.002	1.000	1.006	1.004	1.000	0.991
56	10/2/2010	1.004	1.004	0.996	1.008	1.004	1.006	0.995

The output constancy data measured by central detector from RBA-3. (cont.).

	Date	6MV	10MV	6MeV	9MeV	12MeV	16MeV	20MeV
57	17/2/2010	1.002	1.000	0.996	1.004	1.000	1.004	0.991
58	25/2/2010	1.002	1.002	1.000	1.008	1.002	1.002	0.991
59	5/3/2010	1.000	1.000	1.000	1.008	1.002	1.006	0.993
60	10/3/2010	1.008	1.009	1.007	1.013	1.008	1.008	0.995
61	16/3/2010	1.008	1.007	1.000	1.008	1.008	1.007	0.995
62	26/3/2010	1.004	1.006	1.002	1.006	1.004	1.000	0.993
63	3/4/2010	1.002	0.998	0.998	1.006	1.002	0.998	0.987
64	9/4/2010	1.006	1.004	0.998	1.006	1.004	0.998	0.987
65	22/4/2010	1.002	1.000	0.993	1.002	0.996	0.998	0.986
66	29/4/2010	1.008	1.004	1.000	1.008	1.000	1.002	0.991
67	6/5/2010	1.004	1.002	0.995	1.002	0.996	0.996	0.986
68	12/5/2010	0.996	0.993	0.993	1.002	0.994	0.996	0.984
69	27/5/2010	1.004	1.002	0.993	1.000	0.998	0.996	0.987
70	3/6/2010	1.008	1.004	0.996	1.006	1.002	1.000	0.991
71	11/6/2010	1.008	1.006	1.002	1.012	1.004	1.000	0.993
72	17/6/2010	1.011	1.009	1.002	1.010	1.010	1.004	0.995
73	25/6/2010	1.009	1.007	1.002	1.010	1.002	1.002	0.993
74	30/6/2010	1.019	1.017	1.015	1.021	1.013	1.009	1.004
75	7/7/2010	1.017	1.013	1.009	1.017	1.011	1.009	0.995
76	16/7/2010	1.017	1.013	1.009	1.015	1.010	1.006	0.995
77	22/7/2010	1.021	1.017	1.011	1.021	1.011	1.013	0.998
78	30/7/2010	1.025	1.018	1.016	1.023	1.013	1.013	1.007
79	6/8/2010	1.023	1.015	1.013	1.019	1.015	1.013	1.007
80	9/8/2010	1.021	1.015	1.013	1.017	1.013	1.011	1.004
81	17/8/2010	1.021	1.018	1.011	1.021	1.017	1.013	1.005
82	26/8/2010	1.019	1.013	1.011	1.017	1.010	1.006	0.998
83	30/8/2010	1.019	1.015	1.013	1.019	1.015	1.015	1.004
57	17/2/2010	1.002	1.000	0.996	1.004	1.000	1.004	0.991

APPENDIX IV

The raw data and calculated EWMA, UCL, and LCL of output constancy measurement with 1 month of data to calculate average and SD for $0.1 \hat{\lambda}$ and $2.703 L$ for 6 MV and 12 MeV (in example).

	6MV (Y _t)	EWMA (Y [^] _t)	LCL	UCL
1	1.000	0.998	0.9976	0.9987
2	1.000	0.998	0.9974	0.9989
3	0.996	0.9983	0.9972	0.9991
4	0.996	0.9981	0.9971	0.9991
5	1.000	0.9983	0.9971	0.9992
6	0.993	0.9977	0.9970	0.9993
7	1.002	0.9981	0.9970	0.9993
8	1.000	0.9983	0.9969	0.9993
9	0.989	0.9974	0.9969	0.9994
10	0.989	0.9965	0.9969	0.9994
11	0.991	0.9959	0.9969	0.9994
12	0.991	0.9954	0.9969	0.9994
13	0.985	0.9944	0.9969	0.9994
14	0.994	0.9944	0.9969	0.9994
15	0.985	0.9935	0.9968	0.9994
16	0.996	0.9938	0.9968	0.9995
17	0.998	0.9942	0.9968	0.9995
18	0.994	0.9942	0.9968	0.9995
19	1.000	0.9948	0.9968	0.9995
20	1.002	0.9955	0.9968	0.9995
21	0.994	0.9954	0.9968	0.9995
22	0.998	0.9957	0.9968	0.9995
23	0.996	0.9957	0.9968	0.9995

	12 MeV (Y _t)	EWMA (Y [^] _t)	LCL	UCL
	1.000	0.996	0.9932	0.9974
	1.004	0.997	0.9924	0.9982
	0.991	0.9960	0.9919	0.9987
	0.987	0.9951	0.9916	0.9990
	1.011	0.9967	0.9913	0.9993
	1.002	0.9972	0.9912	0.9995
	1.009	0.9984	0.9910	0.9996
	1.004	0.9990	0.9909	0.9997
	0.989	0.9979	0.9908	0.9998
	0.985	0.9966	0.9907	0.9999
	0.985	0.9955	0.9906	1.0000
	0.983	0.9942	0.9906	1.0000
	0.977	0.9926	0.9906	1.0000
	0.974	0.9907	0.9905	1.0001
	0.955	0.9871	0.9905	1.0001
	1.002	0.9886	0.9905	1.0001
	1.008	0.9905	0.9905	1.0001
	1.004	0.9918	0.9905	1.0001
	1.009	0.9936	0.9904	1.0002
	1.009	0.9951	0.9904	1.0002
	0.998	0.9954	0.9904	1.0002
	1.004	0.9963	0.9904	1.0002
	1.000	0.9966	0.9904	1.0002

The raw data and calculated EWMA, UCL, and LCL of output constancy measurement with 1 month of data to calculate average and SD for $0.1 \hat{\lambda}$ and 2.703 L for 6 MV and 12 MeV (in example) (cont.).

	6MV (Y _t)	EWMA (Y [^] _t)	LCL	UCL
24	0.993	0.9954	0.9968	0.9995
25	0.989	0.9948	0.9968	0.9995
26	0.993	0.9945	0.9968	0.9995
27	0.989	0.9940	0.9968	0.9995
28	0.989	0.9935	0.9968	0.9995
29	0.991	0.9932	0.9968	0.9995
30	0.993	0.9931	0.9968	0.9995
31	0.978	0.9916	0.9968	0.9995
32	0.989	0.9913	0.9968	0.9995
33	0.996	0.9918	0.9968	0.9995
34	0.991	0.9917	0.9968	0.9995
35	0.998	0.9923	0.9968	0.9995
36	0.998	0.9929	0.9968	0.9995
37	0.994	0.9931	0.9968	0.9995
38	0.994	0.9932	0.9968	0.9995
39	0.994	0.9933	0.9968	0.9995
40	0.994	0.9934	0.9968	0.9995
41	1.007	0.9948	0.9968	0.9995
42	1.006	0.9959	0.9968	0.9995
43	0.985	0.9948	0.9968	0.9995
44	0.987	0.9941	0.9968	0.9995
45	1.000	1.0055	1.0050	1.0073
46	1.009	1.0059	1.0046	1.0077
47	1.008	1.0061	1.0044	1.0079
48	1.008	1.0062	1.0042	1.0081

	12 MeV (Y _t)	EWMA (Y [^] _t)	LCL	UCL
	1.000	0.9970	0.9904	1.0002
	0.998	0.9971	0.9904	1.0002
	1.000	0.9974	0.9904	1.0002
	0.996	0.9973	0.9904	1.0002
	0.994	0.9970	0.9904	1.0002
	0.991	0.9963	0.9904	1.0002
	0.996	0.9963	0.9904	1.0002
	0.981	0.9948	0.9904	1.0002
	0.998	0.9951	0.9904	1.0002
	1.002	0.9958	0.9904	1.0002
	0.998	0.9961	0.9904	1.0002
	1.004	0.9968	0.9904	1.0002
	1.008	0.9979	0.9904	1.0002
	0.996	0.9977	0.9904	1.0002
	0.996	0.9976	0.9904	1.0002
	0.998	0.9976	0.9904	1.0002
	1.000	0.9979	0.9904	1.0002
	1.011	0.9992	0.9904	1.0002
	1.013	1.0006	0.9904	1.0002
	0.987	0.9992	0.9904	1.0002
	0.989	0.9982	0.9904	1.0002
	1.000	1.0064	1.0058	1.0085
	1.011	1.0069	1.0053	1.0090
	1.010	1.0072	1.0050	1.0093
	1.008	1.0072	1.0048	1.0095

The raw data and calculated EWMA, UCL, and LCL of output constancy measurement with 1 month of data to calculate average and SD for $0.1 \hat{\lambda}$ and 2.703 L for 6 MV and 12 MeV (in example) (cont.).

	6MV (Y _t)	EWMA (Y [^] _t)	LCL	UCL
49	1.008	1.0064	1.0040	1.0082
50	1.008	1.0065	1.0039	1.0083
51	1.006	1.0064	1.0039	1.0084
52	1.004	1.0061	1.0038	1.0085
53	1.011	1.0067	1.0037	1.0085
54	1.004	1.0064	1.0037	1.0086
55	1.004	1.0061	1.0037	1.0086
56	1.004	1.0059	1.0037	1.0086
57	1.002	1.0055	1.0036	1.0087
58	1.002	1.0051	1.0036	1.0087
59	1.000	1.0046	1.0036	1.0087
60	1.008	1.0049	1.0036	1.0087
61	1.008	1.0052	1.0036	1.0087
62	1.004	1.0050	1.0036	1.0087
63	1.002	1.0047	1.0036	1.0087
64	1.006	1.0048	1.0036	1.0087
65	1.002	1.0045	1.0036	1.0087
66	1.008	1.0048	1.0036	1.0087
67	1.004	1.0047	1.0036	1.0087
68	0.996	1.0039	1.0036	1.0087
69	1.004	1.0039	1.0036	1.0087
70	1.008	1.0042	1.0035	1.0087
71	1.008	1.0046	1.0035	1.0087
72	1.011	1.0052	1.0035	1.0087
73	1.009	1.0057	1.0035	1.0087

	12 MeV (Y _t)	EWMA (Y [^] _t)	LCL	UCL
	1.010	1.0075	1.0046	1.0097
	1.008	1.0075	1.0045	1.0098
	1.004	1.0071	1.0044	1.0099
	1.002	1.0066	1.0043	1.0100
	1.008	1.0067	1.0043	1.0100
	1.004	1.0064	1.0042	1.0101
	1.004	1.0062	1.0042	1.0101
	1.004	1.0059	1.0042	1.0101
	1.000	1.0053	1.0041	1.0102
	1.002	1.0050	1.0041	1.0102
	1.002	1.0047	1.0041	1.0102
	1.008	1.0050	1.0041	1.0102
	1.008	1.0052	1.0041	1.0102
	1.004	1.0051	1.0041	1.0102
	1.002	1.0048	1.0041	1.0102
	1.004	1.0047	1.0041	1.0102
	0.996	1.0038	1.0041	1.0103
	1.000	1.0035	1.0041	1.0103
	0.996	1.0027	1.0041	1.0103
	0.994	1.0019	1.0041	1.0103
	0.998	1.0015	1.0041	1.0103
	1.002	1.0015	1.0041	1.0103
	1.004	1.0018	1.0040	1.0103
	1.010	1.0025	1.0040	1.0103
	1.002	1.0025	1.0040	1.0103

The raw data and calculated EWMA, UCL, and LCL of output constancy measurement with 1 month of data to calculate average and SD for $0.1 \hat{\lambda}$ and 2.703 L for 6 MV and 12 MeV (in example) (cont.).

	6MV (Y _t)	EWMA (Y [^] _t)	LCL	UCL
74	1.019	1.0070	1.0035	1.0087
75	1.017	1.0080	1.0035	1.0087
76	1.017	1.0089	1.0035	1.0087
77	1.021	1.0101	1.0035	1.0087
78	1.025	1.0115	1.0035	1.0087
79	1.023	1.0126	1.0035	1.0087
80	1.021	1.0135	1.0035	1.0087
81	1.021	1.0142	1.0035	1.0087
82	1.019	1.0147	1.0035	1.0087
83	1.019	1.0151	1.0035	1.0087

	12 MeV (Y _t)	EWMA (Y [^] _t)	LCL	UCL
	1.013	1.0036	1.0040	1.0103
	1.011	1.0044	1.0040	1.0103
	1.010	1.0049	1.0040	1.0103
	1.011	1.0055	1.0040	1.0103
	1.013	1.0063	1.0040	1.0103
	1.015	1.0072	1.0040	1.0103
	1.013	1.0078	1.0040	1.0103
	1.017	1.0088	1.0040	1.0103
	1.010	1.0088	1.0040	1.0103
	1.015	1.0095	1.0040	1.0103

APPENDIX V

The percent point dose differences of prostate IMRT QA.

No	%Dose dif.	No	%Dose dif.	No	%Dose dif.	No	%Dose dif.	No	%Dose dif.
1	-0.1	26	1.3	51	2.2	76	2.3	101	1.4
2	-2.2	27	-0.2	52	-2.6	77	-0.8	102	-2.9
3	-1.0	28	-1.1	53	2.0	78	-1.4	103	-3.1
4	3.1	29	-2.7	54	-0.3	79	1.5	104	-0.5
5	1.2	30	-2.1	55	-2.3	80	-0.2	105	2.0
6	2.7	31	0.0	56	3.0	81	-0.3	106	-0.1
7	2.8	32	0.3	57	0.6	82	2.2	107	1.6
8	0.5	33	0.4	58	0.2	83	1.3	108	-0.1
9	2.3	34	-1.0	59	0.0	84	-2.6	109	-2.8
10	-0.9	35	-1.9	60	1.3	85	2.2	110	0.1
11	-1.3	36	-0.2	61	-2.6	86	-2.3	111	-1.5
12	-1.9	37	1.1	62	1.9	87	-1.4	112	1.5
13	-1.2	38	-0.4	63	-0.3	88	1.2	113	0.4
14	0.1	39	0.8	64	0.3	89	-1.7	114	0.2
15	2.1	40	-2.6	65	2.5	90	-2.9	115	-0.4
16	-1.7	41	-0.5	66	1.0	91	1.5	116	3.1
17	0.7	42	-0.7	67	2.6	92	0.1	117	1.7
18	0.9	43	-2.4	68	1.6	93	2.1	118	2.3
19	3.6	44	2.7	69	-1.9	94	1.6	119	2.0
20	1.1	45	-2.1	70	1.4	95	1.1	120	2.6
21	-1.3	46	-1.8	71	-0.2	96	2.3	121	1.0
22	-1.0	47	-2.3	72	-2.2	97	2.2	122	1.7
23	-0.2	48	-0.2	73	-2.2	98	0.9	123	0.8
24	3.9	49	1.6	74	-2.2	99	-2.8	124	1.8
25	-1.2	50	-1.5	75	-1.4	100	0.7	125	-1.2

The percent point dose differences of prostate IMRT QA (cont.).

No	%Dose dif.	No	%Dose dif.	No	%Dose dif.	No	%Dose dif.	No	%Dose dif.
126	0.5	151	1.8	176	1.8	201	2.8	226	3.0
127	0.9	152	-0.1	177	0.2	202	2.6	227	-1.1
128	0.6	153	3.0	178	-0.6	203	0.9	228	1.7
129	-0.9	154	2.9	179	0.8	204	2.5	229	3.8
130	2.6	155	-0.9	180	1.1	205	3.2	230	-2.4
131	0.9	156	0.1	181	-0.1	206	4.1	231	-2.9
132	1.7	157	2.0	182	2.6	207	3.3	232	-0.1
133	2.0	158	3.0	183	2.9	208	3.7	233	-2.7
134	1.4	159	-2.5	184	-0.2	209	2.7	234	2.7
135	-3.4	160	0.0	185	2.5	210	1.0	235	0.5
136	-0.4	161	1.1	186	2.9	211	2.7	236	-0.2
137	-1.5	162	-1.9	187	0.9	212	2.2	237	0.6
138	-0.7	163	2.9	188	-2.8	213	2.6	238	0.1
139	-2.0	164	1.0	189	2.1	214	2.6	239	2.0
140	1.1	165	2.9	190	0.8	215	0.0	240	2.0
141	0.7	166	-1.0	191	0.1	216	2.9	241	-0.4
142	-0.6	167	3.0	192	1.8	217	4.2	242	-1.9
143	3.0	168	2.8	193	1.6	218	0.6	243	-1.1
144	1.4	169	-1.9	194	1.8	219	-2.4	244	3.1
145	2.8	170	2.7	195	-0.2	220	1.2	245	-0.2
146	0.6	171	-2.0	196	1.9	221	1.7	246	0.0
147	-0.6	172	1.9	197	2.9	222	-1.1	247	1.3
148	-0.9	173	-1.6	198	3.0	223	0.5	248	1.2
149	2.8	174	0.9	199	4.6	224	0.7	249	2.6
150	0.6	175	-1.4	200	2.3	225	2.4	250	0.8

The percent point dose differences of prostate IMRT QA (cont.).

No	%Dose dif.	No	%Dose dif.	No	%Dose dif.	No	%Dose dif.	No	%Dose dif.
251	-2.0	276	-1.5	301	0.7	326	-3.2	351	0.3
252	0.9	277	1.1	302	-1.8	327	-0.9	352	2.0
253	1.9	278	1.6	303	-2.5	328	0.2	353	2.4
254	-2.5	279	-2.0	304	1.7	329	0.0	354	0.9
255	2.1	280	-1.6	305	2.2	330	0.8	355	-1.3
256	0.5	281	-0.9	306	1.5	331	-0.2	356	-0.5
257	1.9	282	1.0	307	-3.5	332	2.7	357	3.1
258	-2.1	283	0.9	308	2.0	333	-0.4	358	1.7
259	-0.2	284	2.1	309	-0.9	334	1.2	359	1.9
260	0.6	285	0.3	310	0.8	335	-0.4	360	1.1
261	1.1	286	3.1	311	1.5	336	-1.6	361	-0.3
262	-0.7	287	-1.9	312	0.2	337	-3.2	362	1.3
263	0.6	288	-1.6	313	2.6	338	-2.0	363	-2.1
264	0.5	289	-3.4	314	1.9	339	-1.9	364	1.7
265	0.8	290	-2.0	315	-1.4	340	-2.3	365	2.9
266	2.6	291	2.8	316	-0.6	341	0.3	366	-0.1
267	-0.5	292	1.2	317	2.4	342	0.8	367	2.4
268	0.7	293	-2.8	318	-1.7	343	-1.6	368	-2.3
269	-2.5	294	-1.4	319	2.3	344	-0.5	369	2.9
270	1.5	295	0.0	320	0.5	345	1.6	370	1.7
271	-0.6	296	1.5	321	-1.6	346	0.4	371	2.1
272	0.4	297	1.3	322	3.2	347	-1.7	372	2.6
273	3.0	298	-2.8	323	-2.2	348	-1.2	373	2.5
274	0.9	299	0.1	324	-0.1	349	0.0	374	1.8
275	1.6	300	-1.2	325	0.9	350	-3.1	375	1.6

The percent point dose differences of prostate IMRT QA (cont.).

No	%Dose dif.	No	%Dose dif.	No	%Dose dif.	No	%Dose dif.	No	%Dose dif.
376	-1.2	401	0.3	426	1.6	451	2.0	476	2.1
377	1.3	402	1.6	427	-0.9	452	-1.9	477	-2.4
378	2.4	403	1.4	428	-0.4	453	1.0	478	-0.6
379	0.4	404	-0.1	429	-2.6	454	-2.6	479	-3.2
380	-0.3	405	-2.7	430	-0.8	455	-2.6	480	0.6
381	1.0	406	-2.2	431	0.7	456	2.3	481	-1.7
382	1.0	407	0.1	432	-1.6	457	2.5	482	2.8
383	0.1	408	-3.2	433	-1.2	458	-3.4	483	3.0
384	0.1	409	-1.1	434	-2.5	459	-2.4	484	2.7
385	-1.3	410	1.5	435	-0.6	460	-2.3	485	2.2
386	0.4	411	-0.9	436	0.6	461	-0.4	486	-3.0
387	-1.6	412	-1.3	437	1.6	462	-0.5	487	-2.0
388	-0.7	413	1.0	438	-0.6	463	1.5	488	-2.4
389	-1.2	414	0.8	439	-1.0	464	-0.3	489	-0.2
390	0.7	415	-1.1	440	-1.6	465	0.3	490	-1.7
391	-2.2	416	-0.2	441	-3.0	466	-1.7	491	1.7
392	-1.2	417	-3.1	442	0.4	467	-2.4	492	-1.2
393	1.5	418	0.3	443	-2.0	468	3.2	493	-3.7
394	-2.2	419	0.0	444	-2.3	469	0.0	494	-0.8
395	-1.1	420	-3.4	445	0.7	470	-2.5	495	1.0
396	2.3	421	-2.8	446	-3.1	471	1.5	496	-2.7
397	2.3	422	-3.9	447	1.5	472	1.2	497	-2.8
398	-3.0	423	0.0	448	-0.3	473	1.5	498	0.5
399	2.5	424	0.3	449	-1.2	474	-1.1	499	-1.6
400	0.1	425	-0.5	450	0.2	475	-0.5	500	1.6

APPENDIX VII

The PTV homogeneity index for head and neck VMAT plan.

Number	D _{2%}	D _{98%}	D _{median}	HI
1	7184	6240	6964.7	0.14
2	5861	5096	5565.4	0.14
3	6426	5770	6205.4	0.11
4	6461	5914	6317.5	0.09
5	7506	6914	7297.9	0.08
6	6572	5820	5388.6	0.14
7	6445	5914	6244.5	0.09
8	7534	6889	7327.4	0.09
9	4284	4060	4211.9	0.05
10	5593	5406	5480	0.03
11	7497	6966	7330	0.07
12	5796	5303	5638.8	0.09
13	6719	5658	6350.8	0.17
14	2480	2366	2435.8	0.05
15	6400	6055	6255.4	0.06
16	3824	3470	3706.9	0.10
17	3365	2933	3249.3	0.13
18	5241	5018	5132.6	0.04
19	7477	6810	7298	0.09
20	7618	6965	7397.4	0.09
21	7456	6763	7321	0.09
22	7774	6945	7491	0.11
23	7666	6886	7429.4	0.10
24	5345	4975	5212.6	0.07
25	5785	5131	5556.6	0.12
26	5012	4589	4883	0.09
27	5346	5022	5219.9	0.06
28	6536	5980	6266	0.09
29	7656	6867	7400.6	0.11
30	7748	6925.3	7511.6	0.11
31	5600	5443	5522.5	0.03
32	6958	6301	6701.7	0.10
33	2484	2311	2423	0.07
34	6325	6073	6210.8	0.04
35	7438	6919	7252	0.07
36	6878	5875	6686.5	0.15
37	7872	6866	7544	0.13
38	7638	6799	7440.8	0.11
39	7666	6878	7476.8	0.11
40	7338	6170	7110.8	0.16
41	7990	7618	7850.4	0.05
42	5343	4989	5217.9	0.07
43	5318	4984	5227.9	0.06
44	1339	1243	1295.7	0.07
45	6357	5724	6148.8	0.10
46	7630	7103	7410.9	0.07
47	5679	5319	5541.1	0.06
48	8072	6794	7530	0.17
49	7646	6861	7455.6	0.11
50	7060	6565	6881.4	0.07

The PTV homogeneity index for head and neck VMAT plan (cont.)

Number	D _{2%}	D _{98%}	D _{median}	HI
51	7617	6765	7372	0.12
52	7420	7037	7296	0.05
53	6506	6019	6338.1	0.08
54	6319	5959	6195.8	0.06
55	3309	2955	3222.5	0.11
56	7830	6802	7494.7	0.14
57	7679	6802	7427.5	0.12
58	6681	5579	6425	0.17
59	5521	5202	5433.6	0.06
60	4266	3922	4161	0.08
61	6548	5601	6304.9	0.15
62	7052	5951	6735.2	0.16
63	4403	3885	4256.4	0.12
64	6264	5945	6135.2	0.05
65	7414	6850	7261.1	0.08
66	7305	6877	7148.3	0.06
67	7420	6831	7260.8	0.08
68	7656	6860	7357.6	0.11
69	3178	3045	3114.1	0.04
70	6952	6546	6791.1	0.06
71	5756	5109	5530.4	0.12
72	7099	5577	6900.2	0.22
73	7648	6746	7371.3	0.12
74	7468	6850	7263.1	0.09
75	7470	6950	7250.6	0.07
76	7573	6229	7404.1	0.18
77	5775	5068	5609.7	0.13
78	3252	2921	3155.8	0.10
79	5751	5239	5597.7	0.09
80	5503	5022	5308.8	0.09
81	7827	6935	7521.9	0.12
82	3160	2994	3115.1	0.05
83	4163	3700	3949.9	0.12
84	7544	6816	7346.4	0.10
85	3292	2807	3191.7	0.15
86	5657	4876	5281.4	0.15
87	7191	6261	6942.4	0.13
88	7591	6276	7320.1	0.18
89	5706	5363	5550.5	0.06
90	7633	6923	7389.7	0.10
91	2154	1899	2067.5	0.12
92	7638	7064	7433.2	0.08
93	7547	6773	7345.2	0.11
94	5102	3956	4881.7	0.23
95	5712	5308	5565.8	0.07
96	7550	6736	7312	0.11
97	5980	5483	5845.7	0.09
98	6754	5952	6470.6	0.12
99	5649	4993	5465	0.12
100	6554	5879	6361.8	0.11

The PTV homogeneity index for head and neck VMAT plan (cont.)

Number	D _{2%}	D _{98%}	D _{median}	HI
101	7640	6824	7377.3	0.11
102	7827	6938	7521.9	0.12
103	7730	6877	7501.6	0.11
104	3305	2945	3211.6	0.11
105	5217	4966	5151.2	0.05
106	6437	6013	6230.6	0.07
107	7414	6671	7226.5	0.10
108	6453	6146	6336	0.05
109	6391	5751	6239.3	0.10
110	5715	5052	5582.3	0.12
111	5766	5251	5609.8	0.09
112	5390	4901	5250.4	0.09
113	5914	5349	5640.7	0.10
114	6826	6586	6728.5	0.04
115	7081	6518	6851	0.08
116	5255	5029	5144.3	0.04
117	5877	5323	5700.3	0.10
118	7696	6855	7488.7	0.11
119	7206	6460	7021.2	0.11
120	5388	4970	5255.7	0.08
121	6102	5651	5966.1	0.08
122	7600	6967	7434.3	0.09
123	7819	7474	7650.5	0.05
124	7716	6767	7484.6	0.13
125	7467	6214	6881.9	0.18
Number	D _{2%}	D _{98%}	D _{median}	HI
126	7097	6635	6953.3	0.07
127	6912	6674	6785.1	0.04
128	6457	5776	6247.9	0.11
129	5815	5579	5723.8	0.04
130	7846	7425	7676.5	0.05
131	7594	6652	7310.4	0.13
132	7682	6837	7454.7	0.11
133	7507	6878	7320.6	0.09
134	3292	2956	3191.1	0.11
135	5878	5091	5748.1	0.14
136	6197	6082	6156.5	0.02
137	7615	6949	7399.9	0.09
138	7858	7522	7681.6	0.04
139	6051	4450	5405.2	0.30
140	7400	6837	7256.1	0.08
141	7628	6842	7414.5	0.11
142	5813	5092	5695.3	0.13
143	6531	5857	6362.7	0.11
144	5858	4311	5465.4	0.28
145	5623	5235	5484.8	0.07
146	3217	2548	3125.9	0.21
147	7435	6924	7301.3	0.07
148	5783	5162	5607.4	0.11
149	6464	6034	6245.9	0.07
150	7111	6508	6943	0.09

BIOGRAPHY

NAME	Mr. Taweap Sanghangthum
SEX	Male
NATIONALITY	Thai
DATE OF BIRTH	25 September 1979
PLACE OF BIRTH	Bangkok, Thailand
INSTITUTIONS ATTENDED	Mahidol University, 2001: Bachelor of Science (Radiological Technology) Mahidol University, 2003: Master of Science (Medical Physics) Chulalongkorn University, 2012 Doctoral of Engineering (Nuclear Engineering)
HOME ADDRESS	114/58 Moo.1, Krisana Village, Tiwanont Rd, Ban-Mai, Muang, Pratumthani, Thailand 12000 Tel. 084-901-3475

International publications

- “Statistical process control analysis for patient-specific IMRT and VMAT QA” which is accepted to publication in Journal of Radiation Research (JRR)
- “Retrospective analysis of linear accelerator output constancy checks using process control techniques” which is accepted to publish in Journal of Applied Clinical Medical Physics (JACMP).
- “On setting tolerance limits for process monitoring in radiotherapy” that is on processing to accept in Physics in Medicine and Biology (PMB).

International presentation (with paper proceeding)

- “Radiotherapy quality assurance using control charts” had presented in International Conference on Advances in Radiation Oncology; ICARO, Vienna, Austria.
- “Using control charts to analyze the patient specific Nasopharyngeal Carcinoma IMRT QA” had presented in 52nd Annual American Association Physicist in Medicine meeting, Pennsylvania, USA.
- “The comparison of different control charts to analyze patient specific IMRT QA” had presented in International symposium on Standards, Applications and Quality Assurance in Medical Radiation Dosimetry; IDOS, Vienna, Austria.
- “Dosimetric verification of volumetric modulated arc therapy through ArcCHECK” had presented in 6th Japan-Korea Joint Meeting on Medical Physics; JKMP & 11th Asia-Ocenia Congress of Medical Physics; AOCMP, Fukuoka, Japan.

National presentation

- “QA in advanced treatment techniques” had presented in 20th THASTRO meeting, Dusit Thani, Chonburi.
- “Patient-specific QA on IMRT” had presented in 5th TMPS annual scientific meeting, BP Samila Beach Hotel & Resort, Songkhla.
- “QA in treatment delivery systems” had presented in 6th TMPS annual scientific meeting, Amarin Lagoon Hotel, Phitsanulok.